

SANDIA REPORT

SAND94-1073 • UC-610
Unlimited Release
Printed August 1995

Direct Containment Heating Models in the CONTAIN Code

Kenneth E. Washington, David C. Williams

Prepared by
Sandia National Laboratories
Albuquerque, New Mexico 87185 and Livermore, California 94550
for the United States Department of Energy
under Contract DE-AC04-94AL85000

Approved for public release; distribution is unlimited.

DISTRIBUTION OF THIS DOCUMENT IS UNLIMITED

Issued by Sandia National Laboratories, operated for the United States Department of Energy by Sandia Corporation.

NOTICE: This report was prepared as an account of work sponsored by an agency of the United States Government. Neither the United States Government nor any agency thereof, nor any of their employees, nor any of their contractors, subcontractors, or their employees, makes any warranty, express or implied, or assumes any legal liability or responsibility for the accuracy, completeness, or usefulness of any information, apparatus, product, or process disclosed, or represents that its use would not infringe privately owned rights. Reference herein to any specific commercial product, process, or service by trade name, trademark, manufacturer, or otherwise, does not necessarily constitute or imply its endorsement, recommendation, or favoring by the United States Government, any agency thereof or any of their contractors or subcontractors. The views and opinions expressed herein do not necessarily state or reflect those of the United States Government, any agency thereof or any of their contractors.

Printed in the United States of America. This report has been reproduced directly from the best available copy.

Available to DOE and DOE contractors from
Office of Scientific and Technical Information
PO Box 62
Oak Ridge, TN 37831

Prices available from (615) 576-8401, FTS 626-8401

Available to the public from
National Technical Information Service
US Department of Commerce
5285 Port Royal Rd
Springfield, VA 22161

NTIS price codes
Printed copy: A08
Microfiche copy: A01

DISCLAIMER

**Portions of this document may be illegible
in electronic image products. Images are
produced from the best available original
document.**

SAND94-1073
Unlimited Release
Printed August 1995

Distribution
Category UC-610

Direct Containment Heating Models in the CONTAIN Code

Kenneth E. Washington
Information Systems Applications Department

David C. Williams
Modeling and Analysis Department

Sandia National Laboratories
Albuquerque, NM 87185-5800

ABSTRACT

The potential exists in a nuclear reactor core melt severe accident for molten core debris to be dispersed under high pressure into the containment building. If this occurs, the set of phenomena that result in the transfer of energy to the containment atmosphere and its surroundings is referred to as direct containment heating (DCH). Because of the potential for DCH to lead to early containment failure, the U.S. Nuclear Regulatory Commission (USNRC) has sponsored an extensive research program consisting of experimental, analytical, and risk integration components. An important element of the analytical research has been the development and assessment of direct containment heating models in the CONTAIN code. This report documents the DCH models in the CONTAIN code.

DCH models in CONTAIN for representing debris transport, trapping, chemical reactions, and heat transfer from debris to the containment atmosphere and surroundings are described. The descriptions include the governing equations and input instructions in CONTAIN unique to performing DCH calculations. Modifications made to the combustion models in CONTAIN for representing the combustion of DCH-produced and pre-existing hydrogen under DCH conditions are also described. Input table options for representing the discharge of debris from the RPV and the entrainment phase of the DCH process are also described. A sample calculation is presented to demonstrate the functionality of the models. The results show that reasonable behavior is obtained when the models are used to predict the sixth Zion geometry integral effects test at 1/10th scale.

DISTRIBUTION OF THIS DOCUMENT IS UNLIMITED

OK

MASTER

TABLE OF CONTENTS

1. Introduction	1
2. Model Descriptions and Governing Equations	2
2.1 Multiple Debris Field Code Architecture	3
2.2 Debris Transport and Intercell Flow	5
2.2.1 <u>Gas/Debris Slip Model</u>	6
2.2.2 <u>Gas Mass Conservation</u>	9
2.2.3 <u>Gas Energy Conservation</u>	11
2.2.4 <u>Debris Mass Conservation</u>	12
2.2.5 <u>Debris Energy Conservation Equations</u>	14
2.2.6 <u>Choked Flow</u>	16
2.2.7 <u>Numerical Considerations of the Debris Intercell Flow Model</u>	17
2.3 DCH Trapping Model	18
2.3.1 <u>Rate Equations for Trapping</u>	18
2.3.2 <u>Average Velocities</u>	21
2.3.3 <u>USER Trapping Model</u>	24
2.3.4 <u>GFT Trapping Model</u>	24
2.3.5 <u>TFI Trapping Model</u>	26
2.3.6 <u>TOF/KU Trapping Model</u>	27
2.3.6.1 <u>TOF/KU Case 1: Trapping On First Impact</u>	29
2.3.6.2 <u>TOF/KU Case 2: Trapping On Structures Beyond The First Impact</u>	32
2.3.6.3 <u>TOF/KU Case 3: No Trapping From First or Second Ku Criteria</u>	35
2.3.7 <u>Trapping Model Sensitivity Coefficients</u>	36
2.4 Chemical Reactions	37
2.4.1 <u>Gas Side Transport</u>	38
2.4.2 <u>Drop-Side Transport</u>	43
2.4.3 <u>Reaction Rate Equations</u>	45
2.5 Hydrogen Behavior Under DCH Conditions	52
2.5.1 <u>DCH-Produced Hydrogen Recombination</u>	53
2.5.2 <u>Diffusion Flame Burning</u>	53
2.5.3 <u>Volumetric Hydrogen Recombination</u>	56
2.6 Heat Transfer	56
2.6.1 <u>Convective Heat Transfer</u>	57
2.6.2 <u>Radiative Heat Transfer</u>	58
2.7 Non-Airborne Debris Interactions	60
2.8 Known Limitations	62

TABLE OF CONTENTS (cont.)

3. Input Instructions	63
3.1 Global Control Block	64
3.2 User-Defined Material Input	65
<u>3.2.1 DCH Material Names</u>	65
<u>3.2.2 DCH Material Property Tables</u>	66
3.3 Global DHEAT block	67
3.4 Cell Level DCH-CELL Input Block	72
3.5 Debris Dispersal, Debris Entrainment, and Gas Blowdown Sources	78
3.6 Miscellaneous DCH Related Input	81
<u>3.6.1 Aerosol Condensation Override</u>	81
<u>3.6.2 Fixed Gas Emissivity Option</u>	81
<u>3.6.3 Relevant Structure Input</u>	82
<u>3.6.4 DCH Restart Input</u>	82
4. Generated Output	83
4.1 Output file	83
4.2 Plot file	84
5. Demonstration Calculations	87
6. Summary	98
7. References	99

LIST OF FIGURES

Figure 1. Illustration of the DCH Multifield Debris Representation in CONTAIN	4
Figure 2. Pressure Results From CONTAIN Assessment	90
Figure 3. Hydrogen Production Results From CONTAIN Assessment	91
Figure 4. CONTAIN Nodalization of Zion Geometry Integral Effects Tests in Surtsey . .	92
Figure 5. IET-6 Pressure CONTAIN Results	93
Figure 6. IET-6 Temperature CONTAIN Results	94
Figure 7. IET-6 Debris Trapping CONTAIN Results	95
Figure 8. IET-6 Fe and FeO Airborne Mass CONTAIN Results	96
Figure 9. IET-6 Hydrogen Burned and Inventory CONTAIN Results	97

1. Introduction

The potential exists in a nuclear reactor core melt severe accident for molten core debris to be dispersed under high pressure into the containment building. If this occurs, the set of phenomena that result in the rapid transfer of energy to the containment atmosphere and its surroundings is referred to as direct containment heating (DCH). Because of the potential for DCH to lead to early containment failure, the U.S. Nuclear Regulatory Commission (USNRC) has sponsored an extensive research program consisting of experimental, analytical, and risk integration components. An important element of the analytical research has been the development and assessment of direct containment heating models in the CONTAIN code. The purpose of this report is to document the DCH models in the CONTAIN code.

The key purpose of the DCH models in CONTAIN is to provide an analytical tool for quantifying containment loads in a DCH event. This tool is also intended to be used to gain an understanding of DCH phenomenology through the analysis and interpretation of DCH experiments. This understanding is then transferred to the use of CONTAIN in the prediction of DCH loads at full scale. To achieve this goal, the code has been written to include detailed models in areas where the phenomena are well understood, and more parametric models with flexible input options in phenomenological areas that are more poorly understood. Parametric models are also included instead of detailed models in some cases where the phenomena are understood, but a detailed model could not be included because of an inherent limitation posed by the control volume CONTAIN code architecture.

DCH processes can be divided into two distinct categories. The first category includes the ejection of debris under high pressure from the reactor pressure vessel (RPV), followed by the entrainment of debris from the cavity into the containment atmosphere. The second category includes the transport and trapping of debris in the containment, and the transfer of heat from debris to the containment atmosphere and its surroundings. Models have recently been added to CONTAIN for predicting the debris ejection and entrainment phases of the DCH process¹. Because of their newness, these models have not been fully validated against the available DCH database, nor have they been used to any appreciable extent in DCH full scale plant calculations. These models have been assessed against a large body of cold simulant data; however, at the time of this writing, they have not been assessed to any appreciable extent against the high temperature database.

¹R. O. Griffith, "C110Z Code Change Document: RPV Dispersal and Cavity Models", Letter report to the USNRC, December, 1993.

This report focuses on the DCH models in CONTAIN that have been actively used in the majority of the DCH assessments and full scale plant analyses performed at Sandia National Laboratories. This includes the user specified table options included in CONTAIN for representing the RPV dispersal and cavity entrainment phase of the DCH process, and the models for representing phenomena in the second phase of the DCH process. For the first phase, the user is provided a set of flexible input tools for controlling the amount and rate of debris dispersal and entrainment. Therefore, this information must be known (as in the case of the experiments), or assumed. Often one assumes a dispersed debris mass and then uses a correlation for debris steam coherence to set the rate of debris entrainment. For the second phase the user is provided with a mixture of mechanistic and parametric models for representing the transport and trapping of debris, and the transfer of heat from the debris to the containment atmosphere and surroundings. This includes models for representing the combustion of DCH-produced and pre-existing hydrogen under DCH conditions. In nearly all cases, user input flexibility has been included to facilitate the use of the code in DCH sensitivity studies.

Section 2 describes the models in detail, including the governing equations. The first subsection of Section 2 describes the architecture of the model. In-depth guidance for users of the DCH models is provided in a forthcoming report on the assessment of the CONTAIN DCH models². Input requirements and options specific to a DCH calculation are given in Section 3. General input requirements for performing CONTAIN calculations are given in the CONTAIN 1.1 User's Manual [Mur89]. User information about models added to the code since the publication of Reference Mur89 is available in letter reports called "code change documents" that are produced as part of the CONTAIN quality assurance process. Although these documents are not published in the open literature, they are sent to all NRC-approved users of the code. Section 4 describes the output generated by CONTAIN in a DCH calculation, and a demonstration calculation is presented in Section 5.

2. Model Descriptions and Governing Equations

This section describes the governing equations for direct containment heating processes modeled in CONTAIN. Direct containment heating consists of a collection of complex chemical, thermal, and physical processes resulting in the transfer of mass and energy from dispersed molten debris to the containment atmosphere and its surroundings. The following list shows the phenomena covered by the CONTAIN DCH models along with the subsections where the model is described.

²D. C. Williams, et. al., "Assessment of DCH Models in CONTAIN," in preparation.

CONTAIN DCH Models

Model Descriptions

Phenomena

- Debris transport and intercell flow
- Debris de-entrainment on structures (trapping)
- Chemical interactions
- Hydrogen combustion under DCH conditions
- Convective and radiative heat transfer
- Non-airborne debris interactions

Subsection

- Section 2.2
- Section 2.3
- Section 2.4
- Section 2.5
- Section 2.6
- Section 2.7

The models and associated governing equations in CONTAIN for these processes are described in the sections indicated above. The hydrogen combustion section only describes the models provided for representing the burning of DCH-produced hydrogen as it enters oxygen rich atmospheres, and the volumetric burning of pre-existing hydrogen at user-specified rates. The standard CONTAIN deflagration model described in Reference Mur89 typically does not play a role in DCH calculations. In addition to these models, CONTAIN includes provisions for specifying the discharge rate of debris from the reactor pressure vessel, and the rate and cumulative dispersal fraction of debris from the cavity into the containment atmosphere. Gas discharge is normally calculated by the flow models in CONTAIN. These input provisions are described in Section 3.5. Section 2.8 describes some of the major limitations in the DCH models. The first subsection below is a discussion of how debris is represented architecturally as multiple fields within the code.

2.1 Multiple Debris Field Code Architecture

The CONTAIN DCH model is based on a multiple field representation of debris particles. With this modeling approach airborne debris can be represented by a range of particle sizes and material compositions. Any number of particle fields can be represented in the model, and each field has its own characteristic size, mass, chemical composition, and temperature. The exchange of mass and energy from the debris to the atmosphere and its surroundings are modeled in CONTAIN for each debris field. In principle, the number of fields that can be represented is only limited by the amount of memory and CPU power available to the user. In practice, 10 or fewer fields are recommended for most calculations. The multiple field feature provides for multiple debris fields and multiple "sets" of debris fields. These sets are referred to here as "generations". Each debris field can have its own mean particle size, initial debris composition, mass, and temperature. The composition and temperature of the field will evolve independently of the other debris fields in the atmosphere. Figure 1 illustrates this concept of fields and generations. This figure also shows the trapped field that represents debris that is not airborne. The non-airborne field represents trapped debris and debris in the cavity before it is entrained by the blowdown steam. Debris in this repository can chemically interact with and transfer heat to the blowdown steam.

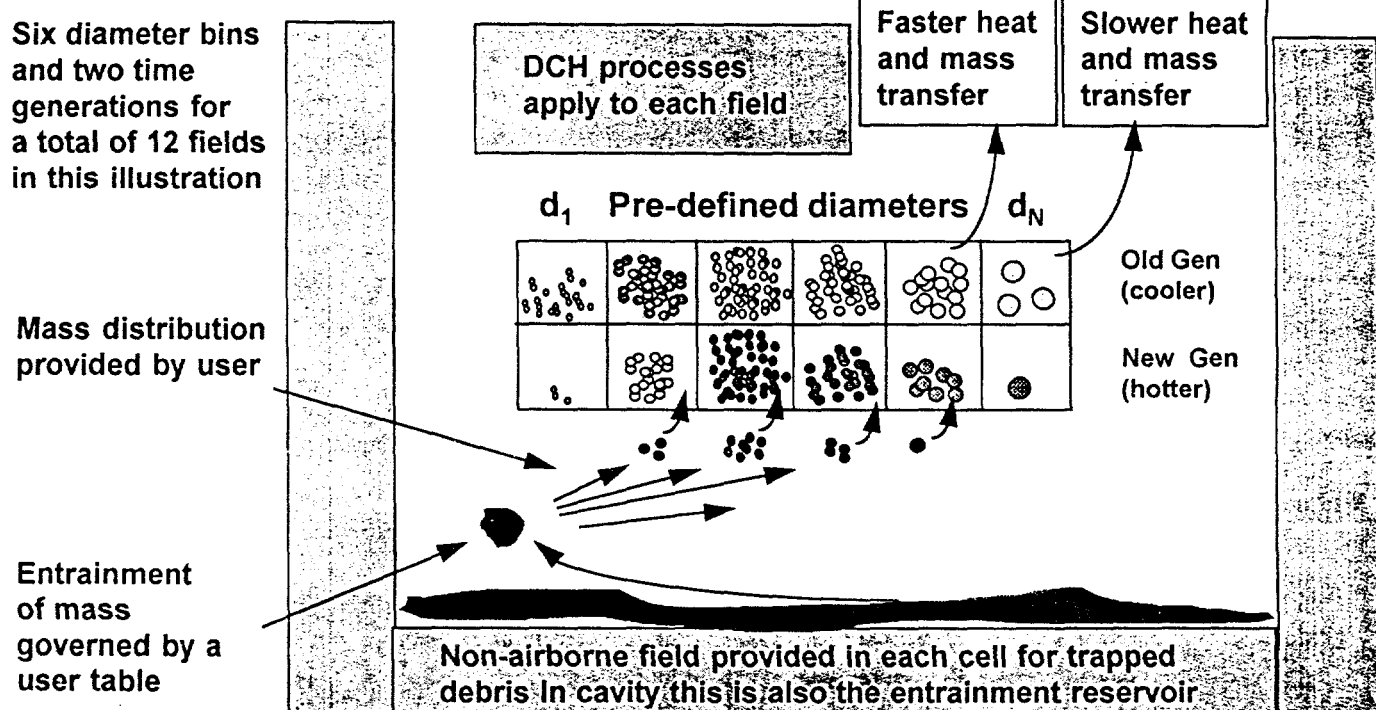


Figure 1. Illustration of the DCH Multifield Debris Representation in CONTAIN

In the multifield DCH modeling approach, the DCH models are evaluated multiple times, once for each field, using the composition, temperature, and other properties of that field. This feature is used to represent the distribution of metals and oxides in the dispersed melt, and to model a particular debris particle size distribution. Using this approach, more realism is possible than before this modeling capability was available. For example, smaller drops in the atmosphere will now react and cool off faster than larger drops if a particle size distribution is represented. The second capability is the provision for modeling multiple "generations" of debris fields. With this capability, the debris fields can be duplicated any number of times into time groups, called generations. This feature of the model can be used to keep freshly dispersed debris from being homogenized with previously dispersed debris. Experience with this capability to date has shown that time resolution often represents a relatively small effect.

The creation of new generations allow freshly dispersed debris to remain separated from previously dispersed debris. This is accomplished by maintaining a current generation of fields. The current generation is simply a group of fields that are populated by external debris sources. All fields in all generations are treated in the flow, trapping, chemistry, and heat transfer models. The non-airborne debris field is not treated in the flow model, and is used as the repository for trapped debris in the trapping model as described in Section 2.3.1. The multiple generation feature does not apply to the non-airborne field.

2.2 Debris Transport and Intercell Flow

The transport of debris in the containment is modeled as flow between control volumes using the control volume based inertial flow momentum equation shown below. In this model, debris and gas are assumed to flow together with a relative slip velocity from upstream cells to downstream cells through one or more interconnecting flow paths. The CONTAIN 1.1 Reference Manual [Was91] describes the control volume inertial flow model and its solution in detail; therefore, these details will not be repeated here. The unique features of the flow model in CONTAIN when debris is present are described.

The mass flow rate of gas and debris combined in flow path (i,j) is governed by the following equation:

$$\frac{dW_{ij}}{dt} = \left[\Delta P_{ij} - \frac{C_{FC} |W_{ij}| W_{ij}}{\rho_{fl} A_{ij}^2} \right] (A/L)_{ij} \quad (1)$$

where,

W_{ij}	=	mass flow rate of gas and debris through a flow path
ΔP_{ij}	=	pressure difference between cell i and j, including gravity head
C_{FC}	=	flow loss coefficient for flow path
A_{ij}	=	area of flow path
A/L_{ij}	=	area to length ratio of flow path
ρ_n	=	effective flow density including effects of debris and gas

This equation is similar to the one used prior to implementation of DCH in CONTAIN, but with two important changes made to the variable definitions. First, the mass flow rate, W_{ij} , is defined here as the total flow rate of gaseous materials and debris, including all dispersed debris fields, through the flow path. The division between gas and debris is discussed in the following sections. Second, the flow density, ρ_n , and the densities imbedded in the gravitational head term of ΔP_{ij} are the densities of gas plus some fraction of airborne debris in each debris field in the upstream cell. The discussion in the next section on the debris/gas slip model describes how the effective flow density is obtained from the slip factor and the upstream gas and debris densities.

Detailed descriptions of the other parameters in Equation (1) as given CONTAIN 1.1 Reference Manual [Was91] also apply to DCH calculations; therefore, they are not repeated here. Note that gravity head component embedded in the ΔP_{ij} term typically plays a small role in DCH calculations. DCH calculated results are also fairly insensitive to C_{FC} values selected for flowpaths in the containment.

2.2.1 Gas/Debris Slip Model.

The governing equations for the effective flow density, ρ_n , which governs the debris flow rate, are based on the assumption that gas and debris flow at different velocities that can be correlated by a slip factor, s . This slip factor is defined as the ratio of the velocity of the gas phase to the velocity of the debris phase as follows,

$$s_n = \frac{v_g}{v_{d,n}} \quad (2)$$

where s_n is the slip ratio for field n, v_g is the gas velocity, and $v_{d,n}$ is the velocity of debris in field n. The slip ratio must be constant over time but can be a function of location. That is, different slip ratios can be specified for flow out of different containment cells. Also, because the DCH model considers multiple debris fields and the diameter of drops in each field can be different, different gas/debris slip ratios may be specified for each field. Therefore, the velocity of debris in fields with differing slip factors will not be the same. The gas velocity will be greater than the debris velocity when slip is greater than one. Note that slip must be greater than or equal to one in the model. Therefore, the gas velocity will always be greater than or equal to the average flow velocity, and the debris velocity will always be less than or

equal to the average flow velocity. This model for gas/debris slip was adopted from the theory of slip in two phase fluid flow, where the ratio of the velocities of the steam and water phases are correlated with a similar slip factor [Elw62].

The sum of the gas and debris mass and momentum fluxes must add up to the total mass and momentum flux. Therefore, the following equations must hold true,

$$\rho_{fl} v_{fl} = \rho_{g,u} v_g + \sum_n^{N_{fields}} \rho_{d,u,n} v_{d,n} \quad (3)$$

and

$$\rho_{fl} v_{fl}^2 = \rho_{g,u} v_g^2 + \sum_n^{N_{fields}} \rho_{d,u,n} v_{d,n}^2 \quad (4)$$

where,

N_{fields}	=	number of debris fields
ρ_{fl}	=	effective flow density including effects of debris and gas
$\rho_{g,u}$	=	density of gas in upstream cell = mass of gas in the upstream cell divided by the cell volume
$\rho_{d,u,n}$	=	density of debris from field n in upstream cell = mass of debris in field n in the upstream cell divided by the cell volume
v_{fl}	=	effective velocity through flow path including effects of debris and gas
v_g	=	velocity of gas through flow path
$v_{d,n}$	=	velocity of debris in field n through flow path

The above equations can be solved for the effective flow density, ρ_{fl} , and the velocity relationships, v_g/v_{fl} , and $v_{d,n}/v_{fl}$.

$$\rho_{fl} = \zeta \left[\rho_{g,u} + \sum_{n=1}^{N_{fields}} \frac{\rho_{d,u,n}}{s_n} \right] \quad (5)$$

$$\frac{v_g}{v_{fl}} = \zeta \quad (6)$$

$$\frac{v_{d,n}}{v_{fl}} = \frac{\zeta}{s_n} \quad (7)$$

where,

$$\zeta = \frac{\left[\rho_{g,u} + \sum_{n=1}^{N_{fields}} \frac{\rho_{d,u,n}}{s_n} \right]}{\left[\rho_{g,u} + \sum_{n=1}^{N_{fields}} \frac{\rho_{d,u,n}}{s_n^2} \right]} \quad (8)$$

Note that when all slip ratios are one, the effective flow density, ρ_{fl} , reduces to the sum of the gas and debris densities, which is equivalent to the heavy-gas no slip assumption. Also, as s_n tends toward infinity, ρ_{fl} tends toward ρ_g as one would physically expect.

From the above equations one can write the gas flow rate, W_g , and the debris field mass flow rate for each field, $W_{d,n}$, in terms of the total combined debris and gas flow rate, W_{fl} ,

$$W_g = \frac{\zeta \rho_{g,u}}{\rho_{fl}} W_{fl} \quad (9)$$

$$W_{d,n} = \frac{\zeta \rho_{d,u,n}}{s_n \rho_{fl}} W_{fl} \quad (10)$$

where W_g is the mass flow rate of gas, and $W_{d,n}$ is the mass flow rate of debris in field n. Physically we know that the sum of W_g and $W_{d,n}$ over all fields must be equal to the total mass flow rate, W_{fl} . It can be shown from the above two equations that this is true.

Gas and debris mass and energy conservation equations are shown in the following sections based on the expressions derived above. Note that the variable ζ defined in Equation (8) turns out to be important for evaluating the effect of flow on the distribution of gases and debris. A different value of ζ is calculated for each cell depending upon the amount of debris in each field in the cell and the slip parameter in each field in the cell.

2.2.2 Gas Mass Conservation

The net gas flow term in the gas mass conservation equation for cell i is written in terms of the gas flow rate, $W_{g,ji}$ into cell i , and $W_{g,ij}$ out of cell i .

$$W_{\text{flow},i,k} = \sum_j \left[\frac{W_{g,ji} \theta_{ji} m_{g,j,k}}{N_{\text{GAS}}} \right] - \left[\sum_j W_{g,ij} \theta_{ij} \right] \left[\frac{m_{g,i,k}}{\sum_k m_{g,i,k}} \right] \quad (11)$$

where $W_{\text{flow},i,k}$ is the net change in mass of gas species k in cell i resulting from flow into and out of the cell, $W_{g,ij}$ is the flow rate of only gas (see Equation 9) from cell i to j , $m_{g,i,k}$ is the mass of gas species k in cell i , N_{gas} is the number of gas species in the cell, and θ_{ij} is a conditional function (1 if $W_{g,ij}$ is positive, 0 otherwise).

Note that the above expression does not contain terms that include debris. Rather than using this equation directly, it is more convenient to incorporate Equation 9 into this equation to express $W_{\text{flow},i,k}$ in terms of the total effective flow rate, W_{fl} . This is done because W_{fl} is determined directly from the flow equation (i.e., it is the flow rate actually calculated in the code), while $W_{g,ij}$ is not. For flow from cell i to cell j , W_{fl} is expressed as W_{ij} in the equations below to remain consistent with the nomenclature in forthcoming CONTAIN code documentation. Substituting Equations 5 through 9 into Equation 11, it can be shown that $W_{\text{flow},i,k}$ can be expressed as,

$$W_{\text{flow},i,k} = \sum_j \left[\frac{W_{ji} \theta_{ji} \zeta_j m_{g,j,k}}{m_{F,j}} \right] - \left[\sum_j W_{ij} \theta_{ij} \right] \left[\frac{\zeta_i m_{g,i,k}}{m_{F,i}} \right] \quad (12)$$

$$m_{F,i} = \zeta_i \left[\sum_k^{N_{GAS}} m_{g,i,k} + \sum_n^{N_{fields}} \sum_k^{N_{DCH}} \frac{m_{d,i,n,k}}{s_{i,n}} \right] \quad (13)$$

where,

ζ_i	calculated slip flow parameter for flow out of cell i (see Equation 8)
θ_{ij}	conditional function: 1 if W_{ij} is positive (flow into j), 0 otherwise
N_{GAS}	number of gas species in a cell
N_{DCH}	number of debris species in a cell
N_{fields}	number of debris fields
$\rho_{g,i}$	density of gas in cell i
$m_{g,i,k}$	mass of gas species k in cell i
$\rho_{d,i,n}$	density of debris in field n of cell i
$m_{d,i,n,k}$	mass of debris species k in field n of cell i
$s_{i,n}$	user specified slip parameter for field n for flow out of cell i

Note that no assumptions were made in going from Equation 11 to Equation 12; thus, they are functionally identical. Equation 11 shows the physical basis of the model more clearly than Equation 12, while the latter shows how the model is actually implemented in the code. Equation 12 also clearly shows that these terms of the mass conservation equation reduce to the proper limits in the absence of debris, where ζ will be one and $m_{F,i}$ and $m_{F,j}$ will be the total mass of gas species only.

The above flow terms are now combined with other source and sink terms to write the mass conservation equation for gases in a DCH calculation.

$$\begin{aligned} \frac{dm_{g,i,k}}{dt} = & \sum_{\substack{j=\text{all} \\ \text{paths}}} \left[\frac{\theta_{ji} W_{ji} \zeta_j m_{g,j,k}}{m_{F,j}} \right] \\ & - \left[\sum_{\substack{j=\text{all} \\ \text{paths}}} \theta_{ij} W_{ij} \right] \left[\frac{\zeta_i m_{g,i,k}}{m_{F,i}} \right] + \left[\frac{dm_{g,i,k}}{dt} \right]_{src} \\ & + \left[\frac{dm_{g,i,k}}{dt} \right]_{chem} + \left[\frac{dm_{g,i,k}}{dt} \right]_{non-DCH} \end{aligned} \quad (14)$$

where,

$m_{g,i,k}$	= mass of gas species k in the cell i
$[dm/dt]_{src}$	= external sources of gas species k into cell i

$[\text{dm}/\text{dt}]_{\text{chem}}$	=	gas mass changes resulting from DCH chemical reactions. This will only be non-zero for O_2 , H_2 , and H_2O species.
$[\text{dm}/\text{dt}]_{\text{non-DCH}}$	=	gas mass sources and sinks from non-DCH processes

The first two terms account for gas flow taking into consideration slip if debris is present as described above. The term with the "chem" subscript is for changes in oxygen, steam, and hydrogen resulting from DCH chemical reactions. The governing equations for these terms are given in Section 2.4. The last term in this equation represents all non-DCH processes that result in changes in gas masses. This term includes a significant number of processes and models that are not the subject of this report (such as condensation and gas releases from core-concrete interactions) and are therefore not described here. The governing equations for these processes are given in the CONTAIN 1.1 Reference Manual [Was91]. Equations for models added to the code since the publication of Was91 are being documented in a forthcoming new manual for version 1.2 of CONTAIN.

The gas energy, debris mass, and debris energy conservation equations are provided in the following sections in a form similar to Equation 14. The above derivation is also applicable to the flow terms in the forthcoming expressions and is therefore not repeated.

2.2.3 Gas Energy Conservation

The energy conservation equation for the atmosphere in a DCH calculation is,

$$\begin{aligned}
 \frac{dU_i}{dt} = & \sum_{\substack{j=\text{all} \\ \text{paths}}} \left[\frac{\theta_{ji} w_{ji} \zeta_j (U_j + P_j V_j)}{m_{F,j}} \right] \\
 & - \left[\sum_{\substack{j=\text{all} \\ \text{paths}}} \theta_{ij} w_{ij} \right] \left[\frac{\zeta_i (U_i + P_i V_i)}{m_{F,i}} \right] \\
 & + \left[\frac{dQ_{g,i}}{dt} \right]_{\text{chem}} + \left[\frac{dQ_i}{dt} \right]_{\text{non-DCH}} \\
 & + \sum_{n=1}^{N_{\text{fields}}} \left\{ \left[\frac{dQ_{d,i,n}}{dt} \right]_{\text{conv}} + \left[\frac{dQ_{d,i,n}}{dt} \right]_{\text{rad,g}} \right\}
 \end{aligned} \tag{15}$$

where,

U_i	= internal energy in cell i
P_i	= pressure in cell i
V_i	= volume of cell i
$[dQ/dt]_{\text{chem}}$	= chemical energy gain rate (or loss rate, if negative)
$[dQ/dt]_{\text{non-DCH}}$	= energy sources and sinks from non-DCH processes
$[dQ/dt]_{\text{conv}}$	= convective heat transfer from debris to gas
$[dQ/dt]_{\text{rad,g}}$	= radiative heat transfer from debris to gas

The first two terms represent the net rate of change in atmosphere energy resulting from flow. The third term represents the energy added to the atmosphere from DCH chemical reactions as described in Section 2.4. This includes the local recombination energy of DCH-generated hydrogen described in Section 2.5.1. It does not include the debris-gas chemical reaction energy as this energy is added to the debris field. The fourth term represents energy sources and sinks from non-DCH processes. The governing equations for most of these processes are given in Reference Was91. The fifth term represents convective heat transfer from debris to gas as described in Section 2.6.1. This term is equal in magnitude but opposite in sign to the counterpart term in the debris energy conservation equation given in Section 2.2.5. The last term represents radiation heat transfer from debris to gas as described in Section 2.6.2. Note that this does not include radiation from debris to structures, where the counterpart radiation term in the debris energy conservation equation does.

2.2.4 Debris Mass Conservation

The mass conservation equation for debris species k , in debris field n , and cell i is given by:

$$\begin{aligned}
 \frac{dm_{d,i,n,k}}{dt} = & \sum_{\substack{j=\text{all} \\ \text{paths}}} \left[\frac{w_{ji} \theta_{ji} \zeta_j m_{d,j,n,k}}{s_{j,n} m_{F,j}} \right] \\
 & - \left[\sum_{\substack{j=\text{all} \\ \text{paths}}} w_{ij} \theta_{ij} \right] \left[\frac{\zeta_i m_{d,i,n,k}}{s_{i,n} m_{F,i}} \right] \\
 & + f_{n,k} \left[\frac{dm_{d,i,k}}{dt} \right]_{\text{src}} - \lambda_{i,n} m_{d,i,n,k} + \left[\frac{dm_{d,i,n,k}}{dt} \right]_{\text{chem}}
 \end{aligned} \tag{16}$$

where,

$m_{d,i,n,k}$	mass of debris species k in field n in the cell i
$s_{i,n}$	slip factor for flow of debris in field n out of cell i
$f_{n,k}$	user-specified distribution factors for source of debris species k into field n
$\lambda_{i,n}$	debris trapping rates for field n in cell i (same for all species)
$[dm/dt]_{\text{src}}$	external sources of debris species k into cell i, or the entrainment of debris species k from the non-airborne field in cell i
$[dm/dt]_{\text{chem}}$	debris mass changes resulting from DCH chemical reactions.

The first two terms on the right hand side of this equation represents the inflow and outflow of debris species k in field n in cell i from and to other cells, respectively. External sources of debris species k into field n of cell i are represented by the third term. This corresponds to debris dispersal from the RPV that the user specifies as a mass source using the CONTAIN source table feature. The external source term also includes debris entrained from the non-airborne debris field that the user specifies using an ENTRAIN type debris source table. The non-airborne debris field is discussed further in Sections 2.3.1 and 2.7. The total source rate of debris given by the third term is the sum of any user specified entrainment source tables and user specified tables of debris directly into the atmosphere. The source rate term would also include sources calculated by entrainment models. These models are described in the letter report identified in the footnote on page one.

The $f_{n,k}$ factors are applied to the total source rate for each species to distribute the mass among the various fields. This two-dimensional parameter is specified by the user as an array in the DCH global input section following the FDISTR keyword. This is the parameter that governs how chemical species are initially distributed into fields when they enter the containment from the RPV. For example, suppose that two fields are being represented in a calculation. Dispersed metals could be separated from dispersed oxides by specifying:

CONTAIN DCH Models

Model Descriptions

$f_{1,k}=1$ and $f_{2,k}=0$ for $k=\text{metals}$
 $f_{1,k}=0$ and $f_{2,k}=1$ for $k=\text{oxides}$

A matrix of factors, $f_{n,k}$, is specified for the first generation of fields and all species represented in a DCH calculation to determine how sources are distributed among the fields. When the first generation fills to its capacity, a second generation of fields is generated. The first group of fields then ceases to be current and the second group becomes current. Becoming current means that $f_{n,k}$ is shifted down such that the values for the first generation of field types are all zero, and the values for the second generation of field types are set to the specified $f_{n,k}$ values. This process repeats as more generations fill and new ones are generated. The user has the flexibility to control whether or not the multiple generation feature of the DCH model will be used by specifying the number of field types and field generations. The rate at which new generations are created is governed by the user-specified maximum allowed mass in a generation of field types (see GRPLIM keyword in Section 3.3). By default only one generation of field types will be modeled. When metals oxidize, oxides normally stay in the same field as their parent metal. An option (see PRODSEP keyword) is provided to allow oxides to be separated from metal when one generation is used. The PRODSEP option can only be used when there is one generation; oxides are never separated from their parent metals when there is more than one generation.

The fourth term represents mass losses resulting from trapping. The governing equation for calculating the trapping rate, λ , and other details of the trapping model are described in Section 2.3. The last term in the debris mass conservation equation represents mass changes resulting from chemical reactions. For reactive metals this term will be negative. The model includes reactions for Zr, Fe, Cr, and Al metals. The term will be positive for the corresponding oxides of these reactive metals. The chemistry model and the governing equations for this term are described in Section 2.4.

2.2.5 Debris Energy Conservation Equations

The energy conservation equation for debris in field n in cell i is given by,

$$\begin{aligned}
 \frac{dH_{d,i,n}}{dt} = & \sum_{\substack{j=\text{all} \\ \text{paths}}} \left[\frac{\theta_{ji} w_{ji} \zeta_j H_{d,j,n}}{s_{j,n} m_{F,j}} \right] \\
 & - \left[\sum_{\substack{j=\text{all} \\ \text{paths}}} \theta_{ij} w_{ij} \right] \left[\frac{\zeta_i H_{d,i,n}}{s_{i,n} m_{F,i}} \right] \\
 & + \sum_{k=1}^{N_{dch}} \left\{ f_{n,k} \left[\frac{dm_{d,i,k}}{dt} \right]_{src} h_k(T_{src}) - \lambda_{i,n} m_{d,i,n,k} h_k(T_{i,n}) \right\} \\
 & + \left[\frac{dQ_{d,i,n}}{dt} \right]_{\text{chem}} - \left[\frac{dQ_{d,i,n}}{dt} \right]_{\text{conv}} - \left[\frac{dQ_{d,i,n}}{dt} \right]_{\text{rad}}
 \end{aligned} \tag{17}$$

where,

$H_{d,i,n}$	= total enthalpy of debris field n in cell i
$h_k(T)$	= specific enthalpy of debris material k at temperature T
$T_{i,n}$	= temperature of debris in field n in cell i
T_{src}	= temperature of the source debris

The first five terms of the energy conservation equation parallel the first five terms of the debris mass conservation equation. The first two terms on the right hand side represent the inflow and outflow of energy resulting from intercell flow. The third term corresponds to the addition of energy from debris sources, such as those to represent debris dispersal from the RPV or user specified entrainment in the cavity. T_{src} will be the temperature of the non-airborne debris field if the source is specified to represent an assumed entrainment rate (i.e., an ENTRAIN type source table). Otherwise, T_{src} will be the temperature specified in the source table. The energy associated with all of the material species that are introduced into the debris field are added together, since one energy conservation equation is used to represent all species in the field. A separate mass conservation equation is used for each species of a field. The fourth term is the energy losses associated with debris trapping, and the fifth term corresponds to the energy release from chemical reactions. The contributions from each species are added together for the trapping term. Trapping is discussed in detail in Section 2.3. The equations that govern the chemical energy term are provided in Section 2.4. Note that the chemical energy includes debris/gas chemical interactions. The energy resulting from the recombination of hydrogen produced in DCH with local oxygen is not included in this term, since this energy is added to the atmosphere.

The sixth term represents convective heat transfer between airborne debris and the cell atmosphere. The DCH convective heat transfer model is described in Section 2.6.1. The seventh and last term represents radiative heat transfer from airborne debris to the cell atmosphere and surrounding structures (including a coolant pool if one is present). The radiation model is described in Section 2.6.2. Convection and radiation are done on a field basis, not a species specific basis; therefore, there is no need to have a summation over species for these two terms. There is no term for decay heat because the time scale for DCH is assumed to be sufficiently short that decay heating of airborne particles can be neglected. Fission products are not allowed to be hosted to debris fields for this reason.

The specific enthalpy functions, $h_k(T)$, are represented by user supplied debris property tables given in the CONTAIN input deck. A set of standard debris property tables have been developed at Sandia National Laboratories³ for use in DCH calculations (see Appendix). These tables include material properties for the following species: Zr, Cr, Fe, Al, ZrO_2 , $CrO_{1.5}$, $AlO_{1.5}$, FeO, and UO_2 .

The total enthalpy of a debris field, $H_{d,i,n}$, must not only satisfy the above equation, but must also equal the sum of the enthalpies of the debris species in the field. This relationship, expressed below in equation form, is what defines the temperature of each debris field.

$$H_{d,i,n} = \sum_{k=1}^{N_{dch}} m_{d,i,n,k} h_k(T_{i,n}) \quad (18)$$

There is only one temperature that will satisfy the above equation. Obviously, this temperature must be solved for numerically.

2.2.6 Choked Flow

In the choked flow model an ideal gas choked flow expression is applied as an upper limit to the calculated intercell gas flow rate. This is done indirectly, since the code actually calculates first a total gas/debris flow rate and then determines the gas and debris flow rates from the specified slip factors. Given this approach, a maximum allowable total flow rate under choked flow conditions must be determined. Equation 9 provides the required relationship between the gas flow rate and the total flow rate, since this condition must also apply when the flow is choked. Therefore, the total flow rate limit under critical flow conditions must be given by,

³ D. C. Williams and M. Pilch, personal communication

$$\begin{aligned}
 W_{ij,c} &= W_{ij,g,c} \left(\frac{\rho_{fl}}{\zeta \rho_g} \right) \\
 &= (\theta_{ij} - \theta_{ji}) A_{ij} v_{ij} [\gamma_u P_u \rho_u \eta_u]^{1/2} \left(\frac{\rho_{fl}}{\zeta \rho_g} \right)
 \end{aligned} \tag{19}$$

where $W_{ij,c}$ is the total critical flow rate, $W_{ij,g,c}$ is the critical gas flow rate, A_{ij} is the flow area, v_{ij} is the vena contracta factor, γ_u is the ratio of specific heat (c_p/c_v) for gas in the upstream cell, P_u is the pressure in the upstream cell, ρ_u is the gas density in the upstream cell, and η_u is a dimensionless parameter given by,

$$\eta_u = \left[\frac{2}{1 + \gamma_u} \right]^{\frac{\gamma_u + 1}{\gamma_u - 1}} \tag{20}$$

Note that only gas is considered in the heat capacity ratio. The vena contracta parameter is specified by the user and is used in place of the flow coefficient under choked conditions. This parameter is generally less than unity, and is defined as the ratio of the minimum area intersected by the flow streamlines to the geometric cross-sectional area of the flow path [Lam45].

The last term in the critical flow rate equation is present to convert the critical gas flow rate to an effective maximum allowable total flow rate. By using this expression to calculate the total maximum flow rate, the gas flow rate will be limited to the ideal gas choked flow rate, and the debris flow rate will meet the specified gas/debris slip velocity criterion. At any time, the total flow rate, W_{ij} , is given by the minimum of W_{ij} from the conservation equations presented earlier and $W_{ij,c}$ as shown below.

$$|W_{ij}| = \min(|W_{ij}|, |W_{ij,c}|) \tag{21}$$

2.2.7 Numerical Considerations of the Debris Intercell Flow Model.

From a numerical standpoint, it is important to understand that the code correctly solves the debris mass conservation equations, the gas mass conservation equations, the debris energy conservation equations, the gas energy conservation equations, and the inertial flow equation for the debris and gas flow rates simultaneously. This solution also includes the evaluation of cell pressures, cell temperatures, and coolant pool conditions. It is also important to understand that the debris to gas heat transfer and chemistry are explicitly coupled to these flow equations. This explicit coupling is what causes small time steps to be required in performing DCH calculations with CONTAIN. The last two terms of the debris mass conservation equation are also calculated outside of the implicit flow solver. The explicitly

coupled rates are time step averaged values evaluated as the mass change from the process divided by the current calculational time step.

There are $N_{DCH} \times N_{fields}$ (one for each debris material in each debris field and generation) mass conservation equations and N_{fields} energy conservation equations that are solved by the code for each flow path connected to a given cell. This includes fields in the current generation and all previous generations. These same equations are then solved for all of the other cells and the flow paths that are connected to them. It should be obvious from the above discussion why DCH calculation can be computationally intensive relative to other CONTAIN calculations.

2.3 DCH Trapping Model

The process of debris removal as a result of interaction with containment structures and/or gravitational fallout is referred to as trapping. This process is still the subject of considerable uncertainty, and plant and experiment analyses have shown that trapping can have an important effect on results. Therefore, the CONTAIN model includes both a mechanistic approach to trapping as well as flexible input for performing sensitivity calculations.

In principle, the CONTAIN DCH trapping model is a simple one, where debris trapping in a given control volume is governed by a first order linear rate equation. As implemented, however, the model has several complexities, where the rate in this equation is calculated within the code according to conditions in the cell atmosphere, attributes of the debris field being de-entrained, and the debris and gas inflow rates. In addition, the trapping rate is recalculated every time step, so that debris trapping reflects changes in the particle field, atmospheric conditions, and inflow rates as the DCH event progresses. The first subsection below describes the trapping rate equation and its solution. The remaining subsections describe the models and options available in CONTAIN for calculating the trapping rates used in this model.

2.3.1 Rate Equations for Trapping

The debris trapping process is governed by a first order linear rate equation for the time rate of change of airborne debris mass in a field.

$$\frac{dm_{d,i,n,k}}{dt} \Big|_{trap} = -\lambda_{i,n} m_{d,i,n,k} \quad (22)$$

where,

$$\lambda_{i,n} = \text{Trapping rate for field } n \text{ in cell } i$$

Notice that each particle field in each cell is governed by its own trapping rate. Therefore, these equations are solved many times throughout a calculation for each particle field, n , and for each cell, i . The model keeps track of the mass of trapped debris by species.

The trapping rate for the different species in a given field and cell are assumed to be the same. The trapping rate, $\lambda_{i,n}$, is also assumed to be constant over a calculational time step. Therefore, the trapping terms in the DCH mass and energy conservation equations in Section 2.2.2 are linear and can be represented by a time-averaged removal rate that depends on the initial mass of airborne debris for each material in a given field and cell. If the time step is given by Δt_c , then an average trapping rate for material k in field n in cell i over the time step is given by,

$$\left[\frac{dm_{d,i,n,k}}{dt} \right]_{\text{trap}} = -m_{d,i,n,k} \times \frac{[1 - e^{-\lambda_{i,n} \Delta t_c}]}{\Delta t_c} \quad (23)$$

The following subsections describe the equations used to calculate the trapping rate, $\lambda_{i,n}$.

Special provisions are made in the trapping model for sending some fraction of the trapped debris material to the intermediate material layer in the lower cell. In the present model, this fraction is specified by the user. The addition of trapped debris to the lower cell is governed by:

$$\frac{dm_{i,LC,k}}{dt} = -f_{LC} \sum_{n=1}^{N_{\text{fields}}} \left[\frac{dm_{d,i,n,k}}{dt} \right]_{\text{trap}} \quad (24)$$

where,

$m_{i,LC,k}$ = mass of material k in the uppermost intermediate layer of the cavity in cell i

f_{LC} = user-supplied fraction of trapped debris to deposit into the uppermost intermediate layer of the cavity of cell i. This is specified using the COOLFRAC keyword in the DCH-CELL input block.

The user-supplied fraction, f_{LC} , governs the fraction of the trapped debris that goes into the uppermost intermediate layer of the lower cell. The remaining fraction, $(1-f_{LC})$, of the trapped debris will be placed in the non-airborne debris field. Note that this option is available in any cell, but is most useful in the cavity cell. The CONTAIN lower cell layer system is described in the CONTAIN 1.1 User's Manual [Mur89]. If there is no intermediate lower cell layer, or if there is no lower cell defined at all, then all trapped debris is placed in the non-airborne debris field regardless of the f_{LC} value. Trapped debris cannot be passed into the CORCON layer system if CORCON is active. Therefore, f_{LC} will be ignored if CORCON is active and all trapped debris will be placed in the non-airborne debris field. This is not considered an important limitation because DCH calculations are typically performed only to predict the peak short term containment load. The f_{LC} parameter is used if CORCON is defined but has not yet been activated; therefore, DCH can be used during the early phase of the accident and CORCON used in a restart or in a new calculation using the trapping results from the DCH run.

In addition to optionally sending trapped debris to the lower cell, the DCH model also stores trapped debris in a special field, called the "non-airborne" debris field. This field also can be used to hold debris in the cavity that has not yet been entrained by the blowdown gas. Debris can be added to the non-airborne field by trapping and as a result of user specified source tables. Typically, user specified sources to the non-airborne field are used to represent the discharge of debris from the RPV into the cavity. Debris can be removed from the non-airborne field also by user specified source tables. User specified tables that remove debris from the non-airborne field are used to represent entrainment. Therefore the removed debris is added to the atmosphere fields as discussed in Section 2.2.4 in connection with the third term in Equation (16)). Such user sources are typically only specified in the cavity cell. The mass of debris in the non-airborne debris field is governed by the following equation,

$$\frac{dm_{d,i,nad,k}}{dt} = - \sum_{n=1}^{N_{fields}} \left[\frac{dm_{d,i,n,k}}{dt} \right]_{trap} + \left[\frac{dm_{d,i,k}}{dt} \right]_{rpv,s} - \left[\frac{dm_{d,i,k}}{dt} \right]_{ent,s} \quad (25)$$

where

$m_{d,i,nad,k}$	=	mass of debris in cell "i" in the non-airborne field
$[dm/dt]_{rpv,s}$	=	discharge source rate from RPV into non-airborne field
$[dm/dt]_{ent,s}$	=	entrainment source rate out of non-airborne field

This equation does not include chemical interaction terms in the non-airborne debris field. These terms would be identical to those described in Section 2.4 for the airborne fields. The first term on the right hand side represents trapping from all airborne fields. The second term represents user sources into the non-airborne field using the TRAPBIN type source tables. The third term represents user specified entrainment rate out of the non-airborne field using the ENTRAIN type source tables. The DCH specific TRAPBIN and ENTRAIN type source tables are described in Section 3.5.

The trapping rate, λ , is either provided by the user or calculated by the code based on cell conditions, particle field attributes, and inflow gas and debris velocities. Four options for determining λ are provided. These options only differ in the way in which the trapping rate, λ , is determined. That is, all models use the first order rate Equation (22), and this equation is always solved in the manner described above to represent de-entrainment. The four trapping options included in the CONTAIN DCH model are:

USER	User-specified trapping rate
GFT	Gravitational fall time
TFI	Time to first impact and fall
TOF/KU	Time of flight/Kutateladze criterion

The USER option is not actually a model, since it is strictly user driven, and does not depend on field attributes, cell conditions, or inflow gas or debris conditions. The GFT model depends on cell conditions and field attributes, but is not dependent upon gas or debris inflow rates. The last two options are dependent upon cell conditions, debris field attributes, and inflow gas and debris conditions. The TOF/KU model is believed to be the most realistic of all the options and is recommended for most situations. There are some situations when use of one of the other options would be more desirable than TOF/KU. For example, one might want to use the USER option to disable trapping in a study to calculate conservative DCH loads. The equations used to calculate λ and the trapping mechanism flags are described in the following sections. The first section below, however, discusses how velocities are calculated that are used in the trapping and heat transfer models.

2.3.2 Average Velocities

The relative velocity between gas and debris, v_{re} , in the GFT and USER trapping models is calculated as the maximum of the gravitational fall velocity and the difference between the average gas velocity and the average debris velocity through the cell. The gravitational fall

velocity, v_{gft} , is defined in Section 2.3.4. The average gas and debris velocities through a cell are calculated in a similar manner as the structure forced convection velocities are calculated, but with one key difference: the average velocities calculated for use in the DCH models do not use the structure-specific flow-path coefficients. The following equations describe the calculation of the average velocities used in the DCH trapping model and the DCH heat transfer model. Note that these velocities are used in all four (USER, GFT, TFI and TOF/KU) of the trapping models, and in the convective heat transfer model.

The average debris velocity for a given cell i and field n , considering all flow paths, is calculated from the debris outflow rates and the debris inflow rates as follows,

$$v_{d,in} = \frac{1}{A_{hyd}} \sum_j \frac{W_{d,n,ji} \theta_{ji}}{\rho_{d,j,n} (P_i/P_j)} \quad (26)$$

$$v_{d,out} = \frac{1}{A_{hyd}} \sum_j \frac{W_{d,n,ij} \theta_{ij}}{\rho_{d,i,n}} \quad (27)$$

$$v_{d,avg} = \max \left[v_{gft}, \left(\frac{v_{d,in} + v_{d,out}}{2} \right) \right] \quad (28)$$

where $W_{d,n,ij}$ is a field and flow path specific expression of the debris mass flux given by Equation 10. The cell hydraulic area, A_{hyd} , is equal to the volume of the cell to the two-thirds power, or the hydraulic area specified for the second structure in the cell if one is provided by the user. Note that the "i" and the "n" for cell i and field n are not included in the symbol names of $v_{d,in}$, $v_{d,out}$, and $v_{d,avg}$ for notational convenience; however, these values are specific to a cell and a field. It is also worth noting that the average debris velocity is not allowed to be smaller than the gravitational fall velocity.

The average gas velocity through a cell, $v_{g,avg}$, is calculated in a similar manner, but the gas mass fluxes and gas densities are used in place of the debris values as shown below. Also, the gas velocity is calculated by assuming isothermal flow and assuming that all incoming gas flow streams mix with each other before they mix with the cell inventory. Again, this is similar to the structure forced convection velocity model. Note that there is only one average gas velocity through the cell which is used to calculate v_{re} for each debris field.

$$\bar{T}_{in} = \frac{\sum_j w_{g,ji} \theta_{ji} T_{g,j} c_{p,j}}{\sum_j w_{g,ji} \theta_{ji} c_{p,j}} \quad (29)$$

$$v_{g,in} = \frac{1}{A_{hyd}} \sum_j \frac{w_{g,ji} \theta_{ji} R \bar{T}_{in}}{MW_j P_i} \quad (30)$$

$$v_{g,out} = \frac{1}{A_{hyd}} \sum_j \frac{w_{g,ij} \theta_{ij}}{\rho_{g,i}} \quad (31)$$

$$v_{g,avg} = \frac{v_{g,in} + v_{g,out}}{2} \quad (32)$$

where $T_{g,j}$ is the temperature, $c_{p,j}$ is the gas heat capacity, and MW_j is the gas molecular weight in the upstream cell, j . R is the universal gas constant. The hydraulic area in the above equations for the gases will be the value specified for the second structure following the HYDAREA keyword in the BCINNER block. If this value is not specified, the hydraulic area will be volume of the cell to the two-thirds power.

In the USER and GFT trapping options, if slip is greater than one, v_{re} is calculated as follows,

$$v_{re} = \max(v_{gft}, |v_{g,avg} - v_{d,avg}|) \quad (33)$$

If slip = 1 in the upstream cell of the dominant flow path, the model uses the following approximate approach similar to the approach used before the slip was added to the model.

$$v_{re} = \max(v_{gft}, v_{d,avg}) \quad (34)$$

Note that the dominant flow path is by default calculated by the code as the flow path with the most debris material flowing through it. It can also be specified by the user. The alternate treatment is provided when slip is equal to one, because the average gas and debris velocities through the cell may be unrealistically close to each other (they may not be exactly equal because of the isothermal flow and mixing assumption applied in calculating the gas velocity). If the newer expression is desired even when slip is essentially 1, then slip can be set to near 1 (slightly larger), but not exactly 1. If slip is greater than 1, the new expression is always used. In most instances when slip is close to one, the gravitational fall velocity will

exceed the difference between the gas and debris velocities, and the two treatments will be equivalent.

The $v_{d,\text{avg}}$ and $v_{g,\text{avg}}$ averages are also used in various places in the TFI and TOF/KU trapping models as described in the following sections.

2.3.3 USER Trapping Model

The simplest and most parametric model is the USER model. In this model, the user simply specifies a trapping rate, λ_i , for each cell. The user-specified trapping rate must be the same for each particle field in a cell. That is, $\lambda_{i,n} = \lambda_i$ for all particle fields, n. This is not true for the other trapping models, since in these models, the rates depend upon the size and composition of the particles in the field.

The user-specified trapping rate is normally a constant; however, time-varying rates can be specified through the use of user tables. To specify a constant trapping rate in a cell the value desired is given in the DCH-CELL block as explained in Section 3.4. User trapping values specified in the global DHEAT block are used as default constant trapping rates for all cells. To specify a time-varying trapping rate, the VAR-PARM keyword is used in the DCH-CELL input block. The name of the VAR-Y variable in the VAR-PARM block must be TRAPRATE to specify the trapping rate as the dependent variable in the table.

2.3.4 GFT Trapping Model

In this model, the trapping rate is taken to be controlled by the gravitational fall rate of a sphere in the cell atmosphere.

$$\lambda_{i,n} = \frac{v_{gft,i,n}}{L_{gft,i}} \quad (35)$$

where,

$v_{gft,i,n}$ = terminal fall velocity for debris particles in field n located in cell i. In the interest of notational convenience, this velocity is simply referred to as v_{gft} hereafter, but the reader should remember that v_{gft} for each field and in each cell is unique.

$L_{gft,i}$ = characteristic gravitational fall height for debris particles in cell i. Again, the i subscript will be dropped for notational convenience, but the reader should remember that L_{gft} for each cell can be unique.

The terminal fall velocity, v_{gft} , is computed using the following drag correlation for spheres:

$$v_{gft} = \left[\frac{-C_1 + \sqrt{C_1^2 + C_1 \cdot C_2}}{2} \right]^2 \left(\frac{\mu_g}{\rho_g d} \right) \quad (36)$$

$$C_1 = 9.06 ; \quad C_2 = \frac{1}{3} \sqrt{\left(\frac{gd}{2} \right) \left(\frac{\rho_d d}{\mu_g} \right) \left(\frac{\rho_g d}{\mu_g} \right)}$$

where,

g	=	the acceleration of gravity
μ_g	=	gas viscosity
ρ_g	=	gas density
ρ_d	=	debris material density
d	=	particle diameter

Note that v_{gft} is dependent upon both cell i and field n , through the gas density, gas viscosity, debris density, and particle diameter. The above correlation assumes that the particles are spheres, the atmosphere is stagnant, and that the particles do not physically interact with each other as they fall.

The characteristic gravitational fall height, L_{gft} , is by default the height of the cell. This value can be specified in the geometry input of the cell, or, if omitted, is calculated to be the cube root of the cell volume (cell volume is a required CONTAIN input). A DCH specific L_{gft} value can also be specified independent of the cell height from the geometry input. This is done using the LENGFT keyword in the DCH-CELL input block.

An important aspect of the CONTAIN trapping treatment is that the GFT trapping rate is computed and used in the TOF/KU model as described in Section 2.3.6. This is based on the assumption that particles cannot de-entrain more slowly than they would fall to the floor by gravity. Details of how this is applied is provided in the following two sections. The GFT rate is not used as a bound if the USER trapping model is selected. The GFT trapping rate is also used in the TFI model to calculate the total debris flight time. The gravitational fall time, t_{gft} , is given by,

$$t_{gft} = \frac{L_{gft}}{v_{gft}} \quad (37)$$

2.3.5 TFI Trapping Model.

The TFI model is based on the assumption that debris will not stick on structures, but will strike only one structure and then rebound and fall to the floor by gravity. This model is provided primarily to facilitate performing sensitivity calculations. Production calculations and most experimental analyses should be performed with the TOF/KU model described in the following section. The TFI and TOF/KU models both use the mass flow rates of gas and debris through the dominant flow path into a cell, and the average flow rate into a cell. By default, the code automatically determines the dominant flow path into a cell. The dominant flow path is defined as the flow path with the most debris material flowing through it. The user can optionally specify the dominant flow path as a regular flow path or an engineered vent using the FROMCELL or FROMVENT keywords. The dominant flow path may not be a suppression pool vent, since debris is not allowed to flow through that flow path. One advantage of using engineered vents is that parallel flow paths may be represented. For any period of time when debris and gas flow is not positive through the identified flow path, the GFT model will be used. Unless there is a good reason to do otherwise, such as performing code testing, the user should let the code automatically determine the dominant flow path.

The CONTAIN flow model calculates the mass flow rate of gas and debris through the flow paths in the containment as described in Section 2.3.2. If slip between gas and debris is being modeled for flow from the upstream cell, then the gas and debris velocities are distinct and their individual values will be used to determine flight times and Ku numbers. However, if slip between gas and debris is not modeled (slip=1), the average flow velocity for gas and debris is used for both. Both cases are included in the descriptions below.

The debris time of flight to the first structure, $t_{s,1}$, is calculated by assuming the debris velocity linearly decreases from the inlet debris velocity, $v_{d,n}$, to the debris velocity at first impact, $v_{d,1}$,

$$t_{s,1} = \frac{L_1}{v_{d,n} - v_{d,1}} \ln\left(\frac{v_{d,n}}{v_{d,1}}\right) \quad (38)$$

where L_1 is the distance to the first structure. This distance must be provided by the user. The debris velocity at first impact is assumed to be equal to the gas velocity at first impact, $v_{g,1}$, if that velocity is slower than the debris inlet velocity.

$$v_{d,1} = \min(v_{d,n}, v_{g,1}) \quad (39)$$

Qualitatively, this is based on the fact that debris/gas drag is assumed to slow down the gas until they both decrease together. The gas velocity at first impact is also used in the

TOF/KU model to evaluate the Kutateladze number; therefore, its governing equations are provided in the following section.

If $v_{d,1}$ is equal to $v_{d,n}$, then the debris flight time to the first structure is given by,

$$t_{s,1} = \frac{L_1}{v_{d,n}} \quad (40)$$

which is the limit of Equation 29 as $v_{d,1}$ approaches $v_{d,n}$. The average debris velocity to the first impact, $v_{d1,avg}$, is given by,

$$v_{d1,avg} = \frac{L_1}{t_{s,1}} \quad (41)$$

The TFI trapping rate is given by the inverse of the sum of the flight time to the first structure and the gravitational fall time.

$$\lambda = \frac{1}{t_{s,1} + t_{gft}} \quad (42)$$

The trapping rate given by the above equations is only calculated if flow through the identified flow path is into the cell. If this is not the case, then the trapping rate will be calculated using the GFT model.

The relative velocity between gas and debris, v_{re} , for heat and mass transfer is given by,

$$v_{re} = \max(v_{gft}, |v_{g1,avg} - v_{d1,avg}|) \quad (43)$$

where $v_{g1,avg}$ is the average gas velocity to the first structure, which is defined in the following section under Case 1 of the TOF/KU model. The reader is referred to that section for a description of the governing equations for this velocity. If slip is equal to 1 in all upstream cells then, $v_{g1,avg}$ is dropped in the above equation.

2.3.6 TOF/KU Trapping Model

Like the TFI model, this model calculates the trapping rate at each calculational cycle according to current conditions of the atmosphere, attributes of the particle field (size, composition, etc), and gas and debris inflow conditions. As the name of the model implies, the TOF/KU model uses a Kutateladze entrainment criterion to determine whether particle re-

CONTAIN DCH Models

Model Descriptions

entrainment occurs after debris impacts structures. If re-entrainment is not indicated, then the debris is assumed to stick and the trapping rate is set to the inverse of the time of flight to the structure. Two de-entrainment criteria are considered which are conceptually related to physical impacts of debris on structures. The first criterion refers to debris impaction upon the first structure debris is likely to encounter as it flows into a cell. The second refers to subsequent structures that debris will impact as a result of average flow through the cell. If the Kutateladze correlation indicates debris re-entrainment for both conditions, then the trapping rate will not be based upon time of flight to structure impacts. Instead the trapping rate will be set to allow most of the debris to flow out of the cell. An option is provided to allow debris to trap at a rate characteristic of gravitational settling under this condition.

The remainder of this section describes the specific equations in the DCH model that implement this trapping strategy. First, however, it is important to understand that the flight of particles in the cell is not actually "tracked" in the TOF/KU model. Without major architectural changes, this would be impossible for a control volume code like CONTAIN to accomplish. Instead, the model relies upon estimates of particle and gas velocities and flight distances to evaluate the Kutateladze numbers for the first two phases. The magnitude of these numbers compared to Kutateladze cutoff numbers for entrainment dictate which calculated debris transport time estimate to use in the evaluation of the trapping rate at that moment in time. This trapping rate applies to all debris that is airborne at that moment in time. If the rate of change in the calculated trapping rate is slow, then this approach should be reasonable.

The Kutateladze number is a dimensionless number given by,

$$Ku \equiv \frac{\rho_g v_g^2}{\sqrt{(\rho_{d,mat} - \rho_g) g \sigma}} \quad (44)$$

where $\rho_{d,mat}$ is the material density of the debris, not the airborne density of debris in the cell. Physically, Ku represents the ratio of the kinetic force of an entraining fluid (with density ρ_g , and velocity v_g) to the geometric mean of gravitational and surface tension forces of the denser fluid being entrained (with density ρ_d). In the context of the TOF/KU debris trapping model, the entraining fluid is the in-flowing debris/gas jet (that tends to re-entrain any trapped debris on structures back into the jet), and the denser fluid is the molten debris in the cell (whose surface tension favors "sticking" the debris to a structure as a film). At some fluid velocity, the kinetic forces will sufficiently overcome the surface tension forces to re-entrain the debris from the surface thereby avoiding trapping on that structure. Below this velocity, debris in the cell is assumed to de-entrain (or trap) at a rate that corresponds to the time of flight to the surface in question. The model uses a default Ku cutoff value of 10 (dimensionless) for the first two phases (or impacts) considered in the TOF/KU model, but the

user may override this value for the first and subsequent impacts. The default is based on droplet entrainment in vertical tubes from the work in Reference Brg81.

The reader should also be aware that the equations presented below are applied to each debris field individually, even though this is not explicitly indicated by the simplified notation used below. Therefore, the trapping rate of one field will typically be different than other fields with different sizes and debris densities.

2.3.6.1 TOF/KU Case 1: Trapping On First Impact. Gases flowing into a cell are assumed to entrain gases in the cell using the Ricou Spalding [Ric61] entrainment correlation. With this correlation, the density of the gas jet impinging the first structure used in evaluating the Ku number is given by,

$$\rho_{g,1} = \frac{\rho_0 \rho_a \xi}{[\rho_a + (\xi-1) \rho_0]} \quad (45)$$

where,

$$\xi = \max \left(\frac{L_1}{x_c}, 1.0 \right) \quad (46)$$

and L_1 is the user-specified distance to the first structure as previously noted, and x_c is a critical cutoff distance below which no entrainment occurs. This distance is given by,

$$\begin{aligned} x_c &= \frac{d_0}{\alpha} \\ d_0 &= \sqrt{\frac{4 A_0}{\pi}} \\ \alpha &= \alpha_0 \sqrt{\frac{\rho_{g,i}}{\rho_0}} \\ \rho_0 &= \rho_{g,u} \left(\frac{P_i}{P_u} \right) \end{aligned} \quad (47)$$

where,

α_0	= user-definable jet expansion coefficient whose default value is 0.32
α	= density corrected jet expansion coefficient
A_0	= Area of the flow path opening
d_0	= hydraulic diameter of flow path opening
$\rho_{g,i}$	= density of gas in the cell
ρ_o	= pressure corrected density of gas from the upstream cell
P_i	= pressure in cell i
P_u	= pressure in the upstream cell

By default the flow path area, A_0 , is the area of the dominant flow path as defined in the FLOWS input. This area can be user-specified using the ADFLOW keyword; however, if this is done the user should also specify the dominant flow path explicitly using either FROMCELL or FROMVENT keywords. This is recommended because the flow path area will not change if ADFLOW is specified, while the dominant flow path may change if it is not also explicitly specified. Specifying the dominant flow path explicitly will prevent an inconsistent area from being used. There may be valid reasons for not following this recommendation; therefore, it is not enforced by the code.

The velocity of gas after it enters a cell is assumed to be constant at $v_{g,in}$ until it travels the cutoff distance x_c . Beyond the cutoff distance it is assumed that the velocity declines linearly as gases are entrained into the flow stream. However, if the estimated forced convection velocity from the flow solver for the first structure in the cell exceeds the jet expansion velocity, the larger forced convection velocity will be used. The gas velocity at the first impact, $v_{g,1}$, is therefore given by,

$$v_{g,1} = \max \left[v_1, v_{g,in} \min \left(1, \frac{x_c}{L_1} \right) \right] \quad (48)$$

where v_1 is the structure convective velocity for the inner face of the first structure in the cell. This velocity is calculated in the structure forced convection model based on the results of the flow model, and can be controlled by specifying a structure-specific hydraulic area and weighting coefficients in the STRUC input block. None of the parameters in the DCH-CELL block have an effect on v_1 . Because of this scheme, it is recommended that at least two structures be defined in subcompartments so that a forced convection velocity will be calculated in the structure heat transfer module and stored in v_1 (and v_2 used under Case 2 in the following section) for use in the TOF/KU model. If no structures are defined, then the model will use the average gas velocity through the cell, $v_{g,avg}$, in place of v_1 in the above expressions.

CONTAIN DCH Models

Model Descriptions

The Kutateladze criterion can be evaluated using one of two options. In the default option, only the gas momentum is included in the numerator. If the RHODG=MIX option is invoked then debris momentum will be included in the numerator of the Ku number.

Under the default RHODG option, the Ku number for the first impact, $Ku_{s,1}$, is given by,

$$Ku_{s,1} = \frac{\rho_{g,1} v_{g,1}^2}{\sqrt{(\rho_{d,mat} - \rho_{g,1}) g \sigma}} \quad (49)$$

If the RHODG=MIX option is specified, then $Ku_{s,1}$ includes the momentum of the debris,

$$Ku_{s,1} = \frac{\rho_{g,1} v_{g,1}^2 + \rho_{d,u} v_{d,1}^2}{\sqrt{(\rho_{d,mat} - \rho_{g,1} - \rho_{d,u}) g \sigma}} \quad (50)$$

where the debris velocity at first impact, $v_{d,1}$, is taken to be the minimum of the debris inlet velocity and the gas velocity at first impact as noted in the previous section on the TFI model (see Eq. 30). In the above equation $\rho_{d,u}$ is calculated as $(\rho_{fl} - \rho_{g,u}) * P_i/P_u$.

De-entrainment on the first impact is assumed to occur if $Ku_{s,1}$ is less than the $Ku_{T,1}$ cutoff value. When $Ku_{s,1} \leq Ku_{T,1}$, the trapping rate, λ , is given by,

$$\lambda = \frac{1}{\min(t_{s,1}, t_{gft})} \quad (51)$$

where $t_{s,1}$ is the debris flight time to the first structure defined in the previous section on the TFI model. The average gas velocity from the inlet to the first impact is calculated by integrating from $v_{g,in}$ to $v_{g,1}$ over the distance x_c to L_1 to give,

$$v_{g1,avg} = \frac{v_{g,in} L_1}{x_c + \frac{(L_1^2 - x_c^2)}{2x_c}} \quad \text{for } x_c < L_1 \quad (52)$$

If x_c is greater than L_1 then $v_{g1,avg}$ will be equal to $v_{g,in}$. If slip is greater than 1 in all upstream cells, the relative velocity between gas and debris for heat transfer and chemical reactions, v_{re} , is given by,

$$V_{re} = \max(V_{gft}, |V_{g1,avg} - V_{d1,avg}|) \quad (53)$$

If slip between gas and debris is exactly equal to 1, then the model only considers the debris velocity to the first structure as was done for the GFT and TFI models,

$$V_{re} = \max(V_{gft}, V_{d1,avg}) \quad (54)$$

The flight time and average velocity to the first structure in Case 1 of the TOF/KU model are the same as they are for the TFI trapping model. Note, however, that the TOF/KU first-structure trapping rate differs from the TFI rate. The TFI model takes the sum of the gravitational fall time and the first impact flight time as the time of flight, while the TOF/KU model takes the shorter of the two as the time of flight. The rates are different because if the debris reaches the first structure under case a of the TOF/KU model, it is assumed to be trapped there. The main input parameter that affects this case of the TOF/KU model is the first trapping length, L_1 . If a direct line of travel from a primary entrance flow path to a structure can be clearly identified, then this distance should be given as L_1 . Otherwise, it is recommended that L_1 be set equal to 6 times the cell volume divided by the surface area of all surfaces in the cell.

An alternate trapping behavior corresponding to only the time of flight to the first structure can be obtained by intentionally specifying an artificially large $Ku_{T,1}$ value. If this is done, the Ku criterion for re-entrainment will never be met and debris will always stick on the first impact. This technique may be useful for performing sensitivity studies. In most predictive calculations, however, the default Ku cutoff values should be used. With the default Ku cutoff value, sticking on the first impact will only be indicated if conditions warrant.

If the Ku criterion for re-entrainment on the first impact is met, sticking on the first impact is not assumed and subsequent impacts on non-horizontal surfaces will be considered as described below.

2.3.6.2 TOF/KU Case 2: Trapping On Structures Beyond The First Impact. The velocity used for evaluating the Ku number for impacts after the first is the structure convective velocity for the second structure, v_2 . Thus, $v_{g,2}$ is equal to v_2 in the expressions below. This velocity is the convective velocity for the inner face of the second structure defined in the structure input block. This velocity can be controlled by changing the default hydraulic area and coefficients in the STRUC input block. Note that none of the parameters specified in the DCH-CELL input block have an effect on v_2 . It is recommended that at least two structures be defined in subcompartments so that either a forced or natural convection velocity is calculated in the heat transfer module and stored in v_2 for use in the TOF/KU model. If less than two

CONTAIN DCH Models

Model Descriptions

structures are defined, then the model will use the average gas velocity through the cell, $v_{g,avg}$, in place of v_2 for $v_{g,2}$.

Under the default RHODG option, Ku for the second trapping criterion is given by,

$$Ku_{s,2} = \frac{\rho_{g,i} v_{g,2}^2}{\sqrt{(\rho_{d,mat} - \rho_{g,i}) g \sigma}} \quad (55)$$

If RHODG=MIX is specified, the second trapping Ku number is given by,

$$Ku_{s,2} = \frac{\rho_{g,i} v_{g,2}^2 + \rho_{d,i} v_{d,avg}^2}{\sqrt{(\rho_{d,mat} - \rho_{g,i} - \rho_{d,i}) g \sigma}} \quad (56)$$

Note that $v_{d,avg}$ as used here is not limited to $v_{g,ft}$ as one might imply from Equation 28. Also notice that the density of the entraining fluid is given by, $\rho_{g,i}$, which is the gas density in the cell and not the upstream entrained density, $\rho_{g,1}$, that was used in evaluating $Ku_{s,1}$. This approach is based on the assumption that the entraining fluid of interest for structure impacts after the first one more closely resembles the debris/gas mixture of the cell itself than the material entering from the upstream cell.

When $Ku_{s,1} > Ku_{T,1}$ and $Ku_{s,2} \leq Ku_{T,2}$, debris is assumed to re-entrain from the first structure but trap (stick) on subsequent non-horizontal structures. For this case the trapping rate, λ , is given by,

$$\lambda = \frac{1}{t_{s,1} + \min(t_{s,2}, t_{gft})} \quad (57)$$

where $t_{s,2}$ is the average debris time of flight from the first impact to subsequent impacts before trapping. The rate is limited to the gravitational fall rate, because physically drops normally would trap at least as fast as they would fall under gravity to horizontal surfaces. The $t_{s,2}$ travel time is given by,

$$t_{s,2} = \frac{L_2}{v_{d,avg}} \quad (58)$$

where L_2 is specified by the user. Because the second trapping criterion applies to generic second impacts, it is recommended that L_2 be set equal to a generic characteristic cell dimension equal to 6 times the cell volume divided by the sum of all exposed surface areas.

The average debris velocity from inlet to trapping on surfaces beyond the first impact is given by $v_{d2,avg}$, which is calculated as follows,

$$v_{d2,avg} = \left[\frac{t_{s,1}\sqrt{v_{d1,avg}} + t_{s,2}\sqrt{v_{d,avg}}}{t_{s,1} + t_{s,2}} \right]^2 \quad (59)$$

This value is used to calculate the relative velocity, v_{re} , between gas and debris used in the heat and mass transfer DCH models in a similar manner as $v_{d1,avg}$ was used under case 1.

If slip is greater than 1 in any upstream cell, the relative velocity between gas and debris for heat transfer and chemical reactions, v_{re} , is given by,

$$v_{re} = \max(v_{gft}, |v_{g,avg} - v_{d2,avg}|) \quad (60)$$

If slip between gas and debris is exactly equal to 1 in all upstream cells,

$$v_{re} = \max(v_{gft}, v_{d2,avg}) \quad (61)$$

If slip = 1 exactly in all upstream cells the model assumes that $v_{d2,avg}$ is representative of the relative velocity between gas and debris. Again, this is done because this was how the model calculated v_{re} prior to the implementation of slip. If the newer formalism is desired even when slip = 1, then the user should specify slip to be slightly larger than one, but not exactly

equal to it (e.g., 1.01). Note that when $\text{slip} = 1$ that $v_{d2,\text{avg}}$ will typically be different from $v_{g,\text{avg}}$ because of the assumed travel distances of the debris as governed by the user-specified L_1 and L_2 parameters.

If $Ku_{s,2} > Ku_{T,2}$, then debris is assumed to remain airborne until it traps by gravity or flows out of the cell. The trapping rate will be calculated as described below.

2.3.6.3 TOF/KU Case 3: No Trapping From First or Second Ku Criteria. This section describes the case where the inflow velocity and other conditions are such that neither of the two Ku re-entrainment criteria are met. Therefore, debris will either gravitationally settle to horizontal surfaces or flow out of the cell. The user has some control over this by specifying the third trapping length, L_3 , and how the debris velocity is treated with the VNOST=GFT and VNOST=CNVEL options. Some guidance on the selection of L_3 and the VNOST option is provided in the following section.

The trapping rate for this case is given by,

$$\lambda = \frac{1}{t_{s,1} + t_{s,2} + \min(t_{gft}, t_{s,3})} \quad (62)$$

where $t_{s,3}$ is the characteristic residence time for debris that is not trapped under the first two de-entrainment criteria. In the VNOST=CNVEL option (the default at the time of this writing, but changed in a later version of CONTAIN) the debris in the cell is assumed to travel at the average debris outlet velocity; therefore, $t_{s,3}$ is given by,

$$t_{s,3} = \frac{L_3}{v_{d,\text{out}}} \quad (63)$$

where L_3 is a user-specified distance for this case. Four reasonable choices for this distance are (1) the GFT height, L_{gft} , (2) the cell height, (3) 6 times the cell volume divided by total surface area as was also suggested for L_2 , and (4) a large value to approximate infinity. The second choice is typically reserved for the VNOST=GFT option described below. The fourth choice causes debris to remain airborne until it is swept out of the cell by flow. Under this approach the VNOST option has no effect. The recommended approach is to use the first choice, which is the default that sets L_3 equal to the L_{gft} value.

If the VNOST=GFT option is invoked, $t_{s,3}$ is given by,

$$t_{s,3} = \frac{L_3}{v_{gft}} \quad (64)$$

Under this option the debris that is not trapped according to the two calculated Ku numbers is assumed to gravitationally settle to horizontal surfaces. The most logical selection of L_3 for this option is the cell height. By default L_3 will be set equal to the "lengtht" value, which will be set equal to the cell height if one is given in the GEOMETRY block. The average velocity of debris for this case, $v_{d,avg}$, will be v_{gft} if VNOST=GFT is specified and $v_{d,out}$ otherwise. The average velocity of debris for this case beginning with its entry into the cell is given by,

$$v_{d3,avg} = \left[\frac{t_{s,1}\sqrt{v_{d1,avg}} + t_{s,2}\sqrt{v_{d,avg}} + t_{s,3}\sqrt{v_{3,avg}}}{t_{s,1} + t_{s,2} + t_{s,3}} \right]^2 \quad (65)$$

The relative velocity for heat transfer and chemistry is given by,

$$v_{re} = \max(v_{gft}, |v_{d3,avg} - v_{g,avg}|) \quad (66)$$

As for the other cases, if slip is exactly equal to 1 in all upstream cells then the relative velocity is simply taken to be the debris velocity, $v_{d3,avg}$.

2.3.7 Trapping Model Sensitivity Coefficients

In addition to the four trapping models and their various options and inputs, three sensitivity coefficients are provided to facilitate performing trapping sensitivity calculations. These coefficients are:

- λ_{min} = slowest allowable trapping rate (default = 0.0)
- λ_{max} = fastest allowable trapping rate (default = ∞)
- λ_{mul} = trapping rate multiplier (default = 1.0)

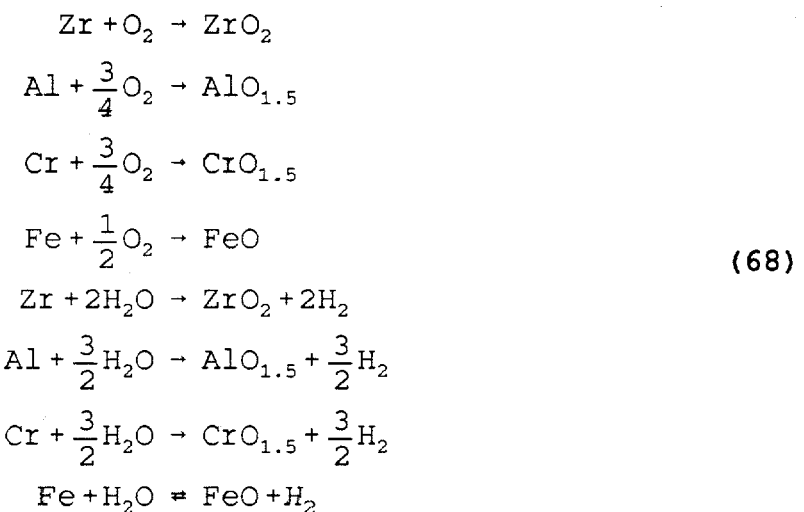
These three coefficients can be specified by the user in the input file using the TRAPMIN, TRAPMAX, and TRAPMUL keywords (see Section 3.4). Regardless of the trapping model selected, the calculated or user-specified trapping rate, λ , will be adjusted as follows:

$$\lambda = \max\{\min[\lambda_{max}, (\lambda \times \lambda_{mul})], \lambda_{min}\} \quad (67)$$

The λ_{mul} coefficient is useful for exploring the sensitivity of a simulation to trapping rate in a relative manner. The other two are useful for limiting the calculated trapping rate to fall within known reasonable bounds.

2.4 Chemical Reactions

Chemical reactions are modeled to occur during a DCH event if reactive metals are present in the dispersed debris fields and if the atmosphere contains oxygen or steam. The following chemical reactions are treated in the model



As indicated, all of these reactions except for the last one for iron/steam are assumed to go to completion. These reactions are treated in a hierarchical fashion within a time step where the order of the reactions is given by the order of the above list. Note that although a hierarchy is assumed during a time step, normally metal is not exhausted during the short time steps typically taken in a DCH calculation. As a result, the reactions of oxygen and steam are effectively calculated to proceed in parallel. Metals, however, do not react in parallel.

Each reaction is treated for every debris field in sequence. Therefore, the reactions are treated for drops in the first field, and then the reactions are considered for the second field, and so on. The exact same equations are applied to each debris field in a calculation; however, the reaction rate calculated for each field can and usually will be different since the models depend on the diameter, composition, and temperature of drops in the field. For example, if a debris field has no reactive metal in it, then chemical reactions will not be modeled at all for that field. Also, if two fields have different diameter drops then the reaction rate for the field with the smaller diameter will be faster than the field with the larger diameter drops. The

model also considers the reaction of drops that are non-airborne if the non-airborne field is assigned a non-zero diameter (see Section 2.7).

The DCH chemistry model consists of four parts. The first part is the modeling of the transport of gases to the surface of drops. This part of the model is described in the first subsection below, where an effective reaction time for the metals in the field based on only gas-side transport limitations is derived. Note that this reaction time is also referred to as a "time constant" in the code output. Because the calculated reaction times change from time step to time step the term "time constant" is not used here. The second part of the model is a drop-side transport model based on the diffusion of oxidant inside the drop. This part of the model is described in the second subsection below, where an effective reaction time for metals in the field based on drop-side transport limitations is derived. The third part of the model is the combination of the gas-side and drop-side reaction rates and the hierarchy scheme used to evaluate the amount of metal that reacts in the debris fields. This part of the model is described in the third subsection below. The equations in the third subsection provide the mass and energy terms that go into the debris and gas mass and energy conservation equations. The final part of the model is the recombination of hydrogen produced by the chemical reactions that is described in Section 2.5.1.

2.4.1 Gas Side Transport.

The gas-side rate model is based on a heat/mass-transfer analogy, where the transport of oxygen and steam to the surface of drops in a field is given by a mass transfer coefficient times a density difference as follows:

$$\left(\frac{dm}{dt} \right)_{O_2} = K_{O_2} A_d \rho'_{O_2} \quad (69)$$

$$K_{O_2} = \frac{Sh_{O_2} D_{O_2}}{d}$$

$$\left(\frac{dm}{dt} \right)_{H_2O} = K_{H_2O} A_d (\rho'_{H_2O} - \rho_{EQ}) ; \text{ if only Fe is present} \quad (70)$$

$$= K_{H_2O} A_d \rho'_{H_2O} ; \text{ otherwise}$$

$$K_{H_2O} = \frac{Sh_{H_2O} D_{H_2O}}{d}$$

where,

K_x	=	mass transfer coefficient for oxidant "x"
Sh_x	=	Sherwood number for oxidant "x"
Sc_x	=	Schmidt number for oxidant "x"
D_x	=	gas diffusivity of oxidant "x" in air
ρ_g'	=	density of oxidant "x" at gas/debris interface
d	=	diameter of debris in the field
ρ_{EQ}	=	equilibrium density of steam at drop surface
A_d	=	surface area for all drops in the debris field
T_{film}	=	film temperature between gas phase and the drop

The subscript "x" in the above definitions refers to oxygen and steam oxidants.

The Sherwood number, analogous to the Nusselt number in heat transfer, is given by the following correlation,

$$Sh_x = 2.0 + 0.6 \sqrt{Re_g} Sc_x^{1/3} \quad (71)$$

The Reynolds and Schmidt dimensionless numbers are given by,

$$Re_g = \frac{\rho_g' v_{re} d}{\mu_g(T_{film})} \quad (72)$$

$$Sc_x = \frac{\mu_g(T_{film})}{(\rho_g' D_x)}$$

where,

$$\rho_g' = \text{gas density at the gas/debris interface}$$

Expressions for the remaining terms in the above equations are provided below.

$$\begin{aligned}\rho_x' &= \rho_x \times \left(\frac{T_{\text{gas}}}{T_{\text{film}}} \right) \\ \rho_g' &= \left(\frac{m_g}{V_{\text{cell}}} \right) \left(\frac{T_{\text{gas}}}{T_{\text{film}}} \right) \\ T_{\text{film}} &= \frac{T_g + T_d}{2}\end{aligned}\quad (73)$$

T_g is the gas temperature, and T_d is the debris temperature of a specific debris field. The diameter, d , is the diameter of drops in the field. As previously noted, the chemistry for each field is calculated separately, using the diameter, composition, and temperature specific to that field.

The Reynolds number in the Sherwood correlation is evaluated using the value of v_{re} , calculated as described in Section 2.3.2.

Note that the density of gas, ρ_g' in the Re and Sc correlations is the density of gas in the atmosphere, but modified to be at the film temperature. The viscosity is the molar average of the viscosities of the gas species in the atmosphere evaluated at the film temperature, T_{film} .

If the debris field has iron metal in it, the equilibrium density of steam, ρ_{EQ} , is given by,

$$\begin{aligned}\rho_{\text{EQ}} &= \frac{p_{\text{EQ}} \text{MW}_{\text{H}_2\text{O}}}{R T_{\text{film}}} \\ p_{\text{EQ}} &= \frac{p_{\text{H}_2\text{O}}^{\text{bulk}} + p_{\text{H}_2}^{\text{bulk}}}{1 + \frac{K}{X_{\text{FeO}}}}\end{aligned}\quad (74)$$

where the p^{bulk} parameters are the partial pressures of steam and hydrogen in the cell atmosphere. The X_{FeO} parameter is the mole fraction of FeO among the other oxides in the debris field. K is the equilibrium constant for the iron/steam reaction and is given by,

$$K = e^{\frac{-\Delta G_{rx}}{RT_d}} \quad (75)$$

where ΔG_{rx} is the net difference in the Gibbs free energy of formation for the reactants and products of the iron/steam reaction. The correlations given in Reference Pow86 are used to evaluate the Gibbs free energies of formation.

As shown by the above equations, the equilibrium density of steam at the surface of drops in the field is set to zero if there are any metals other than iron. If all the steam oxidant is consumed by non-iron metals in the field then this steam transfer rate is used unadjusted. An adjustment is made to the remaining available steam if iron is present in the field and if other metals did not consume all of the steam. This is accomplished in the code by evaluating an effective multiplier on the steam reaction rate for the $P_{EQ}=0$ case that would give the same amount of oxidant reaction as the non-zero case. This multiplier is then used only on the iron/steam reaction, which will only occur if iron is present and if other metals did not exhaust all steam that transported to the drop. If the drop has only iron metal in it, then the steam transport rate is given by Equation (70). This is explained in greater detail in Section 2.4.3.

The following correlations for oxygen and steam diffusivity, D_{O_2} and D_{H_2O} , in the cell atmosphere are derived from a binary diffusion approximation given in Reference Bir60, where the transport medium is assumed to be air.

$$D_{O_2} = \frac{6.40827 \times 10^{-5} (T_{film})^{1.823}}{P} \quad (76)$$

$$D_{H_2O} = \frac{4.40146 \times 10^{-6} (T_{film})^{2.334}}{P} \quad (77)$$

The molecular weights of oxidant and air and various constants specific to air are imbedded within the constants in the above expressions.

The correlation for steam diffusivity is known to overestimate the diffusivity in air at elevated temperatures (above 500 K) [Wil87]. On the other hand, the bulk of the metal-steam reaction in typical DCH calculations takes place in the cavity or subcompartment volumes in which the dominant noncondensable species in the debris-gas boundary layer is hydrogen, not air or nitrogen; often the hydrogen is dominant by large factors. As it happens, these errors cancel at approximately 2000 K and the net error does not exceed 30% over the temperature range 1200-3000 K, assuming a pure steam-hydrogen mixture [Wil87]. While it is obviously unsatisfying to rely upon this essentially fortuitous cancellation of errors, the fact is that the error is sufficiently small for the conditions that typically dominate DCH analysis that only a

relatively sophisticated multicomponent diffusivity formulation would guarantee improvement without risking doing more harm than good. For compartmentalized geometries, the likelihood of important error in the present model is believed to be small. If large amounts of metallic debris are transported to the dome, where concentrations of noncondensables other than hydrogen may not be small, this formulation may overpredict the steam-metal reaction rate somewhat at sufficiently high temperatures.

The gas-side transport rates given by Equations (69) and (70) are used to calculate an oxygen equivalent molar gas transport rate to the surface of drops in the field as follows,

$$\frac{dN_g}{dt} = \frac{2}{MW_{O_2}} \left(\frac{dm}{dt} \right)_{O_2} + \frac{1}{MW_{H_2O}} \left(\frac{dm}{dt} \right)_{H_2O} \quad (78)$$

N_g in this expression is the number of oxygen equivalents of oxidant gas at the surface of the drops in a given debris field available to react. The equation above gives the rate at which N_g can be supplied for chemical reactions.

If only gas-side transport limits the reaction of metals, then the reaction rate of metal expressed in oxygen equivalents must equal the transport rate of gases to the drops. The metal reaction time based on gas-side transport can therefore be expressed as the ratio of metal in oxygen equivalents to the oxidant molar transport rate as follows,

$$\tau_g = \frac{N_{met}}{\left(\frac{dN_g}{dt} \right)} \quad (79)$$

where N_{met} is the amount of metal in the debris field in oxygen equivalents and is given by,

$$N_{met} = \sum_{\substack{k=Zr, Al \\ Cr, Fe}} \frac{v_k m_k}{MW_k} \quad (80)$$

where m_k is the mass of the reactive metal species "k" in the debris field, MW_k is the molecular weight of the reactive metal species and v_k are the oxygen to metal stoichiometry ratios for the metal species in the debris field. The stoichiometry ratios for Zr, Al, Cr, and Fe are 2, 1.5, 1.5, and 1 respectively as readily seen from the reactions as written in Equation (68).

2.4.2 Drop-Side Transport.

In reality, drop-side limitations may slow the reaction rate from the rate given by considering only gas-side limitations. The actual reaction rate used in the chemistry model is therefore a combination of gas-side and drop-side rates. This section describes the drop side rate model and the next section describes how the gas-side and drop-side rate models are combined and used to represent the chemical reactions.

CONTAIN has a rate-limiting drop-side model that is based on the solution of the diffusion equation in spherical coordinates. A useful approximation to the diffusion equation solution in spherical coordinates at early times is,

$$F(y) = 6\sqrt{\frac{y}{\pi}} - 3y ; y \leq 0.2 \quad (81)$$

where,

$$y = \frac{4 D_{liq} t}{d^2} \quad (82)$$

and t is time and D_{liq} is the diffusivity for the drop. This expression holds true until $y = 0.2$ at which time over 90% of the metal has reacted. From this expression it can be seen that the reaction rate initially varies as $t^{1/2}$; therefore, the reaction rate is strongly time-varying at early times. It is not practical, however, to track the thermal history of individual debris droplets with sufficient resolution to use this parabolic reaction rate law directly in CONTAIN. Therefore, the drop-side reaction rate is set such that one obtains the correct time required to react half the metal in an initially fresh drop. In terms of a drop-side reaction time, τ_d ,

$$1 - e^{-\frac{t_{50}}{\tau_d}} = 0.5 \quad (83)$$

where t_{50} is the time that will give $F(y)=0.5$. After a little algebra it can be shown that,

$$\tau_{50} = \frac{0.03055d^2}{4D_{liq}} \quad (84)$$

Substituting this into Equation (83) and solving for the effective drop-side reaction time, τ_d , gives

$$\tau_d = \frac{0.011017d^2}{D_{liq}} \quad (85)$$

If the temperature of a debris field is below a user-specified cutoff temperature, T_{cutoff} , then the diffusivity is set to zero and the drop side reaction time is set to infinity, thereby disabling chemical reactions for that field. The rationale for providing an option to terminate the reaction at low temperatures is to prevent old, cold debris from quenching fresh debris when a limited number of generations is used. The user can disable this feature by setting a zero cutoff temperature through input.

The drop diffusivity, D_{liq} , is given by

$$D_{liq} = \left\{ \begin{array}{ll} \infty ; & \text{if } D_{L1} = D_{L2} = 0 \\ D_{L1} e^{-\frac{E_{L1}}{T_d}} ; & \text{if } D_{L2} = 0 \\ D_{L2} T_d e^{-\frac{E_{L2}}{T_d}} ; & \text{if } D_{L1} = 0 \\ \min \left[D_{L1} e^{-\frac{E_{L1}}{T_d}}, D_{L2} T_d e^{-\frac{E_{L2}}{T_d}} \right] ; & \text{otherwise} \end{array} \right\} \quad (86)$$

where D_{L1} , E_{L1} , D_{L2} , and E_{L2} are specified by the user. Note that if D_{L1} and D_{L2} are set to zero by the user, then D_{liq} will be set to infinity, which corresponds to no drop-side limitations ($\tau_d = 0$).

A few limitations of the drop side model are now discussed. First, the drop-side reaction time given by Equation (85) corresponds to a fixed reaction rate that will match the time required to react half the fresh metal in a drop. Because the reaction rate is time varying as $t^{1/2}$, the drop-side limited reaction rate is underestimated at early times and overestimated at late times. Second, the drop-side model is based on diffusion within a stagnant drop. Other relevant processes such as vibration or circulation within the drop may lower the drop-side resistance below the diffusion limited rate. Also, drop shattering and drop-drop physical

interactions could expose fresh metal which would bypass the diffusion limited rates assumed by this model. Reliable models for these processes are not available; however, their importance can be assessed in CONTAIN by choosing large drop diffusivities or by ignoring drop-side resistance. This is the rationale for the recommendation that infinite diffusivity be used to bypass the drop-side model.

2.4.3 Reaction Rate Equations

The previous two subsections describe gas-side transport and drop-side transport limited reaction times, respectively. The reaction rate will be slower than the rate implied by either the gas-side limited or drop-side limited reaction times. The two reaction times are therefore combined to obtain an effective reaction time, τ_e . The effective reaction time is defined as the root-sum-square of the gas-side and drop-side reaction times as follow:

$$\tau_e = \sqrt{\tau_g^2 + \tau_d^2} \quad (87)$$

The use of a root-sum-square here has no rigorous basis; however, the intent is to account for the fact that the reaction time will be somewhere between the slower reaction time and the sum of the two reaction times.

The effective reaction time is used to calculate the reaction rate of metals in the debris field. The following discussion describes how this calculation is actually performed. First it is important to remember that each debris field is modeled separately and will therefore have its own effective reaction rate time constant. The equations below pertain to one particular field. The total mass and energy changes resulting from chemistry in a cell must include a summation over all debris fields. Another important aspect of the model is that the reaction times are not constant. That is, they are re-evaluated at the beginning of every cell time step.

The reaction rate for metal in oxygen equivalent units for a given debris field is given by,

$$\frac{dN_{met}}{dt} = - \frac{N_{met}}{\tau_e} \quad (88)$$

where N_{met} is the amount of metal in oxygen equivalents in a debris field given by Equation (80). Again, this specific rate only applies to one time step, one cell, and one debris field. The above equation is integrated to give the following expression for the amount of metal in oxygen equivalents that can react in a time step, Δt_c ,

$$\Delta N_{\text{met}} = N_{\text{met}}^0 \times \left(1 - e^{-\frac{\Delta t_c}{\tau_e}}\right) \quad (89)$$

The reacted amounts of all metal species in oxygen equivalents added together must not exceed ΔN_{met} . The reactions are also limited by the amount of oxygen and steam that can transport to the drop surface as given by Equations (69) and (70). Note that this check in the model is redundant, since τ_e is determined from Equations (69) and (70). The following discussion provides more details on how the calculation is actually performed.

The metal species in the debris field are reacted with the available oxygen in the following order: Zr, Al, Cr, and Fe. The reactions will be cut off if there is no oxygen remaining of that available from the gas-side transport calculation, or if the moles of metal reacted in oxygen equivalents exceeds ΔN_{met} . If the reactions are cut off because of oxygen limitations, the metal species are again considered in the same order listed above for reaction with steam. Again, the reaction of each metal species will proceed in the listed hierarchical order until no steam remains of that available from the gas-side transport calculation, or until the moles of metal reacted in oxygen equivalents reaches the maximum allowable amount, ΔN_{met} , from Equation (89).

The iron/steam reaction is the very last one that will be calculated to proceed. Therefore, this reaction will only proceed if other metals in the drop did not consume all the available steam from the gas-side transport Equation (70). The steam transport equation (with $\rho_{\text{EQ}} = 0$) is incorrect for the iron/steam reaction. Note that if iron is the only metal in the drop, the steam transport equation as originally written is correct. For the case where iron is a residual metal, any un-reacted steam available for the iron reaction is reduced by a factor, α_{EQ} , to account for

the fact that $\rho_{EQ} > 0$ for the iron/steam reaction. The parameter α_{EQ} is defined by rewriting the steam gas-side transport Equation (70) as follows,

$$\left(\frac{dm}{dt} \right)_{H_2O} = K_{H_2O} A_d (\rho'_{H_2O} - \rho_{EQ}) = K_{H_2O} A_d \alpha_{EQ} \rho'_{H_2O} \quad (90)$$

$$\alpha_{EQ} = \frac{\rho'_{H_2O} - \rho_{EQ}}{\rho'_{H_2O}}$$

It can be shown from Equation (74) that α_{EQ} is given by,

$$\alpha_{EQ} = \frac{\left(\frac{K}{X_{FeO}} - \frac{P_{H_2}^{bulk}}{P_{H_2O}^{bulk}} \right)}{\left(\frac{K}{X_{FeO}} + 1 \right)} \quad (91)$$

The α_{EQ} parameter is used to adjust the available steam for the iron reaction for fields that have iron and other metals present at the beginning of the time step. The α_{EQ} parameter is applied to account for non-zero ρ_{EQ} values for the iron reaction for such fields. For fields that have only iron present at the start of a time step, the use of ρ_{EQ} given by Equation (74) in the steam transport equation is exactly equivalent to using the α_{EQ} correction and $\rho_{EQ}=0$.

It should be clear from the above discussion that simple differential equations do not describe the rate at which metals are burned. This is primarily because there is no way to know *a priori* which metal in the drop will use the last available mole of oxidant. In fact, there is no way of knowing *a priori* whether the reaction will be oxidant transport limited, oxygen or steam availability limited, or metal limited. In most situations, the reaction will be oxidant transport limited. The following equations describe the amounts of metals and oxidant reacted and oxides produced for metal "k" if metals more reactive than "k" are absent and if metal "k" does not run out during the time step. The quantities in the following equations are

CONTAIN DCH Models

Model Descriptions

subscripted with *i* and *n* to emphasize that the expressions pertain to a particular cell "*i*" and debris field "*n*".

$$\begin{aligned}
 (\Delta O_2)_{i,n} &= \left(\frac{dm}{dt} \right)_{O_2} \Delta t_c \\
 \Delta m_{d,i,n,k} &= -2 \left(\frac{(\Delta O_2)_{i,n}}{MW_{O_2}} \right) \left(\frac{MW_k}{v_k} \right); \quad k = \text{metals Zr, Al,} \\
 &\quad \text{Cr, and Fe} \quad (92) \\
 \Delta m_{d,i,n,k} &= +2 \left(\frac{(\Delta O_2)_{i,n}}{MW_{O_2}} \right) \left(\frac{MW_k}{v_k} \right); \quad k = \text{oxides ZrO}_2, \text{ AlO}_{1.5}, \\
 &\quad \text{CrO}_{1.5}, \text{ and FeO}
 \end{aligned}$$

where MW is molecular weight, *v* is the stoichiometry coefficient, and all other parameters are previously defined. Recall that Δt_c is the time step. Similar expressions apply to the reaction of metals with steam,

$$\begin{aligned}
 (\Delta H_2O)_{i,n} &= \left(\frac{dm}{dt} \right)_{H_2O} \Delta t_c \\
 \Delta m_{d,i,n,k} &= - \left(\frac{(\Delta H_2O)_{i,n}}{MW_{H_2O}} \right) \left(\frac{MW_k}{v_k} \right); \quad k = \text{metals Zr, Al, and Cr} \\
 \Delta m_{d,i,n,k} &= - \left(\frac{(\alpha_{EQ} \Delta H_2O)_{i,n}}{MW_{H_2O}} \right) \left(\frac{MW_k}{v_k} \right); \quad k = \text{Fe metal} \\
 \Delta m_{d,i,n,k} &= + \left(\frac{(\Delta H_2O)_{i,n}}{MW_{H_2O}} \right) \left(\frac{MW_k}{v_k} \right); \quad k = \text{oxides ZrO}_2, \text{ AlO}_{1.5}, \text{ CrO}_{1.5} \\
 \Delta m_{d,i,n,k} &= + \left(\frac{(\alpha_{EQ} \Delta H_2O)_{i,n}}{MW_{H_2O}} \right) \left(\frac{MW_k}{v_k} \right); \quad k = \text{FeO oxide} \\
 (\Delta H_2)_{i,n} &= + \left(\frac{(\Delta H_2O)_{i,n}}{MW_{H_2O}} \right) MW_{H_2}; \quad (\text{from all } k)
 \end{aligned} \quad (93)$$

Similar but more piece-wise expressions (where several if-then branches are included) are used to calculate chemical reactions under other less-ideal conditions. For simplicity sake,

these more involved expressions are not shown, since the physical models are represented adequately by the expressions above for the simplest case.

The gas transport rate in the above expression is calculated for debris field "n" in cell "i" from Equations (69) and (70). As noted previously, the steam transport equation is evaluated with the $\rho_{Eq}=0$, and α_{Eq} is used as shown above to account for non-zero values of ρ_{Eq} . The net effect is that the correct value of ρ_{Eq} is used for all the metals.

The above equations are applied to each debris field sequentially. The metal masses reacted and oxide masses produced in a cell are divided by the time step to give the chemistry terms in the debris mass conservation equation. The same procedure applies to the masses of oxygen and steam consumed and the mass of hydrogen produced, but with two important differences. First, the gas mass changes from the reaction of all debris fields must be added together. Second, hydrogen gas produced can burn if oxygen is available in the cell. This is described in the following section. Note that if multiple generations are included, all sizes in a generation are done first before moving on to the next generation.

The energy released by the chemical reactions is added to the debris field. The amount of metal burned by oxygen and steam is multiplied by the energies of reactions given in the following table.

Table I
DCH Chemistry
Energies of Reaction

Metal Species	ν Oxygen/Metal Stoichiometry Ratio	Q_{rx,o_2} Oxygen Reaction MJ/kg	Q_{rx,h_2o} Steam Reaction MJ/kg
Zr	2	12.023	5.7384
Al	1.5	31.06	15.18
Cr	1.5	10.91	2.442
Fe	1	4.865	-0.2679

This table gives the heat of reaction per unit mass of metal reacted referenced to 273 Kelvin. It is important to note that these numbers are for liquid phase water; therefore, the energy required to vaporize water has been subtracted from the steam reactions. If atmosphere conditions are such that water is in the vapor phase then the heat of vaporization for the water will be added back to the debris field. The energy required to heat oxygen and steam to the drop temperature is also accounted for. These energy exchanges are done in two stages. First, the model takes the difference in enthalpy between the gaseous reactants and products at the debris field temperature and adds it to the debris field and subtracts it from the gas field,

$$\begin{aligned}
 HX_{d,i,n} = & (\Delta O_2)_{i,n} h_{O_2}(T_{d,i,n}) \\
 & + (\Delta H_2O)_{i,n} h_{H_2O}(T_{d,i,n}) \\
 & - (\Delta H_2)_{i,n} h_{H_2}(T_{d,i,n})
 \end{aligned} \tag{94}$$

This is done on a field by field basis. Next, because convective heat transfer results in heating of the reactants above the gas temperature as they transport toward the drop, the

following correction is applied to the convection heat transfer rate as recommended by Collier [Col81],

$$\Delta Q_{cor,i,n} = \Delta Q_c (\xi - 1)$$

$$\xi = \frac{a}{1 - e^{-a}} \quad (95)$$

$$a = \frac{HX_{d,i,n} - HX_{g,i,n}}{\Delta Q_c}$$

where,

$$HX_{g,i,n} = (\Delta O_2)_{i,n} h_{O_2} (T_{g,i,n}) + (\Delta H_2 O)_{i,n} h_{H_2 O} (T_{g,i,n}) - (\Delta H_2)_{i,n} h_{H_2} (T_{g,i,n}) \quad (96)$$

and ΔQ_c is the amount of energy exchanged by convection between the debris field and the atmosphere. Notice that $(1 - \xi)$ is used as a multiplier on the convective heat transfer rate. The convection heat transfer equations and ΔQ_c are described in Section 2.6.1.

Taking these corrections into account, the chemistry term for the debris energy equation for a particular field n in cell i is given by,

$$\left[\frac{dQ_{d,i,n}}{dt} \right]_{chem} = \frac{1}{\Delta t_c} \left\{ \left[\begin{array}{l} \sum_{k}^{Zr, Al} (\Delta m_{d,i,n,k})_{O_2} Q_{rx,O2,k} \\ + (\Delta m_{d,i,n,k})_{H_2 O} Q_{rx,H2O,k} \\ + HX_{d,i,n} + \Delta Q_{cor,i,n} \end{array} \right] \right\} \quad (97)$$

The first term in the summation represents the energy of metals burned in oxygen reactions given by Equation (92). The second term represents the energy of metals burned in steam reactions given by Equation (93). The third term is the difference in enthalpies of the gaseous reactants and products, and the last term is the Collier convection correction factor.

The mass change terms are only given by Equations 92 and 93 under ideal conditions as explained previously.

The chemistry term for the gas energy equation includes the differences in enthalpies of the reactants and products, and the Collier correction for all fields as follows,

$$\left[\frac{dQ_{g,i}}{dt} \right]_{\text{chem}} = \frac{1}{\Delta t_c} \left\{ \sum_{n=1}^{N_{\text{fields}}} -HX_{d,i,n} - \Delta Q_{\text{cor},i,n} \right. \\ \left. + 2.86 \times 10^8 (\Delta H_2)_{i,n} \right\} \quad (98)$$

The last term in this expression is for hydrogen (in kilomoles) produced in DCH chemical reactions that recombines with local oxygen in the cell atmosphere as discussed in the following section.

2.5 Hydrogen Behavior Under DCH Conditions

It has been observed in DCH experiments [All91, All92a-e, All93a-b, Bin92a-d] that hydrogen does not burn as traditional propagating deflagrations under DCH conditions. However, hydrogen combustion does play a significant, and often dominant, role in producing loads in a DCH event. Three burning modes are important in DCH events: (1) recombination of DCH produced hydrogen in the vicinity of the drop, (2) the burning of hydrogen as a jet or diffusion flame as DCH-produced hydrogen flows away from the point of its production into oxygen rich volumes, and (3) the spontaneous recombination of pre-existing hydrogen volumetrically in oxygen rich volumes. The entrainment of pre-existing hydrogen into the burning jet in the oxygen rich volumes is also an important process that must be considered. As noted below, this is included as part of the model for the second combustion mode.

Hydrogen produced by steam/metal reactions can immediately recombine with oxygen if any is available in the vicinity of the reacting drop. The first section below describes the model included in CONTAIN for this process. Normally, however, oxygen is not available in large amounts in the cavity and subcompartment regions where the majority of the hydrogen is produced. Therefore, most of the hydrogen produced by DCH chemical reactions burns continuously as it flows downstream and enters the oxygen rich upper containment volumes. A simple diffusion flame burning (DFB) model is provided in CONTAIN that can be used to represent this process. The second section below briefly describes this model, with emphasis on the two DCH-specific aspects of the DFB model: the option to specify a cutoff temperature for the burning of incoming combustible gas, and the simple model for the entrainment of pre-existing combustible gases in a cell into the diffusion flame jet. The third

section below briefly describes the bulk spontaneous recombination model (BSR) model in CONTAIN for burning pre-existing hydrogen volumetrically at a user specified rate.

2.5.1 DCH-Produced Hydrogen Recombination

Consideration is given to the recombination of hydrogen produced in metal/steam reactions with unburned oxygen in the vicinity of the drop. Hydrogen produced by DCH chemical reactions is assumed to burn instantaneously if oxygen is available in the cell. This can only occur if oxygen is available during the same time step when the hydrogen was produced. The rationale for this approach is that the hydrogen is assumed to be near the surface of the drop during the same time step during which it was produced. If oxygen is not available during this time step, then it will only burn as governed by one of the other containment combustion models (deflagration, diffusion flame burning, or bulk spontaneous recombination). The hydrogen recombination reaction can also be disabled by the user in one or more cells by specifying RCOMH2=OFF in the DHEAT or DCH-CELL input blocks.

The hydrogen burning reaction is given by



where 2.86×10^8 joules of energy are released per kilomole of hydrogen that recombines with oxygen. This reaction is limited by the availability of oxygen in the cell and the amount of hydrogen produced by DCH during the time step. The energy released by the recombination process is added to the atmosphere, not the drop field, as shown in Equation (98).

2.5.2 Diffusion Flame Burning

The dominant mode of combustion for DCH-produced hydrogen is as a diffusion flame or a jet as the hot hydrogen enters an oxygen rich environment in the containment upper regions. A diffusion flame burning (DFB) model is provided in CONTAIN for modeling this process. Under some high temperature conditions, pre-existing hydrogen may also burn. The BSR described in the following section is provided to model this mode of combustion. The DFB model does include a simple model for representing the entrainment and burning of pre-existing hydrogen into the burning jet as described below.

In the DFB model, a user specified fraction of the combustible gases flowing into a cell are assumed to burn at an infinitely fast rate if the model is enabled. The model is enabled using the CONTBURN keyword in the H-BURN block. Within the CONTBURN block the user specifies various parameters that define the conditions under which hydrogen flowing into the cell burns, and what fraction is assumed to burn. These input parameters are applicable to both DCH and non-DCH problems, and are sufficiently described in the C110T code change document that is distributed with the code software. Two DCH-specific parameters are discussed in greater detail below. The burning rate is always controlled by the rate of flow

into the cell; that is, once the hydrogen arrives any amount assumed to burn does so within the time step.

In DCH calculations (and other calculations) the user may specify that, for combustion to occur, the temperature of combustible gases flowing into a cell must exceed a given threshold temperature given by the DFTEMP input. By default this threshold is set to 1000 Kelvin. The temperature of the combustible gases flowing into the cell is taken to be the temperature of the upstream cell. The DFB inflow temperature criterion is a necessary, but not sufficient, condition for combustible gases to burn via the DFB model. Therefore, this criterion can be thought of as a "snuffout" criterion, which will snuff out a DFB if the temperature of the gases is below the cutoff. Finally, the DFB temperature criterion is applied independently to each flow path, including regular flow paths, engineered vents, and the suppression pool vent. That is, hot combustible gases entering a cell through one path may burn via the DFB model, while cooler combustible gases entering the same cell but through other paths may not burn. This will occur if the temperatures of some upstream cells are above the threshold, while the temperatures of other upstream cells are below the threshold. User specified sources are not subject to the DFB temperature criterion.

The temperature cutoff criterion can be expressed using singularity functions as shown in the following governing equations.

$$W_{JET,i,H2} = \sum_j \left[\frac{W_{ji} \theta_{ji} \zeta_j m_{j,H2} \langle T_j - T_{i,DFB} \rangle}{m_{F,j}} \right] \quad (99)$$

$$W_{JET,i,CO} = \sum_j \left[\frac{W_{ji} \theta_{ji} \zeta_j m_{j,CO} \langle T_j - T_{i,DFB} \rangle}{m_{F,j}} \right]$$

where,

- $W_{jet,i,x}$ = effective jet flow rate of x , where x is H2 or CO.
- $m_{j,x}$ = mass of x in the upstream cell, where x is H2 or CO,
- T_i = the temperature of the gas in the upstream cell,
- $T_{i,DFB}$ = the DFB threshold temperature, given by the DFTEMP keyword,
- $\langle x-y \rangle$ = a singularity function, defined as one when $x \geq y$, and zero otherwise.

One can readily see from these expressions that combustible gases flowing into cell i from cells that are cooler than the cutoff temperature will not be included in the jet that can burn as a diffusion flame under the DFB model. Note that these expressions account for debris/gas slip if DCH is being modeled. This is apparent from the fact that they are similar to the first

term of Equation 13 (with the material index set equal to H2 and CO), which was derived to include the effects of debris/gas slip. The effect of non-DCH specific parameters that can be given to conditionally set $W_{jet,i,x}$ to zero in the DFB model are not considered in the above equations.

The entrainment of pre-existing combustible gases is determined assuming that the atmosphere is well-mixed in the cell, and that enough gases from the cell atmosphere are entrained into the jet to burn all of the incoming combustible gas plus the combustible gas entrained along with the oxygen. Under the well-mixed atmosphere assumption, this approach will provide a first order estimate of the amount of combustible gases entrained into jet. This model only considers entrainment, and thus does not account for burning rate limitations imposed by effects such as diffusion and mixing. This approach also does not take into account oxygen entering the cell in the jet. The burning of the diffusion flame jet is represented by the balance equation,

$$N_{cg,jet} + X_{H_2}N_e + X_{CO}N_e = 2X_{O_2}N_e \quad (100)$$

where N_e is the moles of atmosphere entrained into the jet, X is the mole fraction of the gases indicated by the subscripts in the downstream cell atmosphere, and $N_{cg,jet}$ is the moles of combustible gas entering the cell available for burning in the diffusion flame.

$$N_{cg,jet} = f_{cb} \times \left[\frac{W_{jet,i,H_2}}{MW_{H_2}} + \frac{W_{jet,i,CO}}{MW_{CO}} \right] \Delta t_f \quad (101)$$

where MW is molecular weight, Δt_f is the flow time step, and f_{cb} is the fraction of incoming combustible gas allowed to burn as a diffusion flame (see the CFRACB keyword in the H-BURN input). Note that $N_{cg,jet}$ may be less than the actual amount flowing into the cell if f_{cb} is specified. $N_{cg,jet}$ may also be set to zero within the model if the total combustible flow rate ($W_{jet,i,H_2} + W_{jet,i,CO}$) is less than a user-specified minimum value. This minimum value is optionally specified using the H2FLOW keyword in the H-BURN input block.

The balance equation provided above is solved for N_e , and the mole fractions of hydrogen and carbon monoxide in the downstream cell are used to obtain the combustible gas moles to entrain into the jet and include in the DFB model. This solution only applies when mixtures are far from stoichiometric. If $2X_{O_2} \leq X_{H_2} + X_{CO}$ then all of the combustible gas in the cell is assumed to be available for entrainment. Under such conditions this may produce unrealistic results; therefore, the entrained combustible gas is limited to the amount of combustible flowing into the cell in the jet.

$$\begin{aligned}
 N_e &= \min\left[N_{\text{total}}, \frac{N_{\text{cg, jet}}}{\max(\delta, 2X_{\text{O}_2} - X_{\text{H}_2} - X_{\text{CO}})}\right] \\
 N_{\text{H}_2,e} &= \min(N_e X_{\text{H}_2}, N_{\text{cg, jet}}) \\
 N_{\text{CO},e} &= \min(N_e X_{\text{CO}}, N_{\text{cg, jet}})
 \end{aligned} \tag{102}$$

where δ is a small number, N_{total} is the total moles of combustible gas in the cell. $N_{\text{H}_2,e}$ is the moles of hydrogen to entrain into the jet from the cell atmosphere, and $N_{\text{CO},e}$ is the moles of carbon monoxide to entrain into the jet from the cell atmosphere. When the DFB model is used, any hydrogen or carbon monoxide pre-existing in cells will be subject to inclusion in the burning jet as described above. The entrainment of pre-existing combustible gases in the DFB model can also be disabled using the NOBURNEN keyword in the CONTBURN input sub-block of the H-BURN input block.

2.5.3 Volumetric Hydrogen Recombination

Pre-existing hydrogen in the containment can burn in three modes: deflagration, entrainment into diffusion flame, and volumetrically. The deflagration model in CONTAIN for this mode is described in Reference Mur89. Deflagrations are not normally expected under DCH conditions; therefore, they are not discussed further here. Entrainment of pre-existing hydrogen is described in the preceding section. The volumetric burning of hydrogen is briefly described below. The reader is referred to the forthcoming CONTAIN 1.2 Code Manual for more complete documentation on this model.

A parametric Bulk Spontaneous Recombination (BSR) model is provided for representing volumetric burning of hydrogen. In this model, hydrogen in a cell recombines at a user specified constant rate. In the model the hydrogen either burns at this rate or does not burn at all. The user specified burn rate is a fraction of what can burn; i.e., $\text{Min}(N_{\text{H}_2}, 2N_{\text{O}_2})$. The temperature and debris concentration in the cell is used as a switch to govern whether the hydrogen burns at the user specified constant rate. While this model does provide a simple way of representing the effects of pre-existing hydrogen recombination under DCH conditions, the model does have some limitations that prevent it from being a truly predictive tool. Most importantly, the hydrogen recombination is known to occur over a broad temperature range. At low temperatures the recombination rate is slow. Also, in reality the rate of recombination is a function of temperature and composition. These complexities are not accounted for in the simple BSR model.

2.6 Heat Transfer

Models are included for convective and radiative heat transfer between the debris and the atmosphere. The DCH radiation model also includes provisions for direct radiation from the

debris to containment structures, including the pool and ice condenser. The first subsection below describes the convection model. The second subsection describes the DCH radiation model. The models described below apply to debris in all fields, including the airborne fields and the non-airborne debris field. The models do not apply to trapped debris that is transferred to the uppermost intermediate layer in the lower cell cavity. Heat transfer for debris in the lower cell is modeled as part of the lower cell heat transfer model as described in the CONTAIN 1.1 User's Manual [Mur89].

2.6.1 Convective Heat Transfer.

Convection heat transfer from debris to gas is assumed to be by forced convection. The heat transfer coefficient is given by the following Nusselt correlation of Ranz and Marshall [Ran52, Bir60] for forced flow over a sphere.

$$Nu_{i,n} = 2.0 + 0.6 Re_g^{1/2} Pr_g^{1/3} \quad (103)$$

where $Nu_{i,n}$ is the Nusselt number for debris field n in cell i. The convection heat transfer rate for each debris field is individually calculated since each field has its own temperature, $T_{d,i,n}$, and particle size, d_n .

The Re_g and Pr_g parameters in this expression are calculated using gas properties at the film temperature, T_{film} , as recommended in Reference Bir60. The velocity, v_{re} , is used as the forced convection velocity in the Reynolds number. This velocity is calculated within the code from the calculated intercell mass flow rates and the predicted trapping behavior as described in Section 2.3. The user does have the option to override this calculated velocity with either a constant or a table function of time as described in Section 3.4.

The heat transfer coefficient is calculated from the Nusselt number as usual,

$$h_{i,n} = \frac{Nu_{i,n} K_{i,n}}{d_n} \quad (104)$$

where, $K_{i,n}$ is the thermal conductivity of the gas evaluated at the film temperature between the gas and the debris in field n in cell i, and d_n is the diameter of droplets in debris field n. The thermal conductivity of the gas is calculated as a mole-weighted average of the gas species as follows:

$$K_{i,n} = \frac{\sum_{k=1}^{N_{\text{gas}}} N_k K_k (T_{\text{film},n})}{\sum_{k=1}^{N_{\text{gas}}} N_k} \quad (105)$$

where N_{gas} is the number of gas species in the cell, N_k is the number of kilomoles of gas species k in the cell, and $T_{\text{film},n}$ is the film temperature between atmosphere and debris in field n .

The debris-to-gas convective heat transfer rate for a given field, n , in cell, i , is given by,

$$\left[\frac{dQ_{d,i,n}}{dt} \right]_{\text{conv}} = h_{i,n} A_{d,i,n} (T_{d,i,n} - T_{g,i}) \quad (106)$$

where $A_{d,i,n}$ is the surface area of all drops in field n in cell i , $T_{d,i,n}$ is the temperature of debris field n in cell i , and $T_{g,i}$ is the gas temperature in cell i . The $[dQ/dt]_{\text{conv}}$ term is the convection heat transfer rate that is subtracted in the debris energy equation for field n (see Equation (17) in Section 2.2.5), and added to the gas energy equation for all fields.

The amount of energy transferred from the debris field to the atmosphere by convection in a cell time step, Δt_c , is given by,

$$\Delta Q_c = \left[\frac{dQ_{d,i,n}}{dt} \right]_{\text{conv}} \Delta t_c \quad (107)$$

The ΔQ_c term is the convection energy amount used to evaluate the Collier correction factor (see Equation (95)) for the effect of mass transfer on convection heat transfer as described in Section 2.4.3.

2.6.2 Radiative Heat Transfer

Debris radiation to the atmosphere, all structure surfaces, the ice condenser, and the uppermost layer in the cavity are treated in the DCH radiation model. Radiation heat transfer between the debris field and the atmosphere is modeled using a simple gray body law,

$$\left[\frac{dQ_{d,i,n}}{dt} \right]_{rad,g} = \epsilon_{d-g} \sigma A_{d,i,n} (T_{d,i,n}^4 - T_{g,i}^4) \quad (108)$$

where σ is the Stephan Boltzman constant and $A_{d,i,n}$ is the surface area of all drops in debris field n in cell i . The effective emissivity for debris-gas radiation, ϵ_{d-g} , is specified by the user. Values near unity are typically appropriate for this parameter. The default value of ϵ_{d-g} is 1.0.

Radiation from the atmosphere to structures is not a DCH-specific model. The gas-to-structure radiation model is described in the CONTAIN 1.1 Reference Manual [Was91] and is not repeated here. However, there is an important consideration that one must give to the atmosphere-to-structure radiation model in DCH calculations. In DCH calculations the radiative properties of the cell as calculated by the Cess-Lian and Modak correlations described in the CONTAIN Reference Manual may not be appropriate under DCH conditions when airborne debris is present in the cell. To accommodate this, the calculated atmosphere emissivity can be overridden in a DCH calculation by the user as described in Section 3.6.2. Values of approximately 0.8 are appropriate for most DCH applications.

The radiative heat transfer rate from debris field n to surface j is given by,

$$\left[\frac{dQ_{d,i,n}}{dt} \right]_{rad,s,j} = \epsilon_{d-s} \sigma \left(\frac{A_{d,i,n}}{\sum_{nn=1}^{N_{fields}} A_{d,i,nn}} \right) \left(\frac{A_{i,j}}{\sum_{jj=1}^{N_{surf}} A_{s,jj}} \right) \times \min \left(\sum_{nn=1}^{N_{fields}} A_{d,i,nn}, \sum_{jj=1}^{N_{surf}} A_{s,jj} \right) (T_{d,i,n}^4 - T_{s,j}^4) \quad (109)$$

where $T_{s,j}$ is the temperature of surface j , and N_{surf} represents all surfaces, including all structure inner surfaces, the uppermost lower cell layer, and the ice condenser area. For structure surfaces, $T_{s,j}$ is the temperature of the first node (or last if the exposed surface is the outer surface of a structure). Note that the film interface temperature of structures is not used as $T_{s,j}$. Although using the interface temperature might be slightly more accurate than using the first node temperature, doing so can cause numerical instabilities, since there is no heat capacity associated with the film temperature. In practice the two temperatures will be very close to each other for DCH calculations, since small nodes should be used for the surface nodes and water films will typically not be present. Note that water films may be present at the start of some DCH calculations and are surprisingly important because it represents an additional source for steam to interact with debris.

Note that the surface area for debris to gas radiation is weighted such that when all surfaces and debris fields are considered, the smaller of the total debris area and the area of all surfaces will be accounted for. The surfaces considered include all structure surfaces, the ice condenser, and the uppermost layer of the cavity.

The black body multiplier for debris-surface radiation, ϵ_{d-s} , is optionally specified by the user. By default this parameter is zero and debris to structure direct radiation is disabled. This parameter is normally left at or close to its default value of zero in most DCH applications based on the assumption that the atmosphere is opaque from airborne debris and DCH generated aerosols. Heat transfer from debris to heat sinks will be non-zero if a non-zero value is specified for ϵ_{d-s} . If a non-zero ϵ_{d-s} is given, then ϵ_{d-g} should also be specified to ensure that the sum of ϵ_{d-g} and ϵ_{d-s} does not exceed unity.

The total radiative energy loss from debris field n used in the debris energy conservation equation (see Equation (17)) is given by the sum of the debris to structure radiation for all surfaces and the debris to gas radiation,

$$\left[\frac{dQ_{d,i,n}}{dt} \right]_{rad} = \left[\frac{dQ_{d,i,n}}{dt} \right]_{rad,g} + \sum_{j=1}^{N_{surf}} \left[\frac{dQ_{d,i,n}}{dt} \right]_{rad,s,j} \quad (110)$$

The first term on the right hand side of this equation is added to the gas energy conservation equation, and the last term is added to the innermost node of each structure. For cells with a cavity cell, the energy is placed in the uppermost intermediate layer. In the case of the ice condenser, the energy only contributes to the melting of ice and not to the heating of the effluent. For structures, the radiative flux is included in the surface flux used to calculate the structure interface temperature.

2.7 Non-Airborne Debris Interactions

Debris that is airborne and debris that is not airborne can both contribute to DCH by heat transfer and chemical reactions. Non-airborne debris includes debris that has not been entrained into the atmosphere, and debris that was once airborne that has been trapped. To enable consideration of both types of non-airborne debris in the heat transfer and chemistry models, the trapped debris bin in the cavity cell must be used as an intermediate repository for debris between the RPV dispersal phase and the cavity entrainment phase. That is, debris dispersal from the RPV should be represented as a source table of debris into the trapped field of the cavity. This is accomplished using a special DCH source table where the DCHTYPE keyword is specified followed by the TRAPBIN type. Entrainment is then represented as a source table of debris from the trapped field in the cavity into the atmosphere of the cavity. This is accomplished again using the DCHTYPE keyword, but this time followed by the

CONTAIN DCH Models

Model Descriptions

ENTRAIN type in the source tables input. These special DCH source tables are discussed in greater detail in Section 3.5.

The governing equations for heat transfer and chemical reactions given in the previous sections also apply to debris that is not airborne. There are four unique aspects to the heat transfer and chemical reactions models for debris that is not airborne. First, the surface area for heat transfer and mass transfer is based on a unique user-specified effective diameter that applies only to debris in the non-airborne bin. By default this diameter is not defined, thus the model is not active. A diameter must be specified by the user in a given DCH-CELL input block using the DIATRAP keyword to enable non-airborne debris interactions in that cell. Given a specified effective diameter, the area is computed as if the mass in the non-airborne field were airborne as follows,

$$A_{d,i,nad} = \frac{6 \sum_k^{N_{DCH}} m_{d,i,nad,k}}{\rho_{d,i,nad} d_{i,nad}} \quad (111)$$

where,

- $A_{d,i,nad}$ = surface area for the non-airborne field in cell *i*,
- $m_{d,i,nad,k}$ = mass of debris species *k* in the non-airborne field in cell *i*,
- $\rho_{d,i,nad}$ = average material density of debris in the non-airborne field in cell *i*,
- $d_{i,nad}$ = user-specified effective diameter for the non-airborne field in cell *i*.

The mass of non-airborne debris is governed by the rate of debris addition to the non-airborne debris field, the rate of entrainment from the non-airborne debris field, and the trapping rate of debris into the non-airborne debris field. Equation (25) in Section 2.3.1 gives the governing equation for the mass of debris in the non-airborne field that takes into account these three processes. The addition of debris to the non-airborne field and the entrainment of debris out of the non-airborne field is governed by user specified tables as described above.

The average material density of airborne and non-airborne debris is calculated as the inverse of the mass average of specific volume of all materials in the trapped field at the temperature of the trapped field. Normally the densities are taken from the material property tables given in the USERDAT input, but they will be ignored if the DENDRP global input (or VAR-PARM table) is specified, in which case the average density of airborne and non-airborne debris will be set to the specified value. The diameter of debris in airborne fields is given by the required DIABIN or DIADRP keywords. The diameter of non-airborne debris is given by the optional DIATRAP keyword. If this keyword is not given, chemistry and heat transfer for the trapped bin will not be modeled.

The second unique aspect of non-airborne debris heat transfer is that radiation directly to structures or the ice chest is not allowed for debris that is not airborne. Therefore, the non-airborne bin is not included in the effective debris to structure area calculation. The third difference is that the black body multiplier for debris to gas radiation can be specified separately for non-airborne debris. This is done using the RADTRAP input as discussed in the input section. By default this value is zero; therefore, radiation heat transfer for trapped debris is disabled unless the user provides a value using the RADTRAP keyword.

The fourth and final difference for non-airborne debris is that by default the average gas velocity through the cell is used for heat and mass transfer for non-airborne debris. This average is by default calculated using the cell volume to the two-thirds power for the cell hydraulic area. The user can specify a specific hydraulic area for use in calculating the average gas velocity through the cell for DCH calculations as discussed in Section 3.4. This is in contrast to airborne debris, where the trapping conditions and the gas and debris flow velocities are used to calculate an appropriate velocity for heat transfer as described in Section 2.3.2. This is not done for non-airborne debris since this field is not flowing and is not subject to trapping as is the airborne debris fields. The velocity for non-airborne debris heat and mass transfer can also be a user-specified constant using the VELTRAP keyword, or a user-specified time-dependent parameter using the VAR-PARM table input option.

2.8 Known Limitations

The *most significant* known limitations of the DCH model in CONTAIN are summarized below. A more in depth discussion of the modeling limitations along with significant user guidance in applying the models is provided in a report on DCH model assessment that is in preparation.

Debris Interaction With Water

There is no mechanistic model for the interaction of dispersed debris with water in the cavity. Excluding the possibility of a steam explosion, some of the effect of debris/water interactions can be represented parametrically through appropriate user input, but the results are largely governed by the user-controlled input assumptions.

Debris-Gas Slip

There is no mechanistic model for calculating the debris gas slip parameter.

Momentum Driven Transport

Debris is only transported by flow with the gas. Therefore, advection-driven transport of debris, such as through a cell when the entrance and exit flow paths are aligned, is not represented. This is believed to be an important transport mechanism in the Zion geometry IET tests and presumably the plant. The importance for other geometries, such as Surry, is not known at this time.

Trapping Limitations

A number of potentially important processes are not represented in the trapping model, such as drop splashing, surface ablation, and film interactions. Although the TOF/KU model does incorporate a number of modeling sophistications, the flight path of particles is not actually tracked in the **CONTAIN model**. Instead, the model relies upon estimates of flight paths based on inflow and outflow debris/gas velocities.

Non-Airborne Debris Interactions

When debris is trapped it is placed into the non-airborne debris bin. Debris in this bin is allowed to continue participating in DCH; however, the model does not include appropriate mechanistic models for the non-airborne bin. The models used are the same ones used for the airborne fields, which is known to be incorrect because the geometry of the non-airborne debris is different than that of airborne drops. There is also no mechanistic model for estimating the velocity of the gas relative to that of the non-airborne debris field. All of the complexities of non-airborne debris interactions are represented parametrically with an effective non-airborne debris diameter and a user controlled gas/debris relative velocity.

Drop-Drop Interactions

The interaction of airborne debris drops with other airborne drops is not modeled. The importance of this effect is unknown. No plans are underway to address this limitation.

Concrete Ablation

There is no model for the ablation of concrete by the debris jet ejected from the RPV.

3. Input Instructions

This section describes the input needed to perform DCH calculations with CONTAIN. The nomenclature used in this section follows that used in the CONTAIN code documentation as described in Reference Mur89. Some of the DCH input is required to make a DCH calculation, while other parts are optional. This section only describes input that is specific to the **DCH model**. It is important to note, however, that choices for other facets of the CONTAIN input can have an effect on the behavior of the code for DCH. For example, the selection of diffusion flame burn and bulk spontaneous recombination options over the default discrete deflagration model in the hydrogen burn input can have a dramatic effect on the calculated peak pressures. Input descriptions for non-DCH models are given in Reference Mur89. Input descriptions for some of the newer models, such as the diffusion flame and bulk spontaneous recombination hydrogen burning options, are at the time of this writing not in published form; however, they are provided in the CONTAIN code change documents that are distributed to all active code users.

The first subsection below describes the global control parameter input. These parameters are used to efficiently reserve memory for the DCH model. The second subsection below

describes the material property input specific to DCH. The third subsection describes the global DHEAT input block, where parameters common to all cells are specified. The fourth subsection describes the cell-specific DCH-CELL input block. The fifth subsection describes how to model debris dispersal and gas blowdown in a DCH calculation. The final subsection covers a number of miscellaneous DCH related input requirements and options.

It should also be noted that the input requirements associated with some of the previously existing control parameters are different during a DCH calculation. The DCH-related input requirements associated with these control variables are described in detail. This document does not describe the non-DCH related input requirements associated with these variables in detail; the reader is referred to the CONTAIN User's Manual [Mur89] for more detail.

3.1 Global Control Block

The following keywords in the global control input block are required to make a DCH calculation. The remainder of the global control block remains as described in the CONTAIN User's Manual.

CONTROL

...

NDHSPC = ndhspc
 [NDHBIN = ndhbin] [NDHGRP = ndhgrp]
 [PRODSEP] [NWDUDM = nwdudm]

...

EOI

NDHSPC = ndhspc

maximum number of species that can be present in each debris field. This corresponds to the N_{dch} parameter used in Section 2, and sets the number of DCH species that must be given in the USERDEF and USERDAT input blocks. This is required input.

NDHBIN = ndhbin

optional parameter for the number of debris fields per generation. By default only one debris field will be modeled. The maximum number of fields in the calculation is the product of "ndhbin" and "ndhgrp". This product corresponds to N_{fields} in Section 2. (default = 1).

NDHGRP = ndhgrp

optional parameter for the number of generations. A new generation is created with "ndhbin" fields in it when the

amount of debris added to the previous generation (from sources) has exceeded the allowable mass threshold, "grplim". This threshold is specified in the global DHEAT block. The maximum number of fields in the calculation is the product of "ndhbin" and "ndhgrp". This product corresponds to N_{fields} in Section 2. (default = 1).

PRODSEP

keyword to enable the distribution of chemistry oxide products into bins according to the FDISTR array. This option is only available when there is one generation (NDHGRP=1). If this option is not used, then oxides stay in the field with the metal that generated it.

NWDUDM = nwdudm

amount of space to reserve for user-specified material property data. If a DCH run is being performed this input should be specified to increase the amount of reserved space from the default value to accommodate the DCH material property tables. A value of 5000 is suitable for most DCH calculations. (default = 1000).

3.2 User-Defined Material Input

DCH calculations require the user to specify the names and properties of the debris species that can be present. This is done using the CONTAIN user defined material input. The user defined properties input feature is described in detail in the CONTAIN User's Manual. Specific requirements that apply only to DCH calculations are described below.

3.2.1 DCH Material Names.

The species that can be included in the debris field must be named in the USERDEF global input block as described in this subsection.

MATERIAL

COMPOUND (names)
USERDEF (unames)

...

USERDEF

keyword to initiate the specification of user defined material species. The DCH material species must be named here in a DCH calculation. The actual properties are provided in the USERDAT input block.

The DCH model recognizes the following specific names of materials as reactive metals: ZRD, ALD, CRD, and FED. These names and only these names may be used as reactive zirconium, aluminum, chromium, and iron respectively. The following oxide names must also be specified if the corresponding metal is given: ZRO2D, ALOXD, CROXD, and FEOD. Again, these names and only these names will be recognized as the oxide products of the four reactive metals. Any number of additional material species with any name may be specified in addition to the special four species above. Any such species will be treated as inert and will be assumed to reside in the oxide phase, even if the name suggests that it is a metal.

At least one of the DCH user-defined metals must be named in order to model chemical reactions of debris in the atmosphere. Also, if a metal is specified then its oxide must also be specified in the **USERDEF** block. For example, if FED is specified, then FEOD **must** also be specified since FED (iron) is assumed to oxidize to FEOD (iron oxide). If either of these rules is violated, an input error will occur and the calculation will not proceed. An oxide can be specified, however, without specifying its metal counterpart.

Any number of additional species may be specified as direct heating materials with phase type DEBRIS in addition to the special ones discussed above. These materials will be inert and will therefore not chemically react. However, as long as the phase of the specified material is DEBRIS, any sources of this material to the atmosphere will be added to the debris fields as discussed in the later subsection on debris sources. The names of user-defined DCH materials must be different than the names of materials in the CONTAIN material library. It is suggested that DCH materials be named ending with a "D" to ensure that the names are unique from the names of the materials in the CONTAIN library.

3.2.2 DCH Material Property Tables

The material properties of all species identified in the USERDEF block must be provided in the global USERDAT input block. The syntax for this input for DCH is exactly as described in the CONTAIN 1.1 User's Manual. The one very important difference between DCH user-defined species and other user-defined materials is that the phase type for DCH material is DEBRIS. The word DEBRIS is specified after the material name in the USERDAT input block. Within the code the phase number for debris will be 4, which is distinct from the phase numbers for gas (1), liquids (2), and solids (3). The DEBRIS phase identifier is extremely important, since this is the only way the code knows that the DCH species given in the USERDEF list are to be treated as species in the debris field.

The CONTAIN code project has developed a standard set of material property tables for the following DCH materials: ZRD, ALD, CRD, FED, ZRO2D, ALOXD, CROXD, and UO2D. These tables include properties for thermal conductivity, specific enthalpy, density, and specific heat at resolutions adequate for most DCH analyses. These tables are included as part of the sample input deck included in the Appendix.

The enthalpy function data in the tables in the Appendix include the heat of fusion associated with debris phase transitions. The specific heat tables are the derivative of the corresponding enthalpy table, but they do not include a representation of a delta function at the phase changes. Debris specific heats are only used in the calculation of the characteristic time constant output variables, while the calculations rely solely upon the enthalpy functions. The delta function was omitted from the specific heat tables because it was discovered that including approximations to the delta function gave unrealistic values for the calculated time constants.

If the user wishes to make his or her own DCH property tables, care should be taken to include the heat of fusion in the enthalpy tables. To avoid numerical difficulties the heat of fusion should be spread over approximately 50 Kelvin. Also, the resolution of the tables in temperature should be approximately every 50 Kelvin.

A few things are important to note about the material property data tables for DCH. First, the oxides ALOXD and CROXD correspond to $\text{AlO}_{1.5}$ and $\text{CrO}_{1.5}$ respectively. These names must be used if CRD and ALD reactive metals are also present. Second, the molecular weight of these oxides must correspond to the species as they are written; for example, the molecular weight of ALOXD must be $\text{MW}_{\text{Al}} + 1.5 \text{ MW}_{\text{O}}$. If oxides of the reactive metals are present in the initial debris sources, the user may employ the standard oxide names (ALOXD, etc) for these sources. Alternatively, if the user wishes to track the oxide introduced as a source separately from that produced by metal reactions, a different name (e.g., AL2O3D) may be assigned. The user must remember, however, that the code will make no connection between the second material and the reactive metal oxide. In this example, the user must define all properties of AL2O3D in addition to those of ALOXD even though they are exactly the same other than molecular weight. Both ALOXD and AL2O3D will be inert material; however, ALOXD will be the oxidation product of ALD metal. In summary, only ZRO2D, ALOXD, CROXD, and FEOD can be used as the ZRD, ALD, CRD, and FED reaction products, respectively.

3.3 Global DHEAT block

The DHEAT block at the global level is used to specify parameters for a CONTAIN DCH run. A counterpart DCH-CELL block at the cell level is also used to specify parameters that pertain to a particular cell. The DHEAT and DCH-CELL block are nearly identical; however, some options are available in DHEAT that are not in DCH-CELL and vice versa. The

CONTAIN DCH Models

Input Instructions

DHEAT block is required in order to perform a direct containment heating calculation. Cell level DCH-CELL input blocks are optional but in reality are usually provided to set the trapping parameters. Some of the parameters in the DHEAT block may also be specified at the cell level in the DCH-CELL block. For these parameters, default values can be specified in the global DHEAT block for all cells, and then cell-specific values can be specified in a DCH-CELL block for one or more cells. DCH-CELL blocks are also needed to specify DCH parameter tables. Unless otherwise specified, the parameters in the global DHEAT block may also be given in the DCH-CELL block where they will only apply to the given cell.

DHEAT

{DIADRP=diadrp **or** DIABIN=(diabin)}
 {FDISTR = (fdistr) **or** FDEVEN}
 [GRPLIM = grplim] [DENDRP = dendrp]
 [RADGAS = radgas] [RADMUL = radmul]
 [DIFO2 = difo2] [DIFH2O = difh2o] [HTCMUL = htcmul]
 [IEQOPT = ieqopt] [THRESH = thresh]
 [LIQSIDE dl1 el1 dl2 el2]
 [RCOMH2 = {ON **or** OFF}]
 [VELOCITY = (velcty)]
 [TRAPRATE = (trprat)]

EOI

DHEAT

initiates the input of DCH parameters for all cells. This is used at the global level.

DIADRP = diadrp

drop diameter for every debris field. The diameter of droplets in every field will be set to the specified value. Drop diameters must be the same in every cell; therefore, DIADRP and DIABIN may not be specified in a DCH-CELL input block. (m)

DIABIN = (diabin)

drop diameter for each field specified individually. Exactly "ndhbin" values must be specified, one for each field. This is the input one uses to specify a particle size distribution for the debris fields. Drop diameters must be the same in every cell; therefore, DIADRP and DIABIN can not be specified in a DCH-CELL input block. (m)

FDISTR = (fdistr)

an array of dimension "ndhspc" by "ndhbin". Exactly this many values must be specified. This corresponds to the matrix

CONTAIN DCH Models

Input Instructions

of $f_{n,k}$ parameters discussed in Section 2.1 and in the debris mass conservation equation (see Equation (16)). "ndhspc" values are specified in the first row, and "ndhbin" rows must be given. The sum of each column should add up to one. If they do not, the code will normalize the values to one. This input can not be specified in the DCH-CELL input block.

FDEVEN

keyword to specify even distribution of debris sources into the fields. This is equivalent to specifying 1/"ndhbin" for each element of "fdistr". This input can not be specified in the DCH-CELL input block.

GRPLIM = grplim

maximum mass of debris allowed to be dispersed into each generation. A new generation is created with "ndhbin" fields when the dispersed mass entering the previous generation has exceeded the allowable limit, "grplim". The number of generations will be limited to the maximum value specified in the global control block, "ndhgrp". Therefore, the mass dispersed into the last generation may exceed the value of "grplim". This input can not be specified in the DCH-CELL input block. Default = 10^{20} (kg).

DENDRP = dendrp

optional user-specified fixed density for all debris fields. If this is omitted, then the density of each field will be computed at each timestep from the density of the species present in the field at that time. The density of each species will be taken from the user-defined RHO or RHOT material table in the USERDAT input block. This input can not be specified in the DCH-CELL input block. (kg/m^3)

RADGAS = radgas

optional radiation blackbody multiplier for radiative heat exchange between the debris and the atmosphere in all cells. This corresponds to debris to gas black body multiplier, $\epsilon_{d,g}$, in Equation (108). This input can also be specified in the DCH-CELL block. The sum of "radmul" and "radgas" should be less than or equal to 1. Default = 1.

CONTAIN DCH Models

Input Instructions

RADMUL = radmul

optional radiation blackbody multiplier for radiative heat exchange between the debris and structure surfaces in all cells. This corresponds to debris to surfaces black body multiplier, $\epsilon_{d,s}$, in Equation (109). The sum of "radmul" and "radgas" should be less than or equal to 1. Default = 0.

DIFO2 = difo2

optional multiplier on the mass transfer coefficient for the transport of oxygen to the surface of drops as determined using the mechanistic mass transfer correlation. This parameter is not shown in Section 2; however, the rate given by Equation (69) is simply multiplied by this value. This parameter can also be specified in the DCH-CELL block. Default = 1.

DIFH2O = difh2o

optional multiplier on the mass transfer coefficient for the transport of steam to the surface of drops as determined using the mechanistic mass transfer correlation. This parameter is not shown in Section 2; however, the rate given by Equation (70) is simply multiplied by this value. Default = 1.

HTCMUL = htcmul

optional multiplier on the convective heat transfer coefficient for the convective transfer of heat between drops and the atmosphere as determined using the mechanistic heat transfer correlation. This parameter is not shown in Section 2.6.1; however, the rate given by Equation (106) is simply multiplied by this value. Default = 1.0.

IEQOPT = ieqopt

optional flag to select alternate treatments for iron/steam equilibrium. A value of 0 means no equilibrium modeling (reaction can go to completion). A value of 1 means that the reaction equilibrium will be evaluated assuming unity for the mole fraction FeO among the oxides. The default value of 2 means that the equilibrium will be evaluated using the calculated mole fraction of FeO. Default = 2.

THRESH = thresh

optional temperature cutoff for chemical reactions for all cells. When the temperature of a debris field in a given cell falls below the "thresh" value, chemical reactions between reactive debris in that field and the atmosphere will be turned off. Default = 1200. (K)

LIQSIDE = dl1,el2,dl2,el2

parameters that specify the temperature-dependent drop diffusivity used in the drop-side diffusion model. These

CONTAIN DCH Models

Input Instructions

parameters are used as shown in Equation (86). This input can also be specified in the DCH-CELL block. Defaults: $dl1 = 10^{-8}$ (m^2/s), $el1 = 0. (K^{-1})$, $dl2 = 0. (m^2/s)$, $el2 = 0. (K^{-1})$ - Note: the default $dl1$ value is potentially non-conservative; therefore, the user may want to specify $dl1 = 0$ to obtain a more conservative result where the diffusion limited drop side model is bypassed.

RCOMH2 = {ON or OFF}

hydrogen recombination keyword followed by the word ON or OFF. The default of ON indicates that hydrogen produced by debris/steam reactions is to be immediately combined with any available bulk oxygen, with the energy being released into the atmosphere. OFF disables this option so that any hydrogen produced will not be immediately combined; however, it may eventually burn if one of the hydrogen burn models are enabled. Default = ON.

VELOCITY = (velcty)

user specified constant relative velocity between debris and the gas for each cell. Exactly "ncells" velocities, one for each cell, are specified following the VELOCITY keyword. This input is provided for compatibility with older input decks and is not recommended. The preferred method is to use the cell-level VELOCITY input to specify the relative velocity between gas and debris. If both the global-level VELOCITY and cell-level USER keywords are given, the cell level input will take precedence.

TRAPRATE = (trprat)

user-specified debris trapping rates for each cell. Exactly "ncells" trapping rates, one for each cell, are specified following the TRAPRATE keyword. This input has the same meaning as the USER="trpval" input in the TRAPPING input block that is specified at the cell level within the DCH-CELL block, except that trapping values for all cells can be specified in one place. If cell-level trapping input is not given, this input is required. This input is provided for compatibility with older input decks and is not recommended. The preferred method is to always specify a cell-level TRAPPING block in the DCH-CELL input. If both the global-level TRAPRATE keyword and cell-level TRAPPING blocks are specified, the cell-level blocks will take precedence in the cells that have them.

EOI

terminator for the global level DHEAT block.

3.4 Cell Level DCH-CELL Input Block

The DCH-CELL block is used to specify DCH parameters specific to a given cell. Therefore, this block need not be given if the parameters in the global DHEAT block do not need to be changed for a given cell. Note, however, that certain important features can only be activated through DCH-CELL input parameters. Perhaps the most important use of the DCH-CELL input is to specify the desired debris trapping model, which cannot be done using the global-level DHEAT input block. *Time dependent parameter tables* (see VAR-PARM below) also must be specified in the DCH-CELL input block. Other uses of the DCH-CELL input block include making parameter changes or disabling certain models such as trapping for a particular cell for a sensitivity study.

The following keywords and associated input in the DCH-CELL input block have the same meaning as they do when given in the DHEAT global block: RADGAS, RADMUL, DIFO2, DIFH2O, HTCMUL, IEQOPT, THRESH, LIQSIDE, RCOMH2, and VELOCITY. Therefore, their input descriptions are not repeated here. The primary difference is that the value specified in the DCH-CELL block applies only to the cell being defined. The only other difference is that only one value is given for the VELOCITY keyword when given in the DCH-CELL block. This one value corresponds to the cell being defined. The values for other cells remain as defined in the DHEAT block or as specified in the DCH-CELL block of other cells.

DCH-CELL

```

[RADGAS = radgas] [RADMUL = radmul]
[DIFO2=difo2] [DIFH2O=difh2o] [HTCMUL=htcmul]
[IEQOPT = ieqopt] [THRESH=thresh] [LIQSIDE dl1 el1 dl2 el2]
[RCOMH2 = { ON or OFF } ] [VELOCITY = velcty]
[ { SDSLIP=(sdslip) or SDEVEN=sdeven } ]
[DIATRAP=diatrp] [VELTRAP=veltrp] [RADTRAP=radtrp]
[TRAPPING
  {GFT or TFI or TOFKU or USER=trpval}
  [{FROMCELL=icell or FROMVENT=ivent}]
  [LEN1=xlen1] [LEN2=xlen2] [LENGFT=xleng] [LEN3=xlen3]
  [KU1=xku1] [KU2=xku2] [SURTEN=surten]
  [RHODG={GAS or MIX}] [VNOST={GFT or CNVEL}]
  [TRAPMIN=trpmin] [TRAPMAX=trpmax] [TRAPMUL=trpmul]
  [COOLFRAC=(cfrac)]]
EOI]
[(VAR-PARM
  [FLAG=iflag]
  [NAME=oname]
  VAR-X=oxvar X=nx (xpts)
  VAR-Y=oyvar Y=ny (ypts)
EOI)]
EOI
*****
```

DCH-CELL

keyword to initiate the input of DCH parameters for a particular cell. Thus, values can be specified in the global DHEAT block for all cells and then a DCH-CELL block can be given at the cell level to specify exceptions for one or more particular cells.

SDSLIP = (sdslip)

slip ratios of gas to debris velocities for each of debris field for debris flow out of the cell. Exactly "ndhbin" values must be specified. The slip ratios apply to flow out of the cell through all flow paths. These values correspond to the s_n slip ratios in the gas and debris flow equations (default=1.)

SDEVEN = sdeven

slip ratio of gas to debris velocities for debris flow out of the cell. This input corresponds to the same parameter as the SDSLIP input, except that only one value is specified and the

slip ratio for all fields is set to this single specified value
(default=1.)

DIATRAP = diatrp

effective diameter for debris chemistry and heat transfer for non-airborne debris (in the trapped field). This diameter is used to calculate the heat and mass transfer rates as long as debris is present in the trapped field. This value can be overridden by a user table (see VAR-PARM below) to obtain time dependent behavior. Unlike the airborne diameters, the trapped field diameter may be different in each cell. (The airborne diameters are restricted to being the same in each cell because mass in the airborne fields can flow between cells.) If the trapped field diameter is zero for a given cell, heat and mass transfer for the trapped field in that cell is disabled. (default=0. m)

VELTRAP = veltrp

user override for the relative gas-debris velocity for the trapped field. If this optional input is omitted the code will use the calculated average gas velocity through the cell for the relative velocity. The specified value or the default can both be overridden by a user table (see VAR-PARM below).
(default=calculated m/s)

RADTRAP = radtrp

black body multiplier for debris to gas radiation heat transfer for the trapped field. Using this parameter allows the trapped field to radiate to the gas. By default this parameter is set to zero thus disabling radiation for trapped debris. The user must specify a value here to enable radiation for the trapped field. Note also that the trapped field does not radiate to structures.
(default=0.)

TRAPPING

keyword to initiate the specification of the trapping model to use to describe debris de-entrainment. If both global and cell-level trapping input are given, the cell-level values in the TRAPPING block override the global level trapping input for that cell only.

GFT

keyword to use the "gravitational fall time" trapping model discussed in Section 2.3.4.

TFI

keyword to use the "time to first impact" trapping model described in Section 2.3.5.

CONTAIN DCH Models

Input Instructions

TOFKU

keyword to use of the "time of flight Kutateladze" trapping model described in Section 2.3.6.

USER = trpval

user-specified constant trapping rate in the cell. If different constant values are to be given for each cell, this input can be given in separate DCH-CELL blocks; alternatively, the TRAPRATE option can be used in the global DHEAT input block. Note that time-dependent "trpval" values may also be specified using VAR-PARM tables as described below.
Default = 0. (s⁻¹)

FROMCELL = icell

the regular flow path to use for the primary flow of debris into the cell. This path is identified by cell "icell" at the other end of the flow path. The flow rate through this flow path is used to calculate various flow parameters, including the debris velocity, in the TFI and TOF/KU trapping models as described in Section 2.3.5 and 2.3.6. This input is optional, if not specified the code will set "icell" or "ivent" equal to the cell where the most mass flux is flowing from.

FROMVENT = ivent

the engineered vent flow path to use for the primary flow for debris into the cell. The integer "ivent" is a vent number, not a cell number. The flow rate through this flow path is used to calculate various flow parameters, including the debris velocity, in the TFI and TOF/KU trapping models as described in Section 2.3.5 and 2.3.6. This input is optional, if not specified the code will set "icell" or "ivent" equal to the cell where the most mass flux is flowing from.

LEN1 = xlen1

the distance to first impact that is used in the TFI and TOF/KU trapping models to calculate flight time. Default = cell height if non-zero height is specified in the GEOMETRY input, and the cube root of the cell volume if height is specified to be zero. (m)

LEN2 = xlen2

the distance to second impact that is used in the TOF/KU trapping model to calculate flight time. Default: same as described under LEN1 above. (m)

LENGFT = lengft

gravitational fall distance used in the GFT, TFI, and TOF/KU trapping models. Default: same as described under LEN1 above. (m)

CONTAIN DCH Models

Input Instructions

LEN3 = xl3	third length considered in the TOF/KU trapping model. Default: same as "lengft". (m)
KU1 = xkul	Kutateladze number cutoff for the first impact used in the TOF/KU trapping model. Values of the calculated Kutateladze number greater than the value of "xkul" indicate that debris remains airborne after the first impact. Default = 10.
KU2 = xku2	Kutateladze number cutoff for the second impact used in the TOF/KU trapping model. Values of the calculated Kutateladze number greater than the value of "xku2" indicate that debris remains airborne after the second impact. Default = 10.
SURTEN = surten	the debris surface tension used in the evaluation of the Kutateladze number for the TFI and TOF/KU trapping models. Default = 1. (N/m)
RHODG = {GAS or MIX}	specifies whether debris is to be included in the upstream and downstream densities in evaluating the Ku number. The default is to exclude the debris, although MIX may be a more reasonable option. The MIX option is also the more conservative of the two. Thus, the use of RHODG=MIX is recommended even though it is not the default for upward compatibility reasons. (Default = GAS)
VNOST = {GFT or CNVEL}	specifies whether or not GFT rules apply after the second impact if the Ku re-entrainment criterion is met. Default = CNVEL.
TRAPMIN = trpmin	the smallest allowable value of the trapping rate. Smaller values calculated by any of the trapping model methods will be overridden by the specified value. Default = 0. (s ⁻¹)
TRAPMAX = trpmax	the largest allowable value of the trapping rate. Larger values calculated by any of the trapping model methods will be overridden by the specified value. Default = 10 ²⁰ . (s ⁻¹)
TRAPMUL = trpmul	a multiplicative factor for the calculated trapping rate. Whether trapping is specified as a constant rate or calculated using one of the provided models, the trapping rate will be multiplied by the value of "trpmul" and then limited to "trpmin" or "trpmax" range. Default = 1.

CONTAIN DCH Models

Input Instructions

COOLFRAC = (cfrac)

the fraction of trapped debris to send to the atmosphere, structure surfaces, and the uppermost intermediate layer. Thus, exactly $1 + "nhtm" + 1$ values must be given, where *nhtm* is the number of structures in the cell, and the two "1"'s corresponds to the atmosphere and the uppermost lower cell layer. At present, only the last value is used by the code, which corresponds to f_{LC} lower cell layer fraction described in Section 2.3.1. Note that this fraction only affects the non-airborne debris field if there is an intermediate lower cell layer. Any debris placed there will not be placed in the non-airborne debris field. The default for this fraction is 0. for all entries.

VAR-PARM

optional keyword to initiate a table for various direct heating parameters described above. VAR-PARM tables are used to specify time- or temperature-dependent direct heating parameters. Any number of tables may be given, with each one initiated with the VAR-PARM keyword and terminated by an EOI. The total number of VAR-PARM tables plus other cell-level user tables must not exceed the value of the cell control parameter "numtbc", and the number of points in any one table may not exceed the value of the cell control parameter "maxtbc".

FLAG = iflag

optional flag indicating the interpolation option for the parameter table. A value of 1 is for step interpolation, and 2 is for linear interpolation. Default = 1.

NAME = oname

the optional name for the table.

VAR-X = oxvar

the independent variable. This input is required for VAR-PARM DCH tables, and "oxvar" must be TIME for the problem time.

VAR-Y = oyvar

the dependent variable. This input is required for VAR-PARM DCH tables. The names of any one of the following DCH-CELL keywords may be specified: DIADRP, DENDRP, THRESH, RCOMH2, DIFO2, DIFH2O, HTCMUL, RADMUL, RADGAS, DL1, EL1, DL2, EL2, VELOCITY, TRAPRATE, SURTEN, LEN1, LEN2, LEN3, LENGFT, KU1, KU2, DIATRAP, VELTRAP, and RADTRAP. The values specified in the table will replace the values given for the associated keyword. Two things are worth noting about the use of VAR-

PARM tables. First, if RCOMH2 is the dependent variable, any value greater than 0.5 will be interpreted as ON. Second, the values specified for the dependent variable will be used for all debris fields, except for the xxxTRAP variables which apply to the trapped field only. This means that the VAR-PARM tables are of limited use for the dependent variables that are field dependent, such as DIADRP, DENDRP, VELOCITY, and TRAPRATE.

X = nx	the number of independent variable values in the table.
xpts	"nx" values of the independent variable.
Y = ny	the number of dependent variable values in the table. The value of "ny" should be equal to "nx".
ypts	"ny" values of the dependent variable.
EOI	terminator for the DCH-CELL input block. A separate terminator is required for the TRAPPING block and for each VAR-PARM table.

3.5 Debris Dispersal, Debris Entrainment, and Gas Blowdown Sources

User-supplied source tables are specified in a DCH calculation to simulate the debris dispersal phase of a high pressure melt ejection event. Typically, side calculations using simple correlations are used to determine the dispersal rate. The dispersed mass is typically assumed in a plant calculation and known a priori in an experiment analysis. DCH source tables have the following format

```
*****
SOURCE=nso
(lename=n
  DCHTYPE={TRAPBIN or ENTRAIN or AIRBORNE}
  [DCHBIN=nfield]
  [IFLAG=ival]
  T=(times)
  MASS=(masses)
  [TEMP=(temps)]
  EOI)
*****
```

With the exception of the DCHTYPE and DCHBIN keywords, this format is the same as the format used to specify atmosphere material sources. One other difference is that DCH tables must use temperature; specific enthalpy cannot be used. DCH source tables are included in the atmosphere source table input block as additional entries along with any other atmosphere source material. Descriptions for the standard source table keywords can be found in the CONTAIN User's Manual [Mur89].

DCHTYPE

keyword to specify the type of DCH source table. This keyword is only allowed if "oname" is the name of a DCH material as defined in the USERDEF block. If TRAPBIN is specified, the source enters the non-airborne field. If ENTRAIN is specified, the debris is entrained out of the non-airborne field at the rate specified. Temperature and specific enthalpy inputs have no effect on DCH tables that have DCHTYPE=ENTRAIN because the entrained debris is assigned the temperature of the non-airborne field. If AIRBORNE is specified, the debris enters the airborne fields. In both the ENTRAIN and AIRBORNE cases the debris is partitioned into fields according to the FDISTR input given in the global DHEAT block.

DCHBIN=nfield

a specific field that the debris in the source table will enter. This input is not allowed if DCHTYPE=TRAPBIN. If this optional input is not given, the debris in the table will be distributed among fields according to the FDISTR input given in the global DHEAT block.

The following types of source tables are typically specified to represent the dispersal and entrainment phases of DCH. First, molten debris ejected from the RPV is modeled as a group of user-defined debris tables into the cavity trapped field. This is accomplished by specifying DCHTYPE=TRAPBIN as noted above. At least one separate table is required for each debris material. The timing of this table is not critical as long as the source table ends prior to the time gas blowthrough is assumed to occur. The FDISTR array has no effect on these source tables and the DCHBIN input is not allowed for these source table types. Second, a group of tables is specified to represent the entrainment rate of debris out of the trapped field. Again, at least one separate table must be given for each debris species that is to be entrained from the trapped field. This is accomplished by specifying the DCHTYPE=ENTRAIN in the source input block. The entrained mass will be divided among the various airborne fields according to the FDISTR array. If the DIABIN option is used the entrained mass will be placed into a specific airborne field. DCH source tables used as an entrainment rate from the trapped field only use the specified mass, since the temperature of the entrained debris will be the temperature of the trapped field. Appropriate checks are made to ensure that the specified entrainment sources do not exceed the available mass in the trapped field. Under the above

described scheme the trapped field in the cavity holds debris that has not yet been entrained. The debris source table feature is general enough to introduce debris directly into the atmosphere of the cavity or any other cell. This is done by specifying DCHTYPE=AIRBORNE or by omitting the DCHTYPE keyword altogether.

Gas Blowdown Sources

The blowdown of gases from the vessel can be treated using either of the following two approaches. The first approach is simply to specify the gas blowdown using user-defined source tables just like the debris dispersal. The materials named in the blowdown tables are standard CONTAIN materials such as H2OV or H2 and should not be specified as user-defined materials with a phase of DEBRIS. If this method is used, the gas blowdown rate is governed by the manually specified source tables. As with the debris, the gas blowdown sources may be represented in any number of source tables.

The second approach that can be used to model the gas blowdown is more involved, but also potentially more realistic, since it will provide inlet gas velocities to the cavity cell. In this approach one includes in the CONTAIN control volume nodalization one or more cells corresponding to the reactor pressure vessel. The hole in the bottom of the lower head that initiates the DCH event is then modeled as a variable area flow path between the RPV cell and the cavity cell. When using this approach to model the gas blowdown, the following should be considered. The opening of the hole must be timed to match the occurrence of gas blowthrough. The debris dispersal source tables described above must also be coordinated with this timing. Typically, side calculations are used to predict the timing of gas blowthrough and the RPV ablation rate which is used to determine the time-dependent area of the hole after blowthrough occurs. One approach for performing such calculations is provided by the work of Pilch and Griffith [Pil92]. Time-dependent areas are specified using the VAR-AREA input in the FLOWS or the AREA-T keyword in the ENGVENT input block as described in the CONTAIN 1.1 User's Manual [Mur89].

The conditions of the RPV, including the steam and hydrogen inventories should be initially set to the vessel conditions. In setting these conditions, errors in the total blowdown mass will result if the default CONTAIN ideal equation of state for steam is used. This can be compensated for by increasing the volume above the actual value. This increase in volume is important to match both the steam mass and the RPV pressure. A recent addition to the CONTAIN code has provided a realistic equation of state for steam, which if used will avoid the need to use the above work-arounds.⁴

⁴Murata, K. K., "Code Change Document for UPDATE C11AA: Realistic Equation of State for Steam," a letter report to USNRC, January, 1994.

3.6 Miscellaneous DCH Related Input.

This section describes the remaining DCH related input requirements and options.

3.6.1 Aerosol Condensation Override.

It may be desirable in a DCH run to disable steam condensation onto aerosols in one or more cells without affecting the other condensation models in CONTAIN. This is most useful when a CONTAIN cell is used to model the RPV to treat blowdown steam as discussed in Section 3.5. The advantage of skipping condensation is that computational time is not wasted evaluating condensation and evaporation equations under conditions where these phenomena will not occur. A new keyword has been added to the global aerosol block for this purpose.

AEROSOL

[NOCONEVA [(ncls)]]

NOCONEVA = (ncls)

keyword to disable aerosol condensation and evaporation for the specified cells. If the NOCONEVA keyword is given alone, aerosol condensation and evaporation in all cells will be disabled. A list of cell numbers, "ncls", can be specified following the NOCONEVA keyword to disable condensation and evaporation in just those cells.

3.6.2 Fixed Gas Emissivity Option.

A user-specified constant gas emissivity option has been added to the radiation input, RAD-HEAT, that is only available in a DCH calculation. This option is provided so that the effect of airborne debris on the gas emissivity, if known, may be accounted for by manually overriding the value determined by the Cess-Lian or Modak correlations. The utility of this option is somewhat limited by the fact that the user-specified emissivity must be a constant value for the entire calculation.

RAD-HEAT

KMX = -emix

EOI

KMX = -emix

a negative value that overrides the calculated gas emissivity. The input must be specified as the negative of the desired gas mixture emissivity as shown. The negative sign is required since the KMX keyword followed by a positive number is used as an aerosol density multiplier as described in the CONTAIN User's Manual.

3.6.3 Relevant Structure Input.

None of the input options in the structure (STRUC) input module are DCH-specific; however, there is one potentially important part of the STRUC block that must be taken into *consideration in a DCH calculation*. The most fundamental consideration is the order in which the structures are defined in a cell. The order is important because the trapping model uses the calculated forced convection velocity across the face of the first two structures in the TOF/KU trapping model as described in Section 2.3. If there are no structures in the cell, the TOF/KU trapping model will be bypassed and the GFT trapping rate will be used. If only one structure is in the cell, then the trapping model will use the velocity for the first structure for both impacts considered by the TOF/KU model.

3.6.4 DCH Restart Input.

Direct heating calculations may be restarted like any other CONTAIN run. Any of the parameters in the DHEAT block may be changed in a restart run, or direct heating processes may be disabled altogether. Once DCH is disabled in a restart run, it cannot be re-enabled in a subsequent restart calculation.

If the DHEAT keyword is left out of the restart input deck, the calculation will restart with the same direct heating parameters as the parent run. If the DHEAT keyword is given, it must be followed by the word "ON" or "OFF". If "OFF" is specified, no further DHEAT input will be accepted and all direct heating processes will be disabled for the restart run. If "ON" is specified, any or all of the originally specified DHEAT input parameters may be re-specified and altered. Parameters not re-specified will assume the value that was given in the parent run. The recommended procedure is to copy the DHEAT input block from the parent run and then modify only those parameters that need to be changed for the restart run. The format of a direct heating restart run is briefly outlined below. Note that both the global and cell level DCH parameters can be changed in a DCH restart run. The general format of the CONTAIN restart input is described in further detail in the CONTAIN 1.1 User's Manual [Mur89].

Global and cell-specific changes may be made in a restart run using the DHEAT and DCH-CELL keywords, respectively. Both input blocks are given at the global level.

```
*****
```

```
CRAY
```

```
RESTART
```

```
TIMES cput tstart (timinc edtdto tstop)
```

```
...
```

```
DHEAT={OFF or ON (...)}
```

```
...
```

```
DCH-CELL=ncell {OFF or ON (...)}
```

```
...
```

```
EOF
```

```
*****
```

Any of the input parameters that can be specified in a parent run may also be specified in a restart except for additional parameter tables. New VAR-PARM tables cannot be specified nor may any existing direct heating VAR-PARM tables be modified in a restart input deck. Any VAR-PARM tables specified in the parent run will remain in effect in the restart run.

4. Generated Output

The first subsection below describes the output generated in a DCH run in the main CONTAIN ASCII output file, called "output". Section 4.2 describes the binary records written onto the plot file called "pltfil". The CONTAIN post-processor, POSTCON, has been modified to read these records and produce formatted tables and plots. Therefore, this information is not needed to use post-process CONTAIN results. It is included here for completeness sake only.

4.1 Output file

DCH calculations with CONTAIN automatically generate three output tables for every cell during a long print edit: a mass table by field and species, a trapping information table, and an effective DCH time constant printout. There is not a flag to control whether or not this output is generated; if the calculation includes DCH modeling then the output will always be generated. The frequency of the output is governed by the standard output edit parameters described in the CONTAIN 1.1 User's Manual. The DCH tables are printed immediately following the atmosphere material mass output table. All of the DCH output tables are self-explanatory, and is therefore not described in any detail here. Most users will find it more efficient to use the CONTAIN post-processing program, POSTCON, to examine DCH output. The following section describes the information that is written to the binary plot file. This is the file that POSTCON uses to generate concise tables and plots.

4.2 Plot file

The following flags associated with DCH are written onto the CONTAIN binary plot file. The POSTCON code [Was87] is used to process this file. Upgrade 1.04D⁵ to the POSTCON code or later is required to read the flags listed below.

The records written to the plot file are shown below in a format that shows the order that the variables are written. Arrays are shown as the variables with the number of elements written in parentheses. For example, 20 elements of the variable x would be shown as x(20). Variables that start with "o" are character*8 variables, variables that start with "i" through "n" are integers, and anything else is a floating point real. The character variable "oblank" is a blank character*8 word.

DCH Control: oflag = 16

```
oflag,oblank,ndhspc,0.0
oblank,oblank,ndhspc,ndhbin,ndhgrp,nfields,kmapd(ndhspc)
```

This flag is a control flag that POSTCON 1.04D and later reads to obtain the number of bins, generations, fields, and species modeled in the DCH calculation. "Ndhspc", "ndhbin", "ndhgrp" are the variables specified in the global control block, and "nfields" is the product, "ndhbin" * "ndhgrp". The "nfields" variable corresponds to N_{fields} in the earlier sections. The two copies of "ndhspc" should equal each other. The copy is provided in the first record so that POSTCON can use it to read the array in the second record. The last variable is an integer array of pointers into the master material property list. This list is used to obtain the names and material properties of the species. For example, if ZRD is the 19th material in the master CONTAIN list, but the first material among the DCH species, then kmapd(1) = 19. The master CONTAIN list will be longer than the DCH list because it includes non-DCH materials, such as gases, concrete, and water.

DCH Time Constants: oflag = 109

```
oflag,oblank,ncell,0.0
oblank,oblank,timcon(20)
```

The "timcon" variable contains the time constants shown in Section 4.1. Although 20 numbers are printed, only certain elements of this array are meaningful. Also, the 19th and 20th elements of this array are not time constants. They are included in this flag because of their use in evaluating the time constants. The meanings of the array elements are as follows:

⁵ K. C. Rentczsh, "Upgrade 1.04D to the POSTCON code," letter report to the USNRC, August, 1993.

CONTAIN DCH Models

Generated Output

- 1 average debris trapping
- 2 average debris/gas convection
- 3 average debris/gas radiation
- 4 average debris/gas total heat transfer
- 5 average debris chemical reactions (mass basis)
- 6 average debris/wall direct radiation
- 7 fastest bin debris trapping
- 8 fastest bin debris/gas convection
- 9 fastest bin debris/gas radiation
- 10 fastest bin debris/gas total heat transfer
- 11 fastest bin debris chemical reactions (mass basis)
- 12 atmosphere cloud to structure heat transfer
- 13 gas transport into/out of cell
- 14 debris transport into/out of cell
- 15 - 18 unused
- 19 total gas heat capacity
- 20 total debris heat capacity

The average time constants include the effects of all debris fields, while the fastest time constants only reflect the field that has the smallest time constant for that process. The field number for one process does not have to be the same as another.

DCH Average Temperature: oflag = 131
 oflag,oblank,ncell,tdavg

This flag writes the average temperature, "tdavg", of all airborne debris. This is the same temperature that is written to the output file at the bottom of the DCH mass output table. As noted earlier, physically this temperature is the temperature that would result if one lumped all the airborne debris into a single field.

DCH Total Airborne and Trapped Mass and Energy: oflag = 132
 oflag,oblank,ncell,0.0
 oblank,oblank,totmas,totent,trpmas,trpent,trptmp,binmas(4)

This flag includes a variety of DCH output variables involving totals. The first two, totmas and totent, are the total airborne mass and enthalpy for all fields. The next two, trpmas and trpent, are the total trapped mass and enthalpy. The next variable, trptmp, is the temperature of the trapped debris. The last variable is an array for the trapped mass by repository type. The first three entries are correspond to the three repositories in order. The last entry is the sum of the first three. This value should always match the value of the "trpmas" variable.

DCH Trapped Mass and Energy by Species: oflag = 133

CONTAIN DCH Models

Generated Output

oflag,oblank,ncell,0.0
oblank,oblank,trpmas(ndhspc),trpent(ndhspc)

The mass of material trapped in the cell by species type is given by the first array, "trpmas". The enthalpy of the trapped debris associated with that species is given by the second array, trpent.

DCH Field Specific Temperature: oflag = 134

oflag,oblank,ncell,ssdch
oblank,oblank,tdfield(nfields+1)

The "ssdch" parameter in the first record is a real number that POSTCON 1.04D and later uses to properly read the multifield related flags. The "tdfield" array is the temperature of each field. This includes each debris field and generation. The order of the array is as follows: the first "ndhbin" temperatures are written for the first generation, following by subsequent groups of temperatures, until "ndhgrp" groups have been written to give a total of "nfields" numbers. The last element of this array is for the non-airborne debris field.

The next three flags follow the same format and layout as this flag, where "ssdch" is also written in the first record, and an array of size "nfields"+1 is written to the plot file.

DCH Field Specific Area: oflag = 135

oflag,oblank,ncell,ssdch
oblank,oblank,adrop(nfields+1)

The layout of this flag is identical to flag '134'. The difference is that this flag writes the array of total area of each debris field, adrop.

DCH Field Specific Total Mass: oflag = 136

oflag,oblank,ncell,ssdch
oblank,oblank,totmas(nfields+1)

The layout of this flag is identical to flag '134'. The difference is that this flag writes the array of total mass of debris in each field, totmas.

DCH Field Specific Total Enthalpy: oflag = 137

oflag,oblank,ncell,ssdch
oblank,oblank,totent(nfields+1)

The layout of this flag is identical to flag '134'. The difference is that this flag writes the array of total enthalpy of each debris field, tentent.

DCH Field Specific Masses by Species: oflag = 138
oflag,oblank,ncell,ssdch
oblank,oblank,dchmas(ndhspc,nfields+1)

This flag writes the main two-dimensional array that holds the mass of debris by species in each debris field. The fastest running element of this array is the species number. For example, all of the DCH species masses are written for the first debris field, followed by the species masses for the second field, and so on. The last group of species masses written is for the non-airborne debris field.

5. Demonstration Calculations

The purpose of this section is to demonstrate the key aspects of the DCH models in CONTAIN and to illustrate how the input elements are typically arranged. It is not the intent of this section to document the assessment of the DCH models. The models described in the previous sections have been assessed against a significant portion of the available DCH experimental database. Included in this assessment are the LFP [All91] and WC tests [All92a], the 1/10th scale Zion geometry SNL integral effects tests [All92b-e, All93a-b], 1/40th scale Zion geometry ANL integral effects tests [Bin92a-d], and 1/6th scale Surry geometry SNL integral effects tests [Bla93]. The results of this assessment are being documented in a separate report⁶. This report includes a description of a standard CONTAIN DCH input prescription, detailed interpretation of the assessment calculations performed, and the results of numerous sensitivity calculations using the CONTAIN DCH models. The key results from this work are shown in Figure 2 and Figure 3. These figures show the agreement obtained between CONTAIN and the test data for vessel pressurization and hydrogen generation. These results were obtained using a standard input prescription for the CONTAIN DCH and hydrogen burning models. A detailed description of this prescription is beyond the scope of this report; however, it is included in the IET-6 input deck included in the Appendix.

CONTAIN calculated results for the IET-6 experiment [All93a] are shown in more detail in the remainder of this section. The input deck for this analysis is given in the Appendix. The DHEAT, DCH-CELL, and H-BURN blocks in this input deck include the standard prescription input parameters recommended in the previously footnoted report by Williams et al. A schematic of the nodalization used in this analysis is shown in Figure 4. The volumes of each cell are shown in the center of each box in this figure, the flow path areas shown next to the lines depict the flow path, and the cell numbers are written in the lower right hand corner of each box. Note that the figure is not drawn to scale and the lengths of the flow

⁶D. C. Williams, R. O. Griffith, E. L. Tadios, and K. E. Washington, "Assessment of the DCH Models in CONTAIN," SAND94-1174, to be published.

paths are not indicated by the lengths of the lines. The locations of the boxes are approximately correct with respect to the actual location of the rooms the cells represent.

Figure 5 shows the calculated pressure as a function of time for the IET-6 experiment. This figure shows that the peak load is predicted to occur at approximately 4.5 seconds, after which time the pressure decreases because of heat losses to the surrounding structures. The cavity pressure is also shown on this figure. As expected, the pressure in the cavity exceeds that in the rest of the vessel during the debris entrainment period. Because the duration of the entrainment period was set in this calculation to match the observed duration in the experiment, the duration of the cavity pressure spike in this experiment is very similar to what was observed in the test. It is also worth noting that no FCI spike is shown in Figure 4 because this phenomena is not represented in the CONTAIN DCH models.

Figure 6 shows temperatures predicted in various rooms. The room names match those given in Figure 4. The temperatures in Figure 6 show the expected trend that the upper dome is substantially cooler than the subcompartments. In particular, cell 5 is the hottest as expected since debris enters this cell first as it leaves the cavity and chute. As the debris travels further downstream, there is less of it airborne, and what amount is airborne is cooler. Therefore, the cells further downstream from the basement cell 5 are progressively cooler during the debris entrainment period. After about 2 seconds, the temperatures are driven more by the interaction of the blowdown gas with non-airborne debris, combustion phenomena, and heat transfer processes within each cell. One can see from this curve that the TOF/KU model results in a small debris carryover fraction to the upper dome. This prediction is consistent with what has been observed in the Zion IET tests [All93a].

Figure 7 shows the non-airborne debris mass in various locations as a function of time. This figure demonstrates the debris trapping model and the table options for representing debris discharge from the RPV and entrainment. The cavity curve shows that debris was assumed to discharge from the RPV linearly over the first 0.3 seconds, at which time gas blowthrough is assumed to occur. From 0.3 to 1.0 seconds, the mass of non-airborne debris in the cavity decreases as expected as debris is entrained into the atmosphere. This was done using a user specified entrainment rate table as shown in the input deck included in the Appendix. As debris is entrained into the atmosphere, it flows into the subcompartments where the majority of it is trapped during the first second. This is shown by the rate at which the non-airborne debris mass curve for the subcompartments reaches a plateau. The final curve on this figure shows the small fraction of debris that is calculated to transport outside of the subcompartments.

Figure 8 shows the mass of Fe and FeO in two different cells. These results demonstrate the debris flow model and the chemistry model. Comparing the mass of Fe in Basement B (cell 5) to the mass of Fe in Basement D (cell 9), one can see the effect that transport distance has on airborne debris masses as captured by the model. As expected, the peak mass of airborne

Fe and FeO in Basement D is slightly shifted to the right in time from the peak mass of airborne Fe in Basement B. Note also that the magnitude of the Fe mass curve is smaller in Basement D than it is in Basement B because of Fe trapping and chemical reactions upstream from Basement D. This is expected because Basement D is further downstream from the cavity than Basement B. (Note that Basement D is several times the volume of Basement B.)

Hydrogen burning and inventory in the vessel are shown in Figure 9. This figure is used to demonstrate the DFB and BSR burning models in the code. One can see from the first four seconds of the hydrogen inventory and burning curves that most of the hydrogen produced burns. The burning mode of this hydrogen is as a continuous flame as it flows into the upper dome of the vessel as represented by the CONTAIN DFB model. This is confirmed by Figure 6 that shows that dome temperatures too low to result in bulk spontaneous recombination. In the first second of the calculation, a significant fraction of the produced hydrogen is not burned. This is shown in Figure 9 by the increase in the total hydrogen inventory curve during the first second. This is explained by the fact that the produced hydrogen transports to lower subcompartment volumes that quickly become oxygen starved. At four seconds, some of the hydrogen in the formerly oxygen-starved subcompartments begins to burn. This happens because natural circulation causes oxygen to be circulated to the subcompartments. This is shown in Figure 9 by the initiation of the increase in the subcompartment burning curve and the decrease in the total hydrogen inventory curve after about four seconds. It is worth noting that the hydrogen burns in the subcompartments after four seconds in BSR mode. From Figure 6 one can clearly see that the temperature threshold for the BSR model has been reached in the subcompartments. Notice, however, that this recombination has a small effect on the peak load in this case since the peak load is predicted to occur only slightly after four seconds.

CONTAIN Assessment: DCH Delta-P
Case 1: NAD Cavity & Subcomp., Slip=1

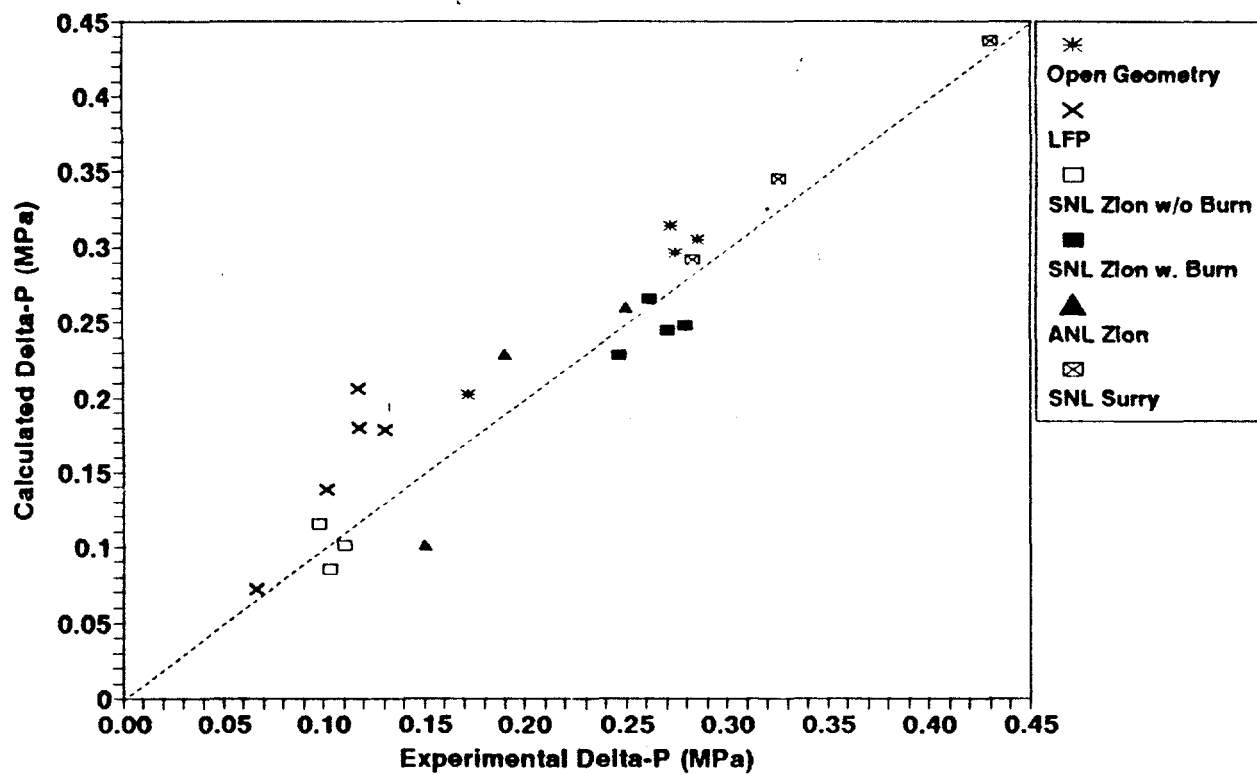


Figure 2. Pressure Results From CONTAIN Assessment

CONTAIN Assessment: Scaled H₂ Produced
Case 1: NAD Cavity & Subcomp., Slip = 1

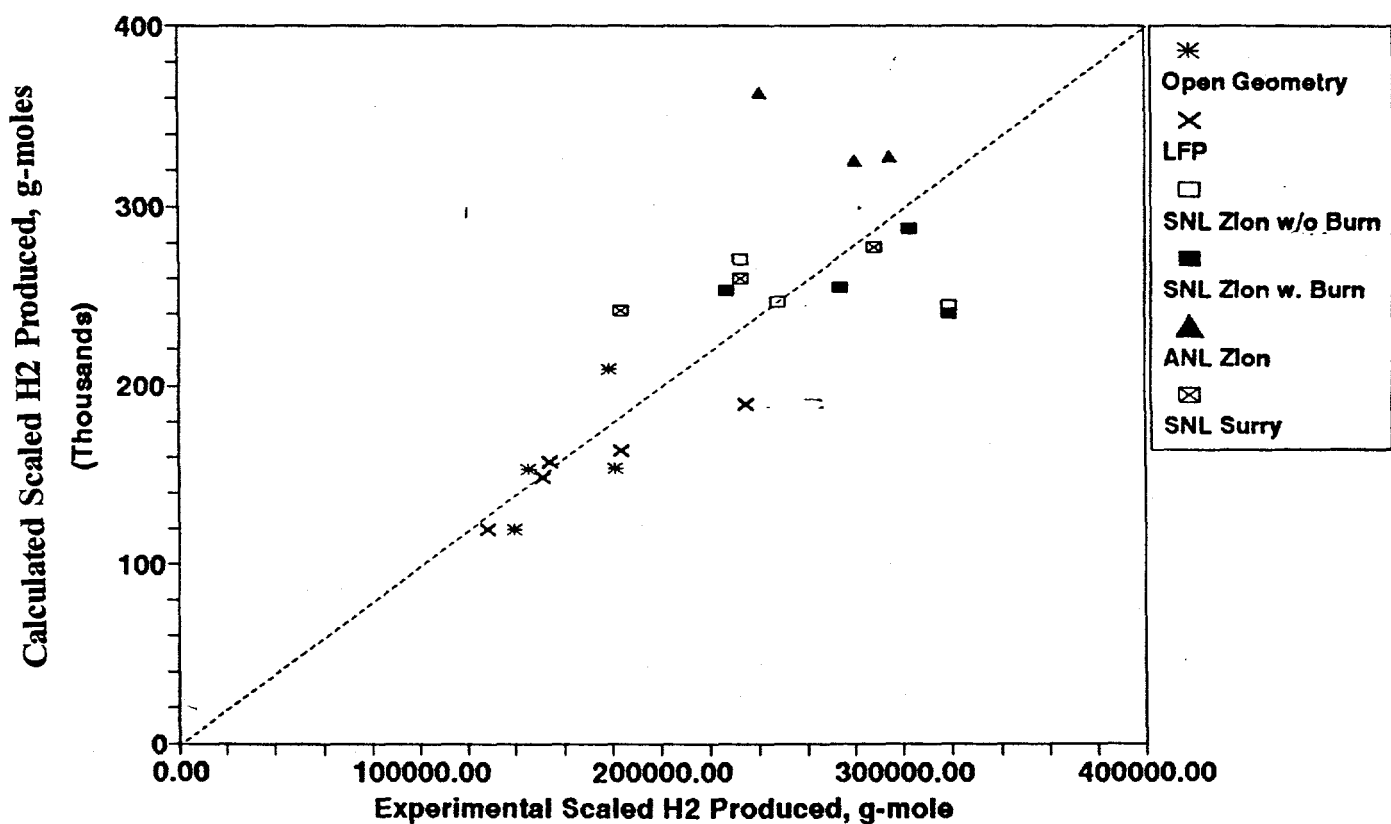


Figure 3. Hydrogen Production Results From CONTAIN Assessment

**CONTAIN 14 Cell Nodalization
Of The Surtsey Zion Configuration**

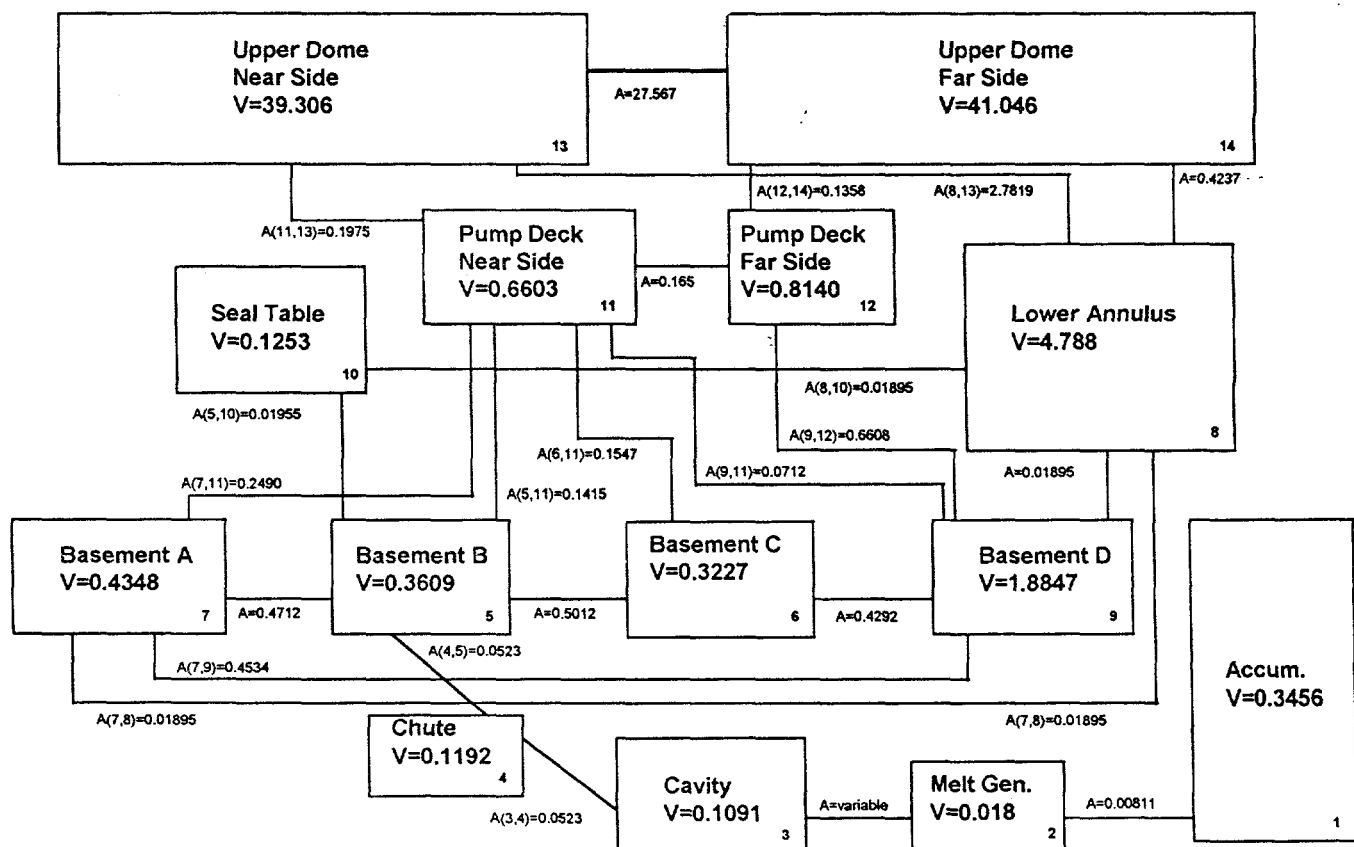


Figure 4. CONTAIN Nodalization of Zion Geometry Integral Effects Tests in Surtsey

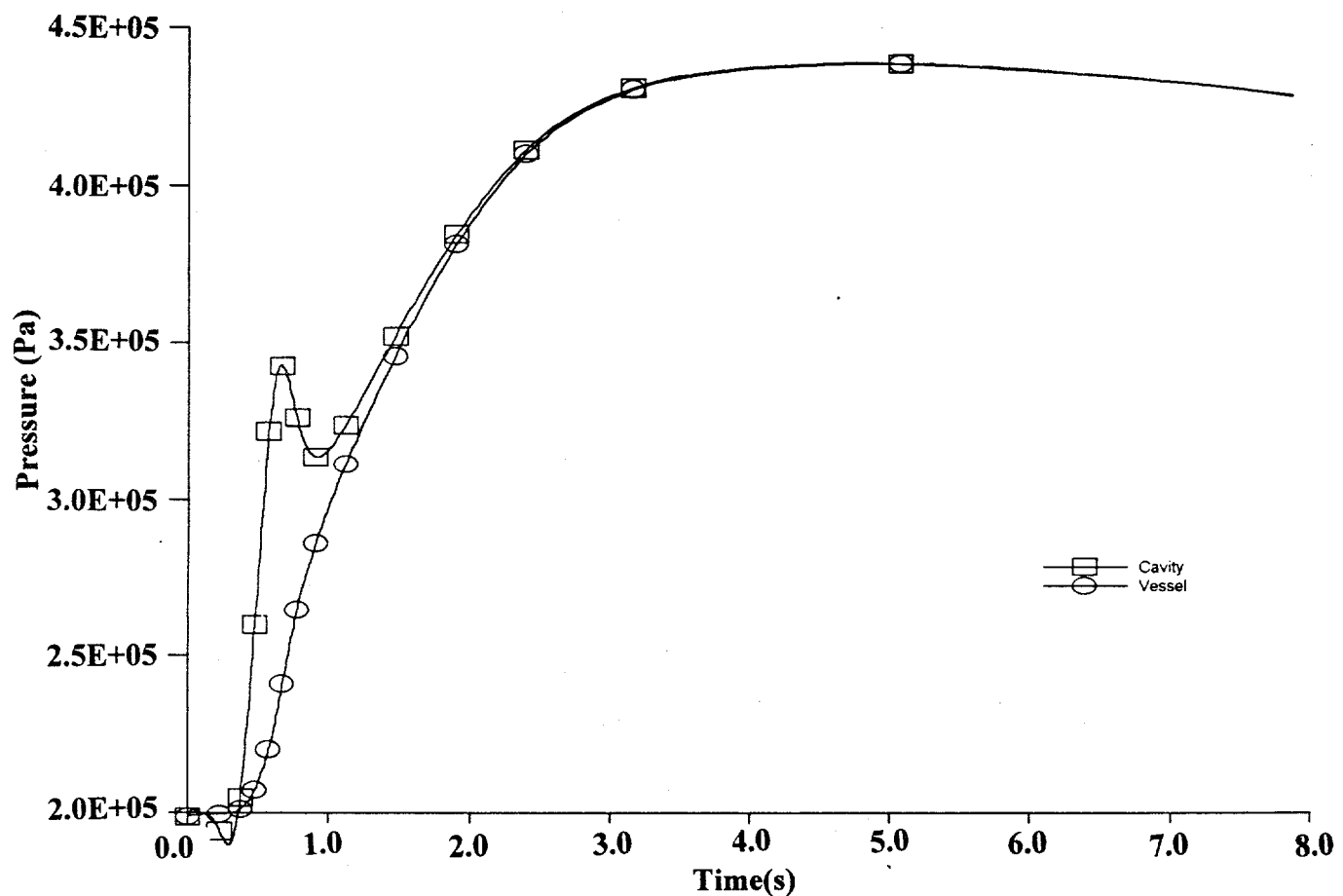


Figure 5. IET-6 Pressure CONTAIN Results

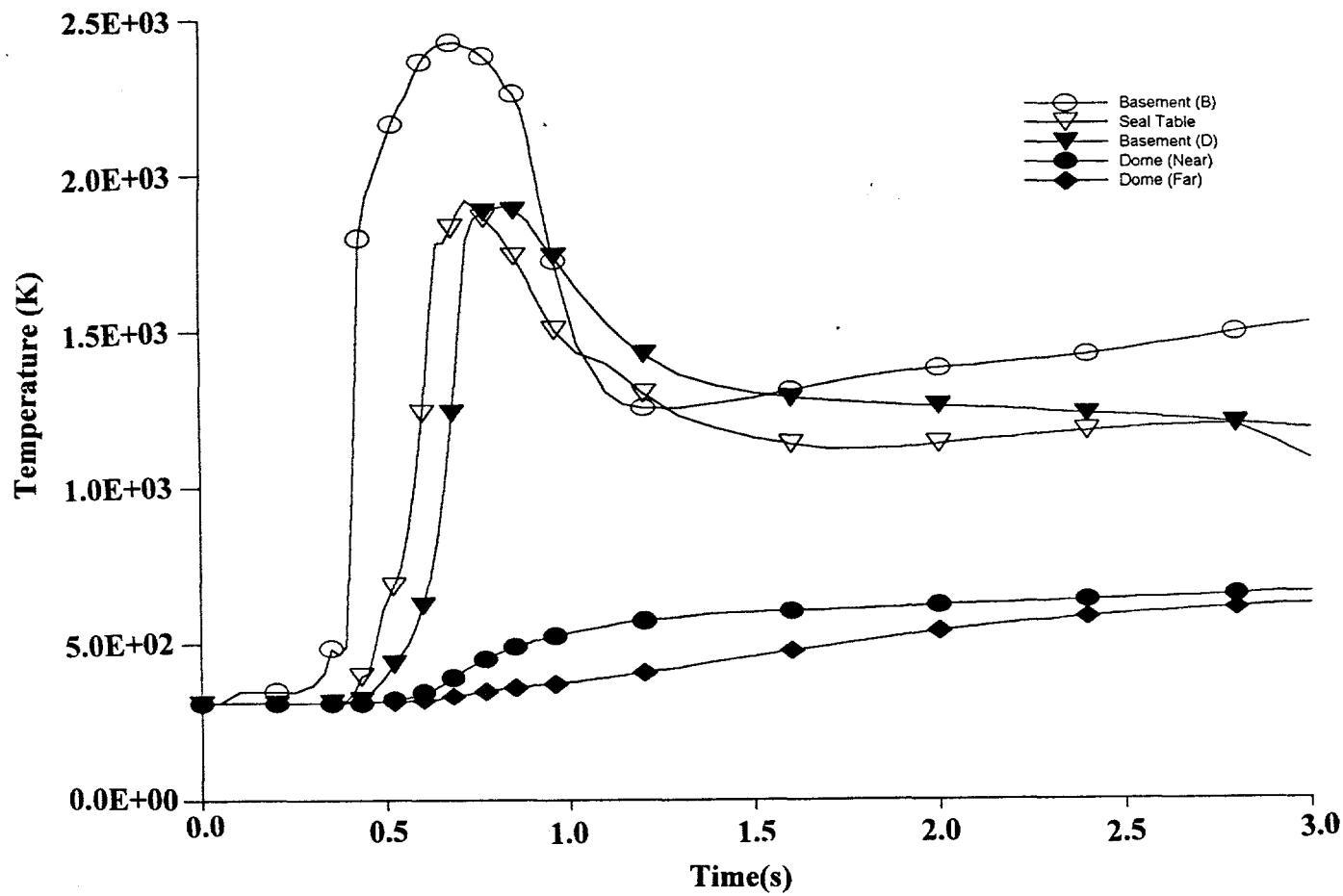


Figure 6. IET-6 Temperature CONTAIN Results

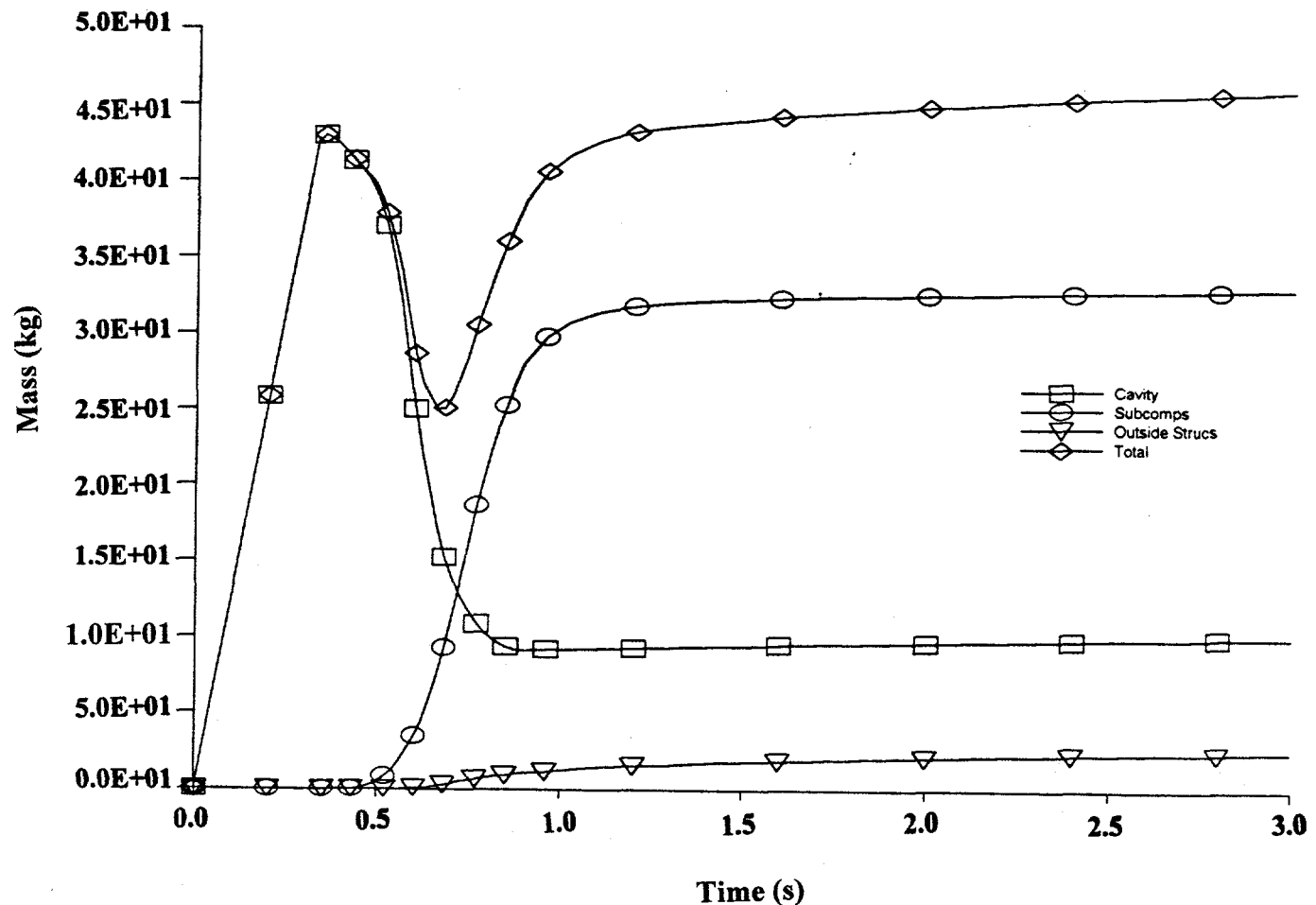


Figure 7. IET-6 Debris Trapping CONTAIN Results

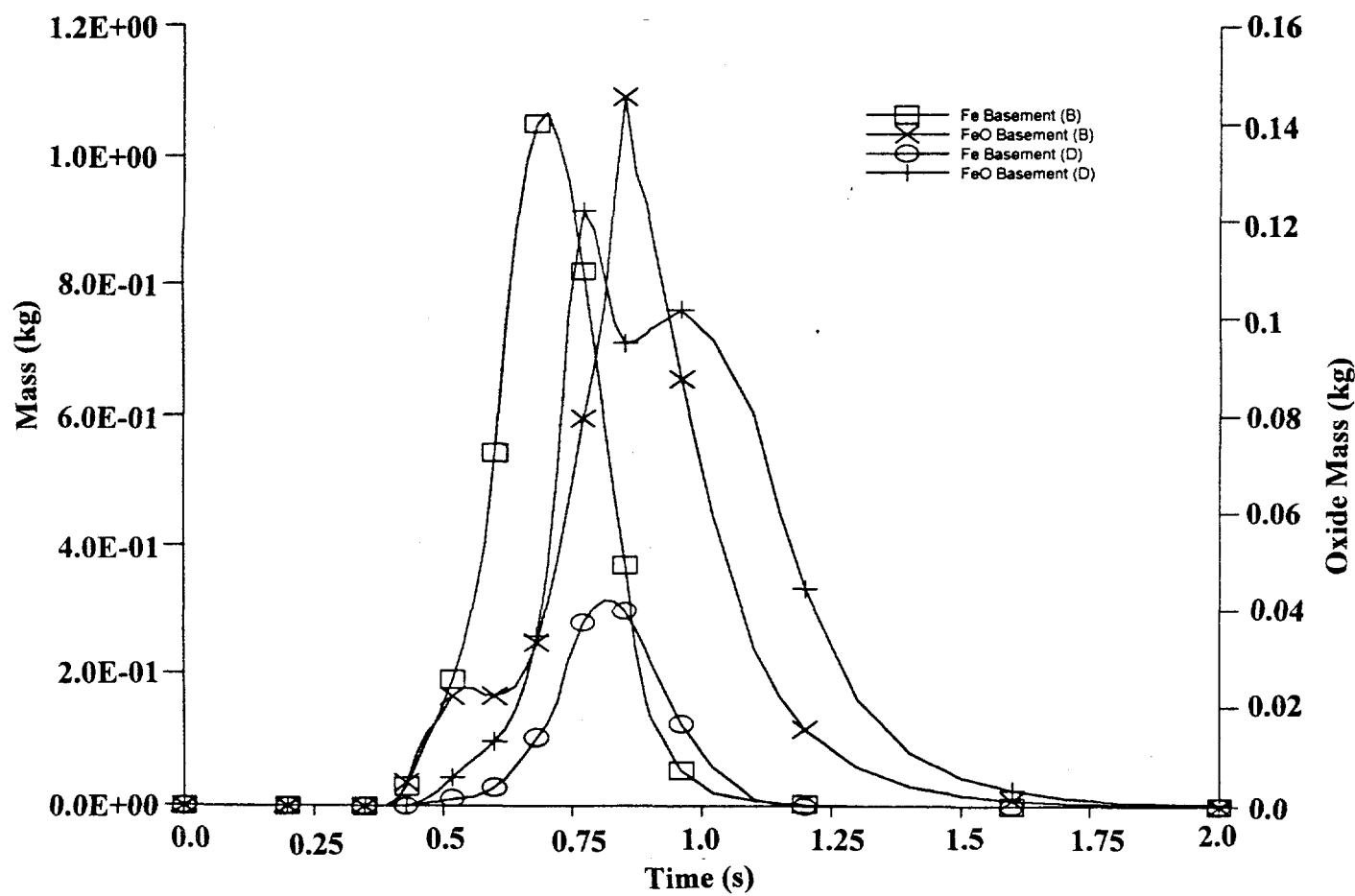


Figure 8. IET-6 Fe and FeO Airborne Mass CONTAIR Results

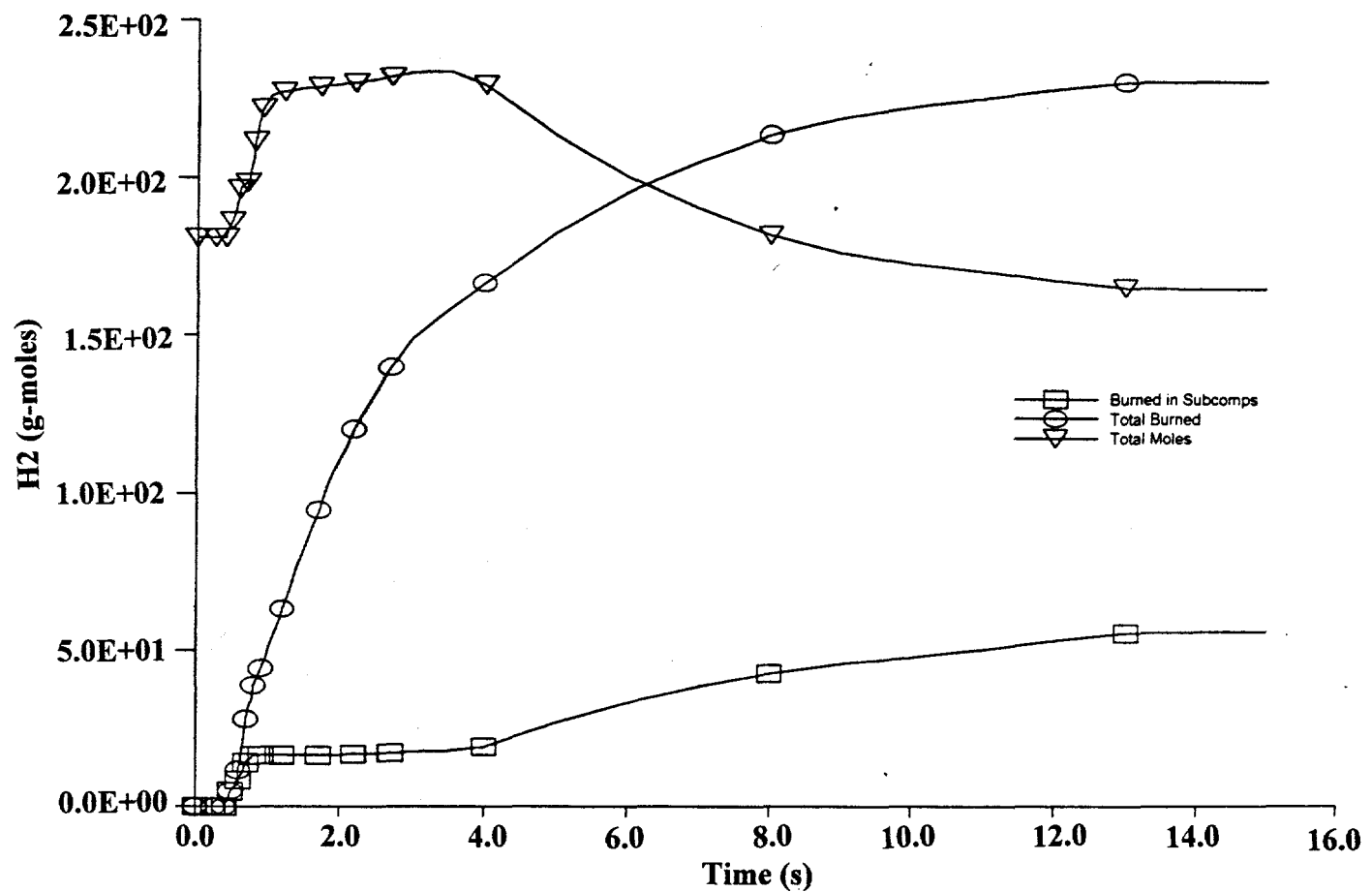


Figure 9. IET-6 Hydrogen Burned and Inventory CONTAIN Results

6. Summary

This report documents the DCH models in the CONTAIN code. These models have been developed to support the U.S. Nuclear Regulatory Commission's effort to understand the direct containment heating process and then apply that understanding to the resolution of the regulatory issue. The governing equations for non-cavity DCH processes modeled in the CONTAIN code have been described. Input instructions for using the DCH models and a description of the output produced has been described in this report. Finally, this report has included a brief description of the overall results of a detailed assessment of the models against a large subset of the available DCH database. Time dependent plots from one of the assessment cases has also been shown to further demonstrate the functionality of the models.

Future plans include documentation of the models that have been included in the CONTAIN code for discharge of molten debris from the RPV, entrainment rate, and entrainment fraction in a separate report. Documentation of the assessment of the CONTAIN DCH models against the DCH database is also the subject of ongoing work. Finally, the DCH models are being applied to support the NRC effort to resolve the DCH issue for large dry Westinghouse PWR containments and to extrapolate the resolution process to other PWR containment designs.

7. References

All91 Allen, M. D., et al., "Experiments to Investigate the Effect of Flight Path on Direct Containment Heating (DCH) in the Surtsey Test Facility," NUREG/CR-5728, SAND91-1105, Sandia National Laboratories, October, 1991.

All92a Allen, M. D., et al., "Experimental Results of Tests to Investigate the Effects of Hole Diameter Resulting From Bottom Head Failure on Direct Containment Heating (DCH) in the Surtsey Test Facility: The WC-1 and WC-3 Tests," SAND91-2153, Sandia National Laboratories, March 1992.

All92b Allen, M. D., et al., "Experiments to Investigate the Effects of 1:10 Scale Zion Structures on Direct Containment Heating (DCH) in the Surtsey Test Facility: The IET-1 and IET-1R Tests," SAND92-0255, Sandia National Laboratories, July 1992.

All92c Allen, M. D., et al., "The Third Integral Effects Test (IET-3) in the Surtsey Test Facility," SAND92-0166, Sandia National Laboratories, March 1992.

All92d Allen, M. D., et al., "Results of an Experiment in a Zion-Like Geometry to Investigate the Effect of Water on the Containment Basement Floor on Direct Containment Heating (DCH) in the Surtsey Test Facility: The IET-4 Test," SAND92-1241, Sandia National Laboratories, September 1992.

All92e Allen, M. D., et al., "Experimental Results of an Integral Effects Test in a Zion-Like Geometry to Investigate the Effect of a Classically Inert Atmosphere on Direct Containment Heating: The IET-5 Experiment," SAND92-1623, Sandia National Laboratories, November 1992.

All93a Allen, M. D., et al., "An Integral Effects Test in a Zion-Like Geometry to Investigate the Effects of Pre-Existing Hydrogen on Direct Containment Heating in the Surtsey Test Facility: The IET-6 Experiment," SAND92-1802, Sandia National Laboratories, January 1993.

All93b Allen, M. D., et al., "An Integral Effects Test in a Zion-Like Geometry to Investigate the Effects of Condensate Levels of Water and Pre-Existing Hydrogen on Direct Containment Heating in the Surtsey Test Facility: The IET-7 Experiment," SAND92-2021, Sandia National Laboratories, January 1993.

CONTAIN DCH Models

References

Bin92a Binder, J. L., et al., "Quick Look Data Report on the Integral Effects Test 1R in the COREXIT Facility at Argonne National Laboratory," LWR-92-2, Argonne National Laboratory, May 1992 (draft).

Bin92b Binder, J. L., et al., "Quick Look Data Report on the Integral Effects Test 1RR in the COREXIT Facility at Argonne National Laboratory," LWR-92-3, Argonne National Laboratory, May 1992 (draft).

Bin92c Binder, J. L., et al., "Quick Look Data Report on the Integral Effects Test 3 in the COREXIT Facility at Argonne National Laboratory," ANL/RE/LWR-92-7, Argonne National Laboratory, July 1992 (draft).

Bin92d Binder, J. L., et al., "Quick Look Data Report on the Integral Effects Test 6 in the COREXIT Facility at Argonne National Laboratory," ANL/RE/LWR-92-8, Argonne National Laboratory, August 1992 (draft).

Bir60 Bird, Stewart, and Lightfoot, Transport Phenomena, Wiley, NY, 1960.

Brg91 Bergeles, A. E., Two Phase Flow in the Power and Process Industries, Hemisphere Publishing Corp., NY, 1981.

Col81 Collier, J. G., Convective Boiling and Condensation, 2nd Edition, McGraw Hill, NY, 1981

Elw62 El-Wakil, M. M., Nuclear Power Engineering, McGraw Hill, NY, 1962.

Mur89 Murata, K. K., et al, "User's Manual For CONTAIN 1.1, A Computer Code For Severe Nuclear Reactor Accident Containment Analysis," NUREG/CR-5026, SAND87-2309, Sandia National Laboratories, 1989.

Mur90 Murata, K. K., et al, "User's Manual For CONTAIN 1.1, A Computer Code For Severe Nuclear Reactor Accident Containment Analysis (Revised For Revision 1.11)," NUREG/CR-5026, SAND87-2309, Sandia National Laboratories, 1990.

Pil92 Pilch, M. and Griffith, R., "An Investigation of Gas Blowthrough and Flow Quality Correlations for Use in the Analysis of High Pressure Meet Ejection Events," SAND91-2322, Sandia National Laboratories, Albuquerque, NM, 1991.

Pow86 Powers, D. A. et al, "VANESA: A Mechanistic Model of Radionuclide Release and Aerosol Generation During Core Debris Interactions with

CONTAIN DCH Models

References

Concrete," NUREG/CR-4308, SAND85-1370, Sandia National Laboratories, Albuquerque, NM, 1986.

Ran52 Ranz, W. E. and Marshall, W. R., "Evaporation from Drops," Chemical Engineering Progress, Vol. 48, No. 3, April 1952.

Ric61 Ricou, F. P., and Spalding, D. B., "Measurements of Entrainment by Axisymmetrical Turbulent Jets," Journal of Fluid Mechanics, 11, pp. 21-32, 1961.

Was87 Washington, K. E., "POSTCON: A Postprocessor and Unit Conversion Program for the CONTAIN Computer Code," NUREG/CR-4887, SAND87-0562, Sandia National Laboratories, Albuquerque, NM, 1987.

Was91 Washington, K. E., et al, "Reference Manual for the CONTAIN 1.1 Code for Containment Severe Accident Analysis," NUREG/CR-5715, SAND91-0835, Sandia National Laboratories, Albuquerque, NM, 1991.

Wil87 D. C. Williams, K. D. Bergeron, D. E. Carroll, G. D. Gasser, J. L. Tills, and K. E. Washington, "Containment Loads Due to Direct Containment Heating and Associated Hydrogen Behavior: Analysis and Calculations With the CONTAIN Code," NUREG/CR-4896, SAND87-0633, Sandia National Laboratories, Albuquerque, NM, 1987.

Wil92 Williams, D. C., "Posttest CONTAIN Calculations for the First Integral Effects Experiment (IET-1) at the Surtsey DCH Facility," A letter report submitted to the USNRC.

CONTAIN DCH Models

Appendix

```

cray
&&
&& ****
&& 14 cell surtsey deck for experiment iet-1, Rev.1
&& created by dave williams, August 1, 1991
&& the test consists of blowing thermite into a 1:10
&& scale zion cavity with high pressure steam. the floor of the
&& cavity may be covered with water. the cavity is connected
&& to the bottom of the surtsey vessel via a chute angled at 25.6 degrees
&& from the vertical.
&& Zion plant features modeled in iet-1 include: seal table, crane wall,
&& shield wall, basement level, pump deck level, operating floor
&& steam generators, reactor coolant pumps, gratings
&& at two levels.
&& there are separate cells for the accumulator and the melt generator
&& there is one cavity cell and one cell for the chute
&& there are four basement cells
&& there is one seal table room cell and two cells for the rest of the
&& pump deck level
&& remainder of Surtsey vessel is divided into three cells: one behind the &&
&& crane wall and two for everything above the operating floor.
&&
&& free volume = 89.971 m**3 (incl. cavity); o2 = 21.9021 kg
&& ****
&&
control ncells=14 ntitl=4 ntzone=8 nac=1 nsectn=20 numtbg=1 maxtbg=95
nengv=5 nwdudm=5000
ndhbin=5 ndhspc=7 ndhgrp=2
eoI
material
compound h2 o2 ar h2ol h2ov fe n2 conc
userdef fed feed a12o3d ald aloxd crd croxd
times 18000.0 0.0

&& -----time zones-----
0.01 0.05 0.33
0.00025 0.02 0.45
0.00025 0.02 0.90
0.0005 0.02 1.05
0.001 0.05 1.2
0.002 0.1 3.0
0.005 0.5 5.0
0.01 1.0 15.0
&& -----
trestart 8 0.5 0.75 1.0 1.5 3.0 5.0 10.0 15.0
&& -----
longedt=5
shortedt=11
&& -----
title
i6c1407: <<iet-6 analogue of i3c1407 (subc. NAD w shutoff, dome len1=lengft)>>
Sd(t) from PcaV(t), etc. <<cntn112z3.x version 12/17/93 run 12/21/93>>
mmd=1 mm, sig-g=4, 10-cell cont., 9.0 m/o o2, p0 = 1.88e5 Pa. 43 kg debris
5 bins, 5 sizes, metals-alox mixed, <<with NAD>>
&& -----

```

CONTAIN DCH Models

Appendix

```

area(7,9)=0.2267 avl(7,9)=0.35 cfc(7,9)=0.5 elevfp(7,9)=2.391
elevfp(9,7)=2.391 && recirculation flows simulated

area(7,11)=0.249 avl(7,11)=0.371 cfc(7,11)=0.5 fpcosn(7,11)=1.0
&& to pump deck level

elevcl(8)=2.958 && Lower surtsey tank, behind crane wall

area(8,9)=0.01895 avl(8,9)=0.02955 cfc(8,9)=1.0 elevfp(8,9)=2.315
elevfp(9,8)=2.315 && recirculation flows simulated

area(8,10)=0.01895 avl(8,10)=0.0733 cfc(8,10)=1.0 elevfp(8,10)=2.96
elevfp(10,8)=2.96 && to seal table room

area(8,13)=2.7819 avl(8,13)=1.8627 cfc(8,13)=0.5 fpcosn(8,13)=1.0
&& to upper surtsey

area(8,14)=0.4237 avl(8,14)=0.2837 cfc(8,14)=0.5 fpcosn(8,14)=1.0
&& to upper surtsey

elevcl(9)=2.572 && basement not adjacent to cavity exit

area(9,11)=0.0712 avl(9,11)=0.1062 cfc(9,11)=0.5 fpcosn(9,11)=1.0
&& to pump deck level

area(9,12)=0.6608 avl(9,12)=0.9849 cfc(9,12)=0.5 fpcosn(9,12)=1.0
&& to pump deck level

elevcl(10)=3.235 && seal table room

area(10,13)=0.0026 avl(10,13)=0.028 cfc(10,13)=0.5 fpcosn(10,13)=1.0
&& seal table room to upper Surtsey (near side)

elevcl(11)=3.552 && pump deck level, near side

area(11,12)=0.165 avl(11,12)=0.2199 cfc(11,12)=0.5 && to far side pump deck

area(11,13)=0.1975 avl(11,13)=0.256 cfc(11,13)=0.5 fpcosn(11,13)=1.0
&& to upper Surtsey (near side)

elevcl(12)=3.552 && pump deck level, far side

area(12,14)=0.1358 avl(12,14)=0.1759 cfc(12,14)=0.5 fpcosn(12,14)=1.0
&& to upper Surtsey (far side)

elevcl(13)=7.474 && upper Surtsey (near side)

area(13,14)=13.788 avl(13,14)=7.539 cfc(13,14)=0.5 elevfp(13,14)=5.589
elevfp(14,13)=5.589

elevcl(14)=7.474 && upper Surtsey (far side)

&&
&& variable flow path for melt. gen. to cavity path --
var-area(2,3) flag=2
var-x=time x=6

```

CONTAIN DCH Models

Appendix

```
&& aerosol tgas2=3000. pgas2=2.0e7
&& h2ol 1.0e-8 0.693 && 'h2ov' is not recommended
thermal
flows
&&
implicit 14
&& --- flow path information ---
&& --flow area, area to length ratio, flow coefficient, open/close--
&& surtsey scale, ambient p, d0 = 0.00082 m.
&&
&& -----centroid of the cells-----
&&
elevcl(1)=1.31 && accumulator cell flow data

&& accumulator/melt generator flow resistance based on M. Pilch's analysis
area(1,2)=0.00811 avl(1,2)=0.00238 cfc(1,2)=3.35

elevcl(2)=0.86 && melt generator cell. Actual area(2,3) is time-dependent

area(2,3)=1.00325e-03 avl(2,3)=0.00153 cfc(2,3)=1.0 fpcosn(2,3)=1.0
contract(2,3)=0.85 topen(2,3)=0.0

elevcl(3)=0.152 && cavity cell

area(3,4)=0.0523 avl(3,4)=0.0305 cfc(3,4)=0.55 fpcosn(3,4)=1.0

elevcl(4)=1.11 && chute between cavity and Surtsey

area(4,5)=0.0523 avl(4,5)=0.0455 cfc(4,5)=0.576 fpcosn(4,5)=1.0

elevcl(5)=2.572 && basement, chute exit region

area(5,6)=0.2506 avl(5,6)=0.47 cfc(5,6)=0.5 elevfp(5,6)=2.391
elevfp(6,5)=2.391 && recirculation flows simulated

area(5,7)=0.2356 avl(5,7)=0.47 cfc(5,7)=0.5 elevfp(5,7)=2.391
elevfp(7,5)=2.391 && recirculation flows simulated

area(5,10)=0.01955 avl(5,10)=0.0428 cfc(5,10)=1.0 && to seal table room

area(5,11)=0.1415 avl(5,11)=0.19 cfc(5,11)=0.5 fpcosn(5,11)=1.0
&& to pump deck level

elevcl(6)=2.572 && basement clockwise from chute exit

area(6,9)=0.2146 avl(6,9)=0.332 cfc(6,9)=0.5 elevfp(6,9)=2.391
elevfp(9,6)=2.391 && recirculation flows simulated

area(6,11)=0.1547 avl(6,11)=0.2305 cfc(6,11)=0.5 fpcosn(6,11)=1.0
&& upward to pump deck level

elevcl(7)=2.572 && basement counterclockwise from chute

area(7,8)=0.01895 avl(7,8)=0.0485 cfc(7,8)=1.98 elevfp(7,8)=2.315
elevfp(8,7)=2.315 && door through crane wall
```

CONTAIN DCH Models

Appendix

```

0.0 0.38 0.39 0.85 1.0 15.0
  var-y=area y=6
  0.0 0.0 2.5e-4 0.750e-3 1.00e-3 1.00e-3
  eoi
  &&

  &&
  engvent && engineered vents used to obtain recirculation flow paths
  &&

from=5 to=6 varea=0.2506 vavl=0.47 vcfc=0.5 velevb=2.752 velevf=2.752
  eoi && recirculation flows simulated

from=5 to=7 varea=0.2356 vavl=0.47 vcfc=0.5 velevb=2.752 velevf=2.752
  eoi && recirculation flows simulated

from=6 to=9 varea=0.2146 vavl=0.332 vcfc=0.5 velevb=2.752 velevf=2.752
  eoi && recirculation flows simulated

from=7 to=9 varea=0.2267 vavl=0.35 vcfc=0.5 velevb=2.752 velevf=2.752
  eoi && recirculation flows simulated

from=13 to=14 varea=13.788 vavl=7.539 vcfc=0.5 velevb=9.359 velevf=9.359
  eoi && recirculation flows simulated

  && -----print options-----
prflow
prburn
prheat
  && prlow-cl
  && prae
debug 4 diffc heatco trap mburn 0.890 0.891 && atrads htsurf cnvnos condns 0.4 0.401
  && -----direct heat parameters-----
dheat
  diabin
    0.1692e-3 0.4834e-3 1.0e-3 2.069e-3 5.911e-3
    thresh=1200.0 rcomh2=on ieqopt=2 && h2 recombination
    difo2=1.0 difh2o=1.0 htcmul=1.0 radmul=0.0 radgas=0.8
  && radimp=on htcimp=on zrrat=0.2600 ferat=0.7400
    liqside 1.0e-4 0.0 0.0 0.0 && radmul = (opaque atmosphere)
    grplim=100.0 && second generation is a "dummy"
  && species assignments to bins
fdistr
  && fed feod a12o3d ald aloxd crd croxd
    0.2 0.2 0.2 0.2 0.2 0.2 0.2
    0.2 0.2 0.2 0.2 0.2 0.2 0.2
    0.2 0.2 0.2 0.2 0.2 0.2 0.2
    0.2 0.2 0.2 0.2 0.2 0.2 0.2
    0.2 0.2 0.2 0.2 0.2 0.2 0.2
  &&
  eoi
  &&
  && ---- material properties for debris ----
userdat

  fed           debris

```

CONTAIN DCH Models

Appendix

molew	5.5847e+01				
temps	38				
	3.0000e+02	4.0000e+02	5.0000e+02	6.0000e+02	7.0000e+02
	8.0000e+02	9.0000e+02	1.0000e+03	1.0500e+03	1.1000e+03
	1.1500e+03	1.2000e+03	1.2500e+03	1.3000e+03	1.3500e+03
	1.4000e+03	1.4500e+03	1.5000e+03	1.5500e+03	1.6000e+03
	1.6500e+03	1.7000e+03	1.7500e+03	1.8000e+03	1.8500e+03
	1.9000e+03	1.9500e+03	2.0000e+03	2.0500e+03	2.1000e+03
	2.1500e+03	2.2000e+03	2.2500e+03	2.3000e+03	2.3500e+03
	2.4000e+03	2.4500e+03	2.5000e+03		
condt					
	4.3270e+01	4.3328e+01	4.0110e+01	3.7659e+01	3.5705e+01
	3.4093e+01	3.2733e+01	3.1562e+01	3.1034e+01	3.0538e+01
	3.0072e+01	2.9633e+01	2.9218e+01	2.8824e+01	2.8450e+01
	2.8095e+01	2.7756e+01	2.7433e+01	2.7123e+01	2.6827e+01
	2.6543e+01	2.6271e+01	2.6009e+01	2.5756e+01	2.5514e+01
	2.5279e+01	2.5053e+01	2.4835e+01	2.4624e+01	2.4419e+01
	2.4222e+01	2.4030e+01	2.3844e+01	2.3663e+01	2.3488e+01
	2.3317e+01	2.3152e+01	2.2991e+01		
entht					
	9.2944e+02	4.7791e+04	9.9091e+04	1.5483e+05	2.1500e+05
	2.7961e+05	3.4866e+05	4.2215e+05	5.4867e+05	5.8240e+05
	6.1613e+05	6.6427e+05	6.9256e+05	7.2172e+05	7.5176e+05
	7.8267e+05	8.1445e+05	8.4710e+05	8.8063e+05	9.1504e+05
	9.5031e+05	1.0038e+06	1.0431e+06	1.0825e+06	1.3693e+06
	1.4087e+06	1.4483e+06	1.4879e+06	1.5276e+06	1.5673e+06
	1.6072e+06	1.6471e+06	1.6871e+06	1.7272e+06	1.7673e+06
	1.8075e+06	1.8478e+06	1.8882e+06		
rhot					
	7.8824e+03	7.8437e+03	7.8050e+03	7.7663e+03	7.7276e+03
	7.6890e+03	7.6503e+03	7.6116e+03	7.5923e+03	7.5729e+03
	7.5536e+03	7.5343e+03	7.5149e+03	7.4956e+03	7.4762e+03
	7.4569e+03	7.4376e+03	7.4182e+03	7.3989e+03	7.3795e+03
	7.3602e+03	7.3409e+03	7.3215e+03	7.3022e+03	6.9768e+03
	6.9350e+03	6.8932e+03	6.8514e+03	6.8096e+03	6.7678e+03
	6.7260e+03	6.6842e+03	6.6425e+03	6.6007e+03	6.5589e+03
	6.5171e+03	6.4753e+03	6.4335e+03		
spht					
	4.4621e+02	4.9058e+02	5.3496e+02	5.7933e+02	6.2370e+02
	6.6808e+02	7.1245e+02	7.5682e+02	6.7459e+02	6.7459e+02
	6.7460e+02	5.5689e+02	5.7436e+02	5.9182e+02	6.0928e+02
	6.2675e+02	6.4421e+02	6.6168e+02	6.7914e+02	6.9661e+02
	7.1407e+02	7.8703e+02	7.8703e+02	7.8703e+02	7.8851e+02
	7.9001e+02	7.9151e+02	7.9301e+02	7.9451e+02	7.9601e+02
	7.9751e+02	7.9901e+02	8.0050e+02	8.0200e+02	8.0350e+02
	8.0500e+02	8.0650e+02	8.0800e+02		
eoi					
feed					
		debris			
molew	7.1850e+01				
temps	38				
	3.0000e+02	4.0000e+02	5.0000e+02	6.0000e+02	7.0000e+02
	8.0000e+02	9.0000e+02	1.0000e+03	1.0500e+03	1.1000e+03
	1.1500e+03	1.2000e+03	1.2500e+03	1.3000e+03	1.3500e+03
	1.4000e+03	1.4500e+03	1.5000e+03	1.5500e+03	1.6000e+03
	1.6500e+03	1.7000e+03	1.7500e+03	1.8000e+03	1.8500e+03
	1.9000e+03	1.9500e+03	2.0000e+03	2.0500e+03	2.1000e+03

CONTAIN DCH Models

Appendix

2.1500e+03	2.2000e+03	2.2500e+03	2.3000e+03	2.3500e+03
2.4000e+03	2.4500e+03	2.5000e+03		
condt				
6.0000e+00	6.0000e+00	6.0000e+00	6.0000e+00	6.0000e+00
6.0000e+00	6.0000e+00	6.0000e+00	6.0000e+00	6.0000e+00
6.0000e+00	6.0000e+00	6.0000e+00	6.0000e+00	6.0000e+00
6.0000e+00	6.0000e+00	6.0000e+00	6.0000e+00	6.0000e+00
6.0000e+00	6.0000e+00	6.0000e+00	6.0000e+00	6.0000e+00
6.0000e+00	6.0000e+00	6.0000e+00	6.0000e+00	6.0000e+00
6.0000e+00	6.0000e+00	6.0000e+00	6.0000e+00	6.0000e+00
6.0000e+00	6.0000e+00	6.0000e+00	6.0000e+00	6.0000e+00
enthf				
1.3835e+03	7.2483e+04	1.4632e+05	2.2212e+05	2.9957e+05
3.7848e+05	4.5878e+05	5.4041e+05	5.8171e+05	6.2333e+05
6.6527e+05	7.0753e+05	7.5009e+05	7.9297e+05	8.3616e+05
8.7966e+05	9.2347e+05	9.6758e+05	1.0120e+06	1.0567e+06
1.4367e+06	1.4842e+06	1.5317e+06	1.5791e+06	1.6266e+06
1.6741e+06	1.7216e+06	1.7691e+06	1.8165e+06	1.8640e+06
1.9115e+06	1.9590e+06	2.0065e+06	2.0540e+06	2.1014e+06
2.1489e+06	2.1964e+06	2.2439e+06		
rhot				
5.7000e+03	5.7000e+03	5.7000e+03	5.7000e+03	5.7000e+03
5.7000e+03	5.7000e+03	5.7000e+03	5.7000e+03	5.7000e+03
5.7000e+03	5.7000e+03	5.7000e+03	5.7000e+03	5.7000e+03
5.7000e+03	5.7000e+03	5.7000e+03	5.7000e+03	5.7000e+03
5.7000e+03	5.7000e+03	5.7000e+03	5.7000e+03	5.4231e+03
5.3907e+03	5.3582e+03	5.3257e+03	5.2932e+03	5.2607e+03
5.2282e+03	5.1958e+03	5.1633e+03	5.1308e+03	5.0983e+03
5.0658e+03	5.0333e+03	5.0008e+03		
spht				
6.9196e+02	7.2646e+02	7.4887e+02	7.6652e+02	7.8193e+02
7.9614e+02	8.0965e+02	8.2274e+02	8.2917e+02	8.3554e+02
8.4186e+02	8.4815e+02	8.5440e+02	8.6062e+02	8.6682e+02
8.7300e+02	8.7916e+02	8.8531e+02	8.9144e+02	8.9756e+02
9.4964e+02	9.4964e+02	9.4964e+02	9.4964e+02	9.4964e+02
9.4964e+02	9.4964e+02	9.4964e+02	9.4964e+02	9.4964e+02
9.4964e+02	9.4964e+02	9.4964e+02	9.4964e+02	9.4964e+02
9.4964e+02	9.4964e+02	9.4964e+02	9.4964e+02	9.4964e+02
eo1				
a12o3d debris & properties adjusted for m.p. < 2300 k				
molew	5.098e+01			
tempo	39			
3.0000e+02	4.0000e+02	5.0000e+02	6.0000e+02	7.0000e+02
8.0000e+02	9.0000e+02	1.0000e+03	1.0500e+03	1.1000e+03
1.1500e+03	1.2000e+03	1.2500e+03	1.3000e+03	1.3500e+03
1.4000e+03	1.4500e+03	1.5000e+03	1.5500e+03	1.6000e+03
1.6500e+03	1.7000e+03	1.7500e+03	1.8000e+03	1.8500e+03
1.9000e+03	1.9500e+03	2.0000e+03	2.0500e+03	2.1000e+03
2.1500e+03	2.2000e+03	2.2500e+03	2.3000e+03	2.3500e+03
2.4000e+03	2.4500e+03	2.5000e+03	2.7000e+03	
condt				
1.0000e+01	1.0000e+01	1.0000e+01	1.0000e+01	1.0000e+01
1.0000e+01	1.0000e+01	1.0000e+01	1.0000e+01	1.0000e+01
1.0000e+01	1.0000e+01	1.0000e+01	1.0000e+01	1.0000e+01
1.0000e+01	1.0000e+01	1.0000e+01	1.0000e+01	1.0000e+01
1.0000e+01	1.0000e+01	1.0000e+01	1.0000e+01	1.0000e+01

CONTAIN DCH Models

Appendix

1.0000e+01	1.0000e+01	1.0000e+01	1.0000e+01	1.0000e+01
1.0000e+01	1.0000e+01	1.0000e+01	1.0000e+01	1.0000e+01
1.0000e+01	1.0000e+01	1.0000e+01	1.0000e+01	1.0000e+01
entht				
1.4330e+03	8.9424e+04	1.9026e+05	2.9814e+05	4.1059e+05
5.2636e+05	6.4477e+05	7.6539e+05	8.2645e+05	8.8798e+05
9.4995e+05	1.0123e+06	1.0752e+06	1.3530e+06	1.4161e+06
1.4796e+06	1.5436e+06	1.6081e+06	1.6731e+06	1.7386e+06
1.8045e+06	1.8709e+06	1.9377e+06	2.0050e+06	2.0728e+06
2.1410e+06	2.2097e+06	2.2789e+06	2.3485e+06	2.4185e+06
2.4890e+06	2.5600e+06	2.6314e+06	3.7701e+06	3.8412e+06
3.9123e+06	3.9833e+06	4.0543e+06	4.3385e+06	
rhot				
3.9650e+03	3.9650e+03	3.9650e+03	3.9650e+03	3.9650e+03
3.9650e+03	3.9650e+03	3.9650e+03	3.9650e+03	3.9650e+03
3.9650e+03	3.9650e+03	3.9650e+03	3.9650e+03	3.9650e+03
3.9650e+03	3.9650e+03	3.9650e+03	3.9650e+03	3.9650e+03
3.9650e+03	3.9650e+03	3.9650e+03	3.9650e+03	3.9650e+03
3.9650e+03	3.9650e+03	3.9650e+03	3.9650e+03	3.9650e+03
3.9650e+03	3.9650e+03	3.9650e+03	3.9650e+03	3.9650e+03
2.9506e+03	2.9130e+03	2.8754e+03	2.725e+03	
spht				
7.7573e+02	9.5800e+02	1.0490e+03	1.1042e+03	1.1424e+03
1.1716e+03	1.1956e+03	1.2163e+03	1.2258e+03	1.2349e+03
1.2436e+03	1.2521e+03	1.2602e+03	1.2557e+03	1.2656e+03
1.2754e+03	1.2851e+03	1.2947e+03	1.3042e+03	1.3136e+03
1.3230e+03	1.3323e+03	1.3416e+03	1.3508e+03	1.3600e+03
1.3691e+03	1.3782e+03	1.3873e+03	1.3964e+03	1.4054e+03
1.4144e+03	1.4234e+03	1.4324e+03	1.4208e+03	1.4208e+03
1.4208e+03	1.4208e+03	1.4208e+03	1.4208e+03	
eo1				
ald	debris			
molew	2.6980e+01			
temps	45			
3.0000e+02	4.0000e+02	5.0000e+02	6.0000e+02	7.0000e+02
8.0000e+02	9.0000e+02	1.0000e+03	1.0500e+03	1.1000e+03
1.1500e+03	1.2000e+03	1.2500e+03	1.3000e+03	1.3500e+03
1.4000e+03	1.4500e+03	1.5000e+03	1.5500e+03	1.6000e+03
1.6500e+03	1.7000e+03	1.7500e+03	1.8000e+03	1.8500e+03
1.9000e+03	1.9500e+03	2.0000e+03	2.0500e+03	2.1000e+03
2.1500e+03	2.2000e+03	2.2500e+03	2.3000e+03	2.3500e+03
2.4000e+03	2.4500e+03	2.5000e+03	2.5500e+03	2.6000e+03
2.6500e+03	2.7000e+03	2.7500e+03	2.8000e+03	2.8500e+03
condt				
2.3904e+02	2.3800e+02	2.3542e+02	2.3130e+02	2.2565e+02
2.1845e+02	2.0972e+02	9.3125e+01	9.4781e+01	9.6374e+01
9.7902e+01	9.9366e+01	1.0077e+02	1.0210e+02	1.0337e+02
1.0458e+02	1.0572e+02	1.0680e+02	1.0782e+02	1.0877e+02
1.0965e+02	1.1048e+02	1.1123e+02	1.1193e+02	1.1256e+02
1.1312e+02	1.1362e+02	1.1406e+02	1.1444e+02	1.1474e+02
1.1499e+02	1.1517e+02	1.1529e+02	1.1534e+02	1.1533e+02
1.1525e+02	1.1511e+02	1.1491e+02	1.1464e+02	1.1431e+02
1.1391e+02	1.1345e+02	1.1292e+02	1.1233e+02	1.1168e+02
entht				
1.6660e+03	9.5040e+04	1.9295e+05	2.9470e+05	4.0088e+05
5.1254e+05	6.3097e+05	1.1479e+06	1.2068e+06	1.2656e+06

CONTAIN DCH Models

Appendix

1.3245e+06	1.3833e+06	1.4421e+06	1.5010e+06	1.5598e+06
1.6186e+06	1.6775e+06	1.7363e+06	1.7951e+06	1.8540e+06
1.9128e+06	1.9717e+06	2.0305e+06	2.0893e+06	2.1482e+06
2.2070e+06	2.2658e+06	2.3247e+06	2.3835e+06	2.4424e+06
2.5012e+06	2.5600e+06	2.6189e+06	2.6777e+06	2.7365e+06
2.7954e+06	2.8542e+06	2.9130e+06	2.9719e+06	3.0307e+06
3.0896e+06	3.1484e+06	3.2072e+06	3.2661e+06	3.3249e+06
rhot				
2.6985e+03	2.6791e+03	2.6588e+03	2.6372e+03	2.6141e+03
2.5891e+03	2.5619e+03	2.3664e+03	2.3524e+03	2.3384e+03
2.3244e+03	2.3104e+03	2.2964e+03	2.2824e+03	2.2684e+03
2.2544e+03	2.2404e+03	2.2264e+03	2.2124e+03	2.1984e+03
2.1844e+03	2.1704e+03	2.1564e+03	2.1424e+03	2.1284e+03
2.1144e+03	2.1004e+03	2.0864e+03	2.0724e+03	2.0584e+03
2.0444e+03	2.0304e+03	2.0164e+03	2.0024e+03	1.9884e+03
1.9744e+03	1.9604e+03	1.9464e+03	1.9324e+03	1.9184e+03
1.9044e+03	1.8904e+03	1.8764e+03	1.8624e+03	1.8484e+03
spht				
9.0135e+02	9.5941e+02	9.9796e+02	1.0381e+03	1.0872e+03
1.1482e+03	1.2226e+03	1.1767e+03	1.1767e+03	1.1767e+03
1.1767e+03	1.1767e+03	1.1767e+03	1.1767e+03	1.1767e+03
1.1767e+03	1.1767e+03	1.1767e+03	1.1767e+03	1.1767e+03
1.1767e+03	1.1767e+03	1.1767e+03	1.1767e+03	1.1767e+03
1.1767e+03	1.1767e+03	1.1767e+03	1.1767e+03	1.1767e+03
1.1767e+03	1.1767e+03	1.1767e+03	1.1767e+03	1.1767e+03
1.1767e+03	1.1767e+03	1.1767e+03	1.1767e+03	1.1767e+03
1.1767e+03	1.1767e+03	1.1767e+03	1.1767e+03	1.1767e+03
eo1				
aloxd	debris	&& ald rx prod.;	properties adjusted for m.p. < 2300 k	
molew	5.098e+01			
temps	39			
3.0000e+02	4.0000e+02	5.0000e+02	6.0000e+02	7.0000e+02
8.0000e+02	9.0000e+02	1.0000e+03	1.0500e+03	1.1000e+03
1.1500e+03	1.2000e+03	1.2500e+03	1.3000e+03	1.3500e+03
1.4000e+03	1.4500e+03	1.5000e+03	1.5500e+03	1.6000e+03
1.6500e+03	1.7000e+03	1.7500e+03	1.8000e+03	1.8500e+03
1.9000e+03	1.9500e+03	2.0000e+03	2.0500e+03	2.1000e+03
2.1500e+03	2.2000e+03	2.2500e+03	2.3000e+03	2.3500e+03
2.4000e+03	2.4500e+03	2.5000e+03	2.7000e+03	
condt				
1.0000e+01	1.0000e+01	1.0000e+01	1.0000e+01	1.0000e+01
1.0000e+01	1.0000e+01	1.0000e+01	1.0000e+01	1.0000e+01
1.0000e+01	1.0000e+01	1.0000e+01	1.0000e+01	1.0000e+01
1.0000e+01	1.0000e+01	1.0000e+01	1.0000e+01	1.0000e+01
1.0000e+01	1.0000e+01	1.0000e+01	1.0000e+01	1.0000e+01
1.0000e+01	1.0000e+01	1.0000e+01	1.0000e+01	1.0000e+01
1.0000e+01	1.0000e+01	1.0000e+01	1.0000e+01	1.0000e+01
1.0000e+01	1.0000e+01	1.0000e+01	1.0000e+01	1.0000e+01
1.0000e+01	1.0000e+01	1.0000e+01	1.0000e+01	1.0000e+01
entht				
1.4330e+03	8.9424e+04	1.9026e+05	2.9814e+05	4.1059e+05
5.2636e+05	6.4477e+05	7.6539e+05	8.2645e+05	8.8798e+05
9.4995e+05	1.0123e+06	1.0752e+06	1.3530e+06	1.4161e+06
1.4796e+06	1.5436e+06	1.6081e+06	1.6731e+06	1.7386e+06
1.8045e+06	1.8709e+06	1.9377e+06	2.0050e+06	2.0728e+06
2.1410e+06	2.2097e+06	2.2789e+06	2.3485e+06	2.4185e+06
2.4890e+06	2.5600e+06	2.6314e+06	3.7701e+06	3.8412e+06

CONTAIN DCH Models

Appendix

	3.9123e+06	3.9833e+06	4.0543e+06	4.3385e+06	
rhct					
	3.9650e+03	3.9650e+03	3.9650e+03	3.9650e+03	3.9650e+03
	3.9650e+03	3.9650e+03	3.9650e+03	3.9650e+03	3.9650e+03
	3.9650e+03	3.9650e+03	3.9650e+03	3.9650e+03	3.9650e+03
	3.9650e+03	3.9650e+03	3.9650e+03	3.9650e+03	3.9650e+03
	3.9650e+03	3.9650e+03	3.9650e+03	3.9650e+03	3.9650e+03
	3.9650e+03	3.9650e+03	3.9650e+03	3.9650e+03	3.9650e+03
	3.9650e+03	3.9650e+03	3.9650e+03	3.9650e+03	3.9650e+03
	2.9506e+03	2.9130e+03	2.8754e+03	2.725e+03	
spht					
	7.7573e+02	9.5800e+02	1.0490e+03	1.1042e+03	1.1424e+03
	1.1716e+03	1.1956e+03	1.2163e+03	1.2258e+03	1.2349e+03
	1.2436e+03	1.2521e+03	1.2602e+03	1.2557e+03	1.2656e+03
	1.2754e+03	1.2851e+03	1.2947e+03	1.3042e+03	1.3136e+03
	1.3230e+03	1.3323e+03	1.3416e+03	1.3508e+03	1.3600e+03
	1.3691e+03	1.3782e+03	1.3873e+03	1.3964e+03	1.4054e+03
	1.4144e+03	1.4234e+03	1.4324e+03	1.4208e+03	1.4208e+03
	1.4208e+03	1.4208e+03	1.4208e+03	1.4208e+03	
eo1					
crd	debris				
	molew	5.2010e+01			
	temps	45			
		3.0000e+02	4.0000e+02	5.0000e+02	6.0000e+02
		8.0000e+02	9.0000e+02	1.0000e+03	1.1000e+03
		1.1500e+03	1.2000e+03	1.2500e+03	1.3000e+03
		1.4000e+03	1.4500e+03	1.5000e+03	1.5500e+03
		1.6500e+03	1.7000e+03	1.7500e+03	1.8000e+03
		1.9000e+03	1.9500e+03	2.0000e+03	2.0500e+03
		2.1500e+03	2.2000e+03	2.2500e+03	2.3000e+03
		2.4000e+03	2.4500e+03	2.5000e+03	2.5500e+03
		2.6500e+03	2.7000e+03	2.7500e+03	2.8000e+03
	condt				
		4.3270e+01	4.3328e+01	4.0110e+01	3.7659e+01
		3.4093e+01	3.2733e+01	3.1562e+01	3.1034e+01
		3.0072e+01	2.9633e+01	2.9218e+01	2.8824e+01
		2.8095e+01	2.7756e+01	2.7433e+01	2.7123e+01
		2.6543e+01	2.6271e+01	2.6009e+01	2.5756e+01
		2.5279e+01	2.5053e+01	2.4835e+01	2.4624e+01
		2.4222e+01	2.4030e+01	2.3844e+01	2.3663e+01
		2.3317e+01	2.3152e+01	2.2991e+01	2.2831e+01
		2.2511e+01	2.2351e+01	2.2191e+01	2.2031e+01
	entht				
		8.3072e+02	4.7601e+04	9.7639e+04	1.5048e+05
		2.6298e+05	3.2191e+05	3.8215e+05	4.1326e+05
		4.7819e+05	5.1194e+05	5.4652e+05	5.8194e+05
		6.5523e+05	6.9308e+05	7.3173e+05	7.7118e+05
		8.5244e+05	8.9425e+05	9.3683e+05	9.8019e+05
		1.0692e+06	1.1149e+06	1.1614e+06	1.2086e+06
		1.6264e+06	1.6642e+06	1.7020e+06	1.7398e+06
		1.8154e+06	1.8532e+06	1.8910e+06	1.9289e+06
		2.0045e+06	2.0423e+06	2.0801e+06	2.1179e+06
	rhct				
		7.1351e+03	7.1230e+03	7.1086e+03	7.0917e+03
		7.0507e+03	7.0266e+03	7.0000e+03	6.9858e+03
		6.9556e+03	6.9396e+03	6.9230e+03	6.9057e+03

CONTAIN DCH Models

Appendix

6.8694e+03	6.8504e+03	6.8307e+03	6.8105e+03	6.7896e+03
6.7681e+03	6.7460e+03	6.7233e+03	6.7000e+03	6.6761e+03
6.6516e+03	6.6265e+03	6.6007e+03	6.5744e+03	6.5475e+03
6.2790e+03	6.2640e+03	6.2490e+03	6.2340e+03	6.2190e+03
6.2040e+03	6.1890e+03	6.1740e+03	6.1590e+03	6.1440e+03
6.1290e+03	6.1140e+03	6.0990e+03	6.0840e+03	6.0690e+03
sph				
4.4940e+02	4.8492e+02	5.1508e+02	5.4101e+02	5.6312e+02
5.8158e+02	5.9644e+02	6.0777e+02	6.3179e+02	6.4931e+02
6.6650e+02	6.8341e+02	7.0009e+02	7.1657e+02	7.3288e+02
7.4905e+02	7.6509e+02	7.8102e+02	7.9686e+02	8.1261e+02
8.2829e+02	8.4390e+02	8.5946e+02	8.7497e+02	8.9042e+02
9.0584e+02	9.2122e+02	9.3657e+02	9.5189e+02	9.6718e+02
7.5619e+02	7.5619e+02	7.5619e+02	7.5619e+02	7.5619e+02
7.5619e+02	7.5619e+02	7.5619e+02	7.5619e+02	7.5619e+02
7.5619e+02	7.5619e+02	7.5619e+02	7.5619e+02	7.5619e+02
eo1				
croxd debris				
molew	7.601e+01			
temps	45			
3.0000e+02	4.0000e+02	5.0000e+02	6.0000e+02	7.0000e+02
8.0000e+02	9.0000e+02	1.0000e+03	1.0500e+03	1.1000e+03
1.1500e+03	1.2000e+03	1.2500e+03	1.3000e+03	1.3500e+03
1.4000e+03	1.4500e+03	1.5000e+03	1.5500e+03	1.6000e+03
1.6500e+03	1.7000e+03	1.7500e+03	1.8000e+03	1.8500e+03
1.9000e+03	1.9500e+03	2.0000e+03	2.0500e+03	2.1000e+03
2.1500e+03	2.2000e+03	2.2500e+03	2.3000e+03	2.3500e+03
2.4000e+03	2.4500e+03	2.5000e+03	2.5500e+03	2.6000e+03
2.6500e+03	2.7000e+03	2.7500e+03	2.8000e+03	2.8500e+03
condt				
1.0000e+01	1.0000e+01	1.0000e+01	1.0000e+01	1.0000e+01
1.0000e+01	1.0000e+01	1.0000e+01	1.0000e+01	1.0000e+01
1.0000e+01	1.0000e+01	1.0000e+01	1.0000e+01	1.0000e+01
1.0000e+01	1.0000e+01	1.0000e+01	1.0000e+01	1.0000e+01
1.0000e+01	1.0000e+01	1.0000e+01	1.0000e+01	1.0000e+01
1.0000e+01	1.0000e+01	1.0000e+01	1.0000e+01	1.0000e+01
1.0000e+01	1.0000e+01	1.0000e+01	1.0000e+01	1.0000e+01
1.0000e+01	1.0000e+01	1.0000e+01	1.0000e+01	1.0000e+01
1.0000e+01	1.0000e+01	1.0000e+01	1.0000e+01	1.0000e+01
entht				
1.2733e+03	7.3338e+04	1.4944e+05	2.2786e+05	3.0787e+05
3.8910e+05	4.7134e+05	5.5447e+05	5.9634e+05	6.3841e+05
6.8067e+05	7.2312e+05	7.6575e+05	8.0855e+05	8.5153e+05
8.9468e+05	9.3801e+05	9.8150e+05	1.0252e+06	1.0690e+06
1.1130e+06	1.1571e+06	1.2014e+06	1.2459e+06	1.2919e+06
1.3379e+06	1.3839e+06	1.4299e+06	1.4759e+06	1.5219e+06
1.5679e+06	1.6139e+06	1.6599e+06	1.7059e+06	1.7519e+06
1.7979e+06	1.8439e+06	1.8899e+06	1.9359e+06	1.9819e+06
2.8872e+06	2.9388e+06	2.9904e+06	3.0420e+06	3.0936e+06
rhot				
5.2091e+03	5.1954e+03	5.1818e+03	5.1682e+03	5.1545e+03
5.1409e+03	5.1272e+03	5.1136e+03	5.1068e+03	5.1000e+03
5.0931e+03	5.0863e+03	5.0795e+03	5.0727e+03	5.0659e+03
5.0590e+03	5.0522e+03	5.0454e+03	5.0386e+03	5.0318e+03
5.0249e+03	5.0181e+03	5.0113e+03	5.0045e+03	4.9977e+03
4.9908e+03	4.9840e+03	4.9772e+03	4.9704e+03	4.9636e+03

CONTAIN DCH Models

Appendix

```
        4.9567e+03 4.9499e+03 4.9431e+03 4.9363e+03 4.9295e+03
        4.9226e+03 4.9158e+03 4.9090e+03 4.9022e+03 4.8954e+03
        4.5736e+03 4.5668e+03 4.5599e+03 4.5531e+03 4.5463e+03
spht
        6.8902e+02 7.4512e+02 7.7433e+02 7.9297e+02 8.0661e+02
        8.1759e+02 8.2702e+02 8.3549e+02 8.3947e+02 8.4333e+02
        8.4708e+02 8.5074e+02 8.5433e+02 8.5786e+02 8.6133e+02
        8.6475e+02 8.6813e+02 8.7148e+02 8.7480e+02 8.7809e+02
        8.8136e+02 8.8461e+02 8.8783e+02 8.9105e+02 9.2001e+02
        9.2001e+02 9.2001e+02 9.2001e+02 9.2001e+02 9.2001e+02
        9.2001e+02 9.2001e+02 9.2001e+02 9.2001e+02 9.2001e+02
        9.2001e+02 9.2001e+02 9.2001e+02 9.2001e+02 9.2001e+02
        1.0321e+03 1.0321e+03 1.0321e+03 1.0321e+03 1.0321e+03
eoil
eoil
&& -----end of global input-----
&& -----cell information-----
&& -----
&&
cell=1 && accumulator cell for blowdown model
control eoi
title
---- cell to generate blowdown sources-----
geometry 0.37835 0.67 && increase volume to correspond to real steam density
atmos=1 0.0 571.0
h2ov= 8.6846
condense
overflow=3
&&
&& -----
&&
cell=2 && melt gen., including pipe between melt gen. & rupture disk
control eoi
title
---- melt generator and connecting pipe to rupture disk ---
geometry 0.018 0.67 && melt gen and pipe -- actual volume
atmos=1 0.0 571.0
h2ov= 0.4132
condense
overflow=3
&&
cell=3 && cavity cell, with DCH sources
&&
control nhtm=4 mxslab=11 nsoatm=9 nspatm=15
    numtbc=1 maxtbc=5
    eoi
geometry 0.1091 0.3048
atmos=3 pgas=1.99e+5 tgas=308.0
molefrac
n2=0.8762 o2=0.0979 h2=0.0259 && n2=0.3950 h2ov=.4600 h2=.0400
eoil
condense
&&
&& -----
&&
```

CONTAIN DCH Models

Appendix

```

h-burn elev=0.152
  contburn
  shratio=20.0
  srtemp=893.0  && bulk spontaneous recombination
  mfscb=0.95
  mfocb=0.01
  debconc=1.e+6 && bsr on gas temp only
  srate=10.46
  eoi
&& for uchb case
  && flam=5.0  cfrmng=1.e-4  mormng=1.e-4  mfcig=1.e-4  mfoig=1.e-4
  && mfsig=0.999 && tactiv=0.4
  eoi
&& overflow to cell 3
overflow=3
rad-heat
  gaswal 0.261
  kmx=-0.8 && -0.741
  emsvt 0.8 0.8 0.8 0.8
  && cess
  eoi
&&
source= 9
&& -----
&& Sources for: IET-6
&&
a72o3d      15 iflag= 2 dchtype=entrain  && integrated mass =12.681
  t=
    0.33      0.4      0.47      0.5      0.53
    0.55      0.57     0.6      0.625     0.65
    0.68      0.75     0.8      0.9      15
  mass=
    0 9.441322 12.42279 24.59713 42.98286
    45.71588 70.80992 64.59852 41.74058 49.69117
    27.33014 13.16816 7.453676      0      0
  temp=
    2500.0    2500.0    2500.0    2500.0    2500.0
    2500.0    2500.0    2500.0    2500.0    2500.0
    2500.0    2500.0    2500.0    2500.0    2500.0
  eoi
ald      15 iflag= 2 dchtype=entrain  && integrated mass = 0.4707
  t=
    0.33      0.4      0.47      0.5      0.53
    0.55      0.57     0.6      0.625     0.65
    0.68      0.75     0.8      0.9      15
  mass=
    0 0.350447 0.461114 0.913005 1.595454
    1.696899 2.628349 2.397792 1.549342 1.844455
    1.01445 0.488781 0.276668      0      0
  temp=
    2500.0    2500.0    2500.0    2500.0    2500.0
    2500.0    2500.0    2500.0    2500.0    2500.0
    2500.0    2500.0    2500.0    2500.0    2500.0
  eoi
crd      15 iflag= 2 dchtype=entrain  && integrated mass = 3.671
  t=

```

A 13
CONTAIN DCH Models

Appendix

```
0.33      0.4      0.47      0.5      0.53
0.55      0.57     0.6      0.625     0.65
0.68      0.75     0.8      0.9      15
mass=
0 2.733281 3.596422 7.120915 12.44362
13.23483 20.4996 18.70139 12.08398 14.38569
7.912128 3.812207 2.157853 0 0
temp=
2500.0 2500.0 2500.0 2500.0 2500.0
2500.0 2500.0 2500.0 2500.0 2500.0
2500.0 2500.0 2500.0 2500.0 2500.0
eo
fed      15 iflag= 2 dchtype=entrain && integrated mass = 17.137
t=
0.33      0.4      0.47      0.5      0.53
0.55      0.57     0.6      0.625     0.65
0.68      0.75     0.8      0.9      15
mass=
0 12.75868 16.78774 33.23972 58.08557
61.77887 95.6901 87.29624 56.4068 67.15095
36.93302 17.795 10.07264 0 0
temp=
2500.0 2500.0 2500.0 2500.0 2500.0
2500.0 2500.0 2500.0 2500.0 2500.0
2500.0 2500.0 2500.0 2500.0 2500.0
eo
&& h2ov      15 iflag= 2 && integrated mass = 3.48
&& t=
&&      0.33      0.4      0.47      0.5      0.53
&&      0.55      0.57     0.6      0.625     0.65
&&      0.68      0.75     0.8      0.9      15
&& mass=
&&      0 2.590909 3.409091      6.75 11.79545
&&      12.54545 19.43182 17.72727 11.45455 13.63636
&&      7.5 3.613636 2.045455 0 0
&& enth=
&&      83940.0 83940.0 83940.0 83940.0 83940.0
&&      83940.0 83940.0 83940.0 83940.0 83940.0
&&      83940.0 83940.0 83940.0 83940.0 83940.0
&& eoi
&& mass= && integrated mass = 0.522
&&      0 0.388636 0.511364 1.0125 1.769318
&&      1.881818 2.914773 2.659091 1.718182 2.045455
&&      1.125 0.542045 0.306818 0 0
&& -----
&& interact <<none>> of 3.48 kg water with debris
h2ov 4 iflag=2
t= 0.0 0.10118 0.20235 0.30353
mass= 0.0 0.0 0.0 0.0
enth= 8.394e+04 8.394e+04 8.394e+04 8.394e+04
eo
&&
&& source debris into reservoir: total mass, includes mass left in melt gen.
&& -----
al2o3d 2 iflag=1 dchtype=trapbin && source mass integral = 16.056 kg
t= 0.0 0.3333333333
```

CONTAIN DCH Models

Appendix

mass= 48.168 0.0
 temp= 2500.0 2500.0
 eoi
 && -----
 ald 2 iflag=1 dchtype=trapbin && source mass integral = 0.596 kg
 t= 0.0 0.3333333333
 mass= 1.788 0.0
 temp= 2500.0 2500.0
 eoi
 && -----
 crd 2 iflag=1 dchtype=trapbin && source mass integral = 4.648 kg
 t= 0.0 0.3333333333
 mass= 13.944 0.0
 temp= 2500.0 2500.0
 eoi
 && -----
 fed 2 iflag=1 dchtype=trapbin && source mass integral = 21.699 kg
 t= 0.0 0.3333333333
 mass= 65.097 0.0
 temp= 2500.0 2500.0
 eoi
 && -----
 && -----heat sink structures-----
 struc
 && outgas && (de)activate outgassing model
 && concdata
 && fh2oe=0.0386 fh2ob=0.200 fco2=0.0150
 && eoi
 name=wall3s type=wall shape=slab chrlen=0.3048 slarea=0.779
 nslab=11 tunif=308.0
 compound= conc conc conc conc conc conc conc conc conc
 x=0.0 1.0e-4 3.0e-4 6.0e-4 1.2e-3 2.4e-3 5.0e-3 1.e-2 2.e-2 4.e-2
 9.e-2 1.83e-1
 bcinner hydarea=0.0813 eoi
 bcoutter tgas=308.0 eoi
 eoi
 && dummy structure to control 2nd impact tof/ku & NAD velocities
 name=dummy3s type=wall shape=slab chrlen=0.3048 slarea=1.0e-10
 nslab=11 tunif=308.0
 compound= conc conc conc conc conc conc conc conc conc
 x=0.0 1.0e-4 3.0e-4 6.0e-4 1.2e-3 2.4e-3 5.0e-3 1.e-2 2.e-2 4.e-2
 9.e-2 1.83e-1
 bcinner hydarea=0.0668 eoi && mean of value for cavity & chute
 bcoutter tgas=308.0 eoi
 eoi
 name=flor3s type=floor shape=slab chrlen=0.612 slarea=0.375
 nslab=11 tunif=308.0
 compound= conc conc conc conc conc conc conc conc conc
 x=0.0 1.0e-4 3.0e-4 6.0e-4 1.2e-3 2.4e-3 5.0e-3 1.e-2 2.e-2 4.e-2
 9.e-2 1.83e-1
 bcinner hydarea=0.0813 eoi
 bcoutter tgas=308.0 eoi
 eoi

CONTAIN DCH Models

Appendix

```

name=roof3s type=roof shape=slab chrlen=0.592 slarea=0.350
  nslab=11 tunif=308.0
  compound= conc conc conc conc conc conc conc conc conc
  x=0.0 1.0e-4 3.0e-4 6.0e-4 1.2e-3 2.4e-3 5.0e-3 1.e-2 2.e-2 4.e-2
  9.e-2 1.83e-1
  bcinner hydarea=0.0813 eoi
  bcouter tgas=308.0 eoi
eoi

dch-cell
  sdeven=5.0
  && interact nonairborne debris
  && diatrap=0.01
    && thresh=1800.0 && stop reacting trapped debris when Fe freezes
  var-parm flag=2
    name=trapreac
    var-x=time x=5 0.0 3.0 4.0 5.0 15.0
    var-y=diatrap y=5 0.01 0.01 0.025 1.0 1.0
  eoi
  trapping user=0.0 && note no trapping in cavity or chute
  && tofku rhodg=mix && fromcell = 2
  && len1=0.406 && height of melt gen. orifice above cavity floor
  && len2=0.940 && distance from melt gen. axis to cavity exit
  && lengft=1000. && trivial trapping if don't de-entrain on second impact
  && ku1=0.0001 ku2=10.0 trapmul=1.0 trapmin=0.0 trapmax=1.0e20
  && vnost=gtf && adfflow=0.1
  eoi
eoi

  cell=4 && chute from cavity to Surtsey
&&
control nhtm=2 mxslab=11
  eoi
geometry 0.1192 0.529
  atmos=3 pgas=1.99e+5 tgas=308.0
  molefrac
  n2=0.8762 o2=0.0979 h2=0.0259 && n2=0.3950 h2ov=.4600 h2=.0400
  eoi
  condense
&&
&& -----
&&
h-burn elev=1.1055
  contburn
  shratio=20.0
  srtemp=893.0 && bulk spontaneous recombination
  mfsccb=0.95
  mfocb=0.01
  debconc=1.e+6 && bsr on gas temp only
  srrate=10.16
  eoi
&& for uchb case
  && flam=5.0 cfrmng=1.e-4 mormng=1.e-4 mfcig=1.e-4 mfoig=1.e-4
  && mfsig=0.999 && tactiv=0.4
  eoi

```

CONTAIN DCH Models

Appendix

```

    && overflow to cell 3
    overflow=3
    rad-heat
        gaswal 0.198
        kmx=-0.8 && -0.690
        emsvt 0.8 0.8
            && cess
    eoi
    && -----heat sink structures-----
    struc
        && outgas && (de)activate outgasing model
        && concdata
        && fh2oe=0.0386 fh2ob=0.200 fco2=0.0150
        && eoi
        name=wall4s type=wall shape=slab chrlen=0.529 slarea=2.087
        nslab=11 tunif=308.0
        compound= conc conc conc conc conc conc conc conc conc
        x=0.0 1.0e-4 3.0e-4 6.0e-4 1.2e-3 2.4e-3 5.0e-3 1.e-2 2.e-2 4.e-2
        9.e-2 1.83e-1
        bcinner hydarea=0.0523 eoi
        bcouter tgas=308.0 eoi
    eoi

    name=floor4s type=floor shape=slab chrlen=0.274 slarea=0.075
    nslab=11 tunif=308.0
    compound= conc conc conc conc conc conc conc conc conc
    x=0.0 1.0e-4 3.0e-4 6.0e-4 1.2e-3 2.4e-3 5.0e-3 1.e-2 2.e-2 4.e-2
    9.e-2 1.83e-1
    bcinner hydarea=0.0523 eoi
    bcouter tgas=308.0 eoi
    eoi

    dch-cell
        sdeven=5.0
        trapping user=0.0 && no trapping in cavity or chute
        && tofku rhodg=mix && fromcell = 3
        && len1=0.331 && 6*(Volume)/(Surface) rule
        && len2=0.331 && 6*V/S rule
        && lengft=1000. && trivial trapping if don't de-entrain on second impact
        && ku1=10.0 ku2=10.0 trapmul=1.0 trapmin=0.0 trapmax=1.0e20
        && vnost=gft && adflow=0.1
    eoi
    eoi

    cell=5 && basement, vicinity of chute exit
    &&
    control nhtm=8 mxslab=11
        numtbc=1 maxtbc=5
    eoi
    geometry 0.3609 0.721
    atmos=3 pgas=1.99e+5 tgas=308.0
    molefrac
    n2=0.8762 o2=0.0979 h2=0.0259 && n2=0.3950 h2ov=.4600 h2=.0400
    eoi
    condense
    &&

```

CONTAIN DCH Models

Appendix

```

&& -----
&&
h-burn elev=2.572
  contburn
    shratio=20.0
    srtemp=893.0  && bulk spontaneous recombination
    mfsrb=0.95
    mfocb=0.01
    debconc=1.e+6 && bsr on gas temp only
    srrate=7.02
  eoi
  && for uchb case
    && flam=5.0  cfrmng=1.e-4  mormng=1.e-4  mfcig=1.e-4  mfoig=1.e-4
    && mfsig=0.999 && tactiv=0.4
  eoi
  && overflow to cell 5
  overflow=5
  rad-heat
    gaswal 0.5028
    kmx=-0.8 && -0.795
    emsvt 0.8 0.8 0.8 0.8 0.8  0.8 0.8 0.8
      && cess
  eoi

  && -----heat sink structures-----
  struc
  && outgas && (de)activate outgassing model
  && concdata
  && fh2oe=0.0386 fh2ob=0.200 fco2=0.0150
  && eoi
  && underside of seal table room floor
  name=roof5s1 type=roof shape=slab chrlen=0.309 slarea=0.0956
  nslab=9 tunif=308.0
  compound= conc conc conc conc conc conc conc conc
  x=0.0 1.0e-4 3.0e-4 6.0e-4 1.2e-3 2.4e-3 5.0e-3 1.e-2 2.e-2 3.05e-2
  eoi

  && bio shield wall
  name=wall5s1 type=wall shape=slab chrlen=0.721 slarea=0.307
  nslab=11 tunif=308.0
  compound= conc conc conc conc conc conc conc conc conc
  x=0.0 1.0e-4 3.0e-4 6.0e-4 1.2e-3 2.4e-3 5.0e-3 1.e-2 2.e-2 3.5e-2
  6.50e-2 0.1067
  eoi

  && crane wall, other outer boundary walls
  name=wall5s2 type=wall shape=slab chrlen=0.584 slarea=0.868
  nslab=10 tunif=308.0
  compound= conc conc conc conc conc conc conc conc conc
  x=0.0 1.0e-4 3.0e-4 6.0e-4 1.2e-3 2.4e-3 5.0e-3 1.e-2 2.e-2 3.5e-2
  5.72e-2
  eoi

  && bottom outside wall seal table room + sides of cross beam
  name=wall5s3 type=wall shape=slab chrlen=0.358 slarea=0.369
  nslab=9 tunif=308.0

```

CONTAIN DCH Models

Appendix

```

compound= conc conc conc conc conc conc conc conc conc
x=0.0 1.0e-4 3.0e-4 6.0e-4 1.2e-3 2.4e-3 5.0e-3 1.e-2 2.e-2 3.83e-2
eoi

&& under side of cross beam
name=roof5s2 type=roof shape=slab chrlen=0.297 slarea=0.0882
nslab=9 tunif=308.0
compound= conc conc conc conc conc conc conc conc
x=0.0 1.0e-4 3.0e-4 6.0e-4 1.2e-3 2.4e-3 5.0e-3 1.e-2 2.e-2 3.83e-2
eoi

&& under side of steam generators
name=roof5s3 type=roof shape=slab chrlen=0.368 slarea=0.2131
nslab=6 tunif=308.0
compound= fe fe fe fe fe
x=0.0 1.0e-4 3.0e-4 6.0e-4 1.2e-3 2.2e-3 3.4e-3
eoi

&& under side of grating at 592' level
name=roof5s4 type=roof shape=slab chrlen=0.37 slarea=0.1396
nslab=3 tunif=308.0
compound= fe fe fe
x=0.0 1.0e-4 3.0e-4 5.57e-4
eoi

&& Surtsey false floor
name=flor5s1 type=floor shape=slab chrlen=0.71 slarea=0.5036
nslab=10 tunif=308.0
compound= conc conc conc conc conc conc conc conc conc
x=0.0 1.0e-4 3.0e-4 6.0e-4 1.2e-3 2.4e-3 5.0e-3 1.e-2 2.e-2 3.5e-2
5.08e-2
bcouter tgas=308.0 eoi
eoi

dch-cell
sdeven=1.0
&& interact nonairborne debris
&& diatrap=0.01
&& thresh=1800.0 && stop reacting trapped debris when Fe freezes
var-parm flag=2
name=trapreac
var-x=time x=5 0.0 3.0 4.0 5.0 15.0
var-y=diatrap y=5 0.01 0.01 0.025 1.0 1.0
eoi
trapping
tofku rhodg=mix && fromcell = 4
len1=0.648 && slant height to underside of seal table room
len2=0.838 && 6V/S estimate
lengft=0.721 && cell height
ku1=10.0 ku2=10.0 trapmul=1.0 trapmin=0.0 trapmax=1.0e20
vnost=gft && adflow=0.1
eoi
eoi

cell=6 && basement, clockwise from chute exit
&&

```

CONTAIN DCH Models

Appendix

```

control nhtm=6 mxslab=11
  numtbc=1 maxtbc=5
  eoi
  geometry 0.3227 0.721
  atmos=3 pgas=1.99e+5 tgas=308.0
  molefrac
  n2=0.8762 o2=0.0979 h2=0.0259 && n2=0.3950 h2ov=.4600 h2=.0400
  eoi
  condense
  &&
  && -----
  &&
  h-burn elev=2.572
  contburn
  shratio=20.0
  srtemp=893.0 && bulk spontaneous recombination
  mfsrb=0.95
  mforb=0.01
  debconc=1.e+6 && bsr on gas temp only
  srrate=7.29
  eoi
  && for uchb case
  && flam=5.0 cfrmng=1.e-4 mormng=1.e-4 mfcig=1.e-4 mfoig=1.e-4
  && mfsig=0.999 && tactiv=0.4
  eoi
  && overflow to cell 5
  overflow=5
  rad-heat
  gaswal 0.578
  kmx=-0.8 && -0.798
  emsvt 0.8 0.8 0.8 0.8 0.8 0.8
  && cess
  eoi

  && -----heat sink structures-----
  struc
  && outgas && (de)activate outgassing model
  && concdata
  && fh2oe=0.0386 fh2ob=0.200 fco2=0.0150
  && eoi
  && bio shield wall + lower RFC wall
  name=wall6s1 type=wall shape=slab chrlen=0.533 slarea=0.3244
  ns1ab=11 tunif=308.0
  compound= conc conc conc conc conc conc conc conc conc conc
  x=0.0 1.0e-4 3.0e-4 6.0e-4 1.2e-3 2.4e-3 5.0e-3 1.e-2 2.e-2 3.5e-2
  6.5e-2 0.1067
  eoi

  && Surtsey false floor
  name=flor6s1 type=floor shape=slab chrlen=0.696 slarea=0.485
  ns1ab=10 tunif=308.0
  compound= conc conc conc conc conc conc conc conc conc conc
  x=0.0 1.0e-4 3.0e-4 6.0e-4 1.2e-3 2.4e-3 5.0e-3 1.e-2 2.e-2 3.5e-2
  5.08e-2
  bcoutner tgas=308.0 eoi
  eoi

```

7/20

```

&& structures forming outer wall of cell 6
name=wall6s2 type=wall shape=slab chrlen=0.721 slarea=0.7913
nslab=10 tunif=308.0
compound= conc conc conc conc conc conc conc conc conc
x=0.0 1.0e-4 3.0e-4 6.0e-4 1.2e-3 2.4e-3 5.0e-3 1.e-2 2.e-2 3.5e-2
5.71e-2
eoi

&& under sides steam gen., pump
name=roof6s1 type=roof shape=slab chrlen=0.368 slarea=0.1476
nslab=6 tunif=308.0
compound= fe fe fe fe fe
x=0.0 1.0e-4 3.0e-4 6.0e-4 1.2e-3 2.2e-3 3.4e-3
eoi

&& under side of grating at 592' level
name=roof6s2 type=roof shape=slab chrlen=0.39 slarea=0.1527
nslab=3 tunif=308.0
compound= fe fe fe
x=0.0 1.0e-4 3.0e-4 5.57e-4
eoi

&& underside of RFC floor
name=roof6s3 type=roof shape=slab chrlen=0.331 slarea=0.1098
nslab=11 tunif=308.0
compound= conc conc conc conc conc conc conc conc conc conc
x=0.0 1.0e-4 3.0e-4 6.0e-4 1.2e-3 2.4e-3 5.0e-3 1.e-2 2.e-2 3.5e-2
6.0e-2 9.4e-2
eoi

dch-cell
sdeven=1.0
&& interact nonairborne debris
&& diatrap=0.01
&& thresh=1800.0 && stop reacting trapped debris when Fe freezes
var-parm flag=2
name=trapreac
var-x=time x=5 0.0 3.0 4.0 5.0 15.0
var-y=diatrap y=5 0.01 0.01 0.025 1.0 1.0
eoi
trapping
tofku rhodg=mix && fromcell = 5
len1=0.9629 && 6V/S rule
len2=0.9629 && 6V/S rule
lengft=0.721 && cell height
ku1=10.0 ku2=10.0 trapmul=1.0 trapmin=0.0 trapmax=1.0e20
vnost=gft adflow=0.5012 && include eng. vent half of entrance
eoi
eoi

cell=7 && basement, counterclockwise from chute exit
&&
control nhtm=6 mxslab=11
numtbc=1 maxtbc=5
eoi

```

CONTAIN DCH Models

Appendix

```

geometry 0.4348 0.721
atmos=3 pgas=1.99e+5 tgas=308.0
molefrac
n2=0.8762 o2=0.0979 h2=0.0259 && n2=0.3950 h2ov=.4600 h2=.0400
eoи
condense
&&
&& -----
&&
h-burn elev=2.572
contburn
    shratio=20.0
    srtemp=893.0    && bulk spontaneous recombination
    mfscb=0.95
    mfocb=0.01
    debconc=1.e+6 && bsr on gas temp only
    srrate=6.60
eoи
&& for uchb case
    && flam=5.0    cfrmng=1.e-4    mormng=1.e-4    mfcig=1.e-4    mfoig=1.e-4
    && mfsig=0.999 && tactiv=0.4
eoи
&& overflow to cell 5
overflow=5
rad-heat
    gaswal 0.702
    kmx=-0.8 && -0.7993
    emsvt 0.8 0.8 0.8 0.8 0.8 0.8
    && cess
eoи
&& -----heat sink structures-----
struc
&& outgas && (de)activate outgassing model
&& concdata
&& fh2oe=0.0386 fh2ob=0.200 fco2=0.0150
&& eoи
&& bio shield wall + lower RFC
name=wall7s1 type=wall shape=slab chrlen=0.533 slarea=0.3056
nslab=11 tunif=308.0
compound= conc conc conc conc conc conc conc conc conc conc
x=0.0 1.0e-4 3.0e-4 6.0e-4 1.2e-3 2.4e-3 5.0e-3 1.e-2 2.e-2 3.5e-2
6.5e-2 0.1067
eoи
&& Surtsey false floor
name=flor7s1 type=floor shape=slab chrlen=0.79 slarea=0.6234
nslab=10 tunif=308.0
compound= conc conc conc conc conc conc conc conc conc conc
x=0.0 1.0e-4 3.0e-4 6.0e-4 1.2e-3 2.4e-3 5.0e-3 1.e-2 2.e-2 3.5e-2
5.08e-2
bcouter tgas=308.0 eoи
eoи
&& structures forming outer wall of cell 7
name=wall7s2 type=wall shape=slab chrlen=0.721 slarea=0.8267
nslab=10 tunif=308.0

```

CONTAIN DCH Models

Appendix

```

compound= conc conc conc conc conc conc conc conc conc
x=0.0 1.0e-4 3.0e-4 6.0e-4 1.2e-3 2.4e-3 5.0e-3 1.e-2 2.e-2 3.5e-2
5.71e-2
eoi

&& under sides steam gen., pump
name=roof7s1 type=roof shape=slab chrlen=0.368 slarea=0.1476
nslab=6 tunif=308.0
compound= fe fe fe fe fe fe
x=0.0 1.0e-4 3.0e-4 6.0e-4 1.2e-3 2.2e-3 3.4e-3
eoi

&& under side of grating at 592' level
name=roof7s2 type=roof shape=slab chrlen=0.496 slarea=0.2459
nslab=3 tunif=308.0
compound= fe fe fe
x=0.0 1.0e-4 3.0e-4 5.57e-4
eoi

&& underside of RFC floor
name=roof7s3 type=roof shape=slab chrlen=0.28 slarea=0.0791
nslab=11 tunif=308.0
compound= conc conc conc conc conc conc conc conc conc conc
x=0.0 1.0e-4 3.0e-4 6.0e-4 1.2e-3 2.4e-3 5.0e-3 1.e-2 2.e-2 3.5e-2
6.0e-2 9.4e-2
eoi

dch-cell
sdeven=1.0
&& interact nonairborne debris
&& diatrap=0.01
&& thresh=1800.0 && stop reacting trapped debris when Fe freezes
var-parm flag=2
name=trapreac
var-x=time x=5 0.0 3.0 4.0 5.0 15.0
var-y=diatrap y=5 0.01 0.01 0.025 1.0 1.0
eoi
trapping
tofku rhodg=mix && fromcell = 5
len1=1.171 && 6V/S rule
len2=1.171 && 6V/S rule
lengtht=0.721 && cell height
ku1=10.0 ku2=10.0 trapmul=1.0 trapmin=0.0 trapmax=1.0e20
vnost=gft adflow=0.4712 && include eng. vent half of entrance
eoi
eoi

cell=8 && lower surtsey, behind the crane wall
&&
control nhtm=3 mxslab=10
eoi
geometry 4.788 1.494
atmos=3 pgas=1.99e+5 tgas=308.0
molefrac
n2=0.8762 o2=0.0979 h2=0.0259 && n2=0.3950 h2ov=.4600 h2=.0400
eoi

```

CONTAIN DCH Models

Appendix

```

condense
&&
&& -----
&&
h-burn elev=2.958
  contburn
    dftemp=400.0
    shratio=9.0
    srtemp=893.0  && bulk spontaneous recombination
    mfscb=0.9
    mfocb=0.01
    debconc=1.e+6 && bsr on gas temp only
    srrate=1.46
  eoi
  && for uchb case
    && flam=5.0  cfrmng=1.e-4  mormng=1.e-4  mfcig=1.e-4  mfoig=1.e-4
    && mfsig=0.999 && tactiv=0.4
  eoi
  && overflow to cell 5
  overflow=5
  rad-heat
    gaswal 0.496
    kmx=-0.8 && -0.794
    emsvt 0.8 0.8 0.8
    && cess
  eoi

  && -----heat sink structures-----
  struc
  && outgas && (de)activate outgassing model
  && concdata
  && fh2oe=0.0386 fh2ob=0.200 fco2=0.0150
  && eoi

  && surtsey outer wall
  name=wall8s1 type=wall shape=slab chrlen=0.75 slarea=17.161
  nslab=8 tunif=308.0
  compound= fe fe fe fe fe fe fe
  x=0.0 1.0e-4 3.0e-4 6.0e-4 1.2e-3 2.4e-3 5.0e-3 9.e-3 1.588e-2
  bcoutter tgas=308.0 eoi
  eoi

  && outside of crane wall
  name=wall8s2 type=wall shape=slab chrlen=0.75 slarea=14.375
  nslab=10 tunif=308.0
  compound= conc conc conc conc conc conc conc conc conc
  x=0.0 1.0e-4 3.0e-4 6.0e-4 1.2e-3 2.4e-3 5.0e-3 1.e-2 2.0e-2 3.5e-2
  5.71e-2
  eoi

  && surtsey false floor
  name=flor8s1 type=floor shape=slab chrlen=0.75 slarea=3.2056
  nslab=10 tunif=308.0
  compound= conc conc conc conc conc conc conc conc conc
  x=0.0 1.0e-4 3.0e-4 6.0e-4 1.2e-3 2.4e-3 5.0e-3 1.e-2 2.e-2 3.5e-2
  5.08e-2

```

CONTAIN DCH Models

Appendix

```

bcouter tgas=308.0 eoi
eoi
dch-cell
sdeven=1.0
trapping
  tofku rhodg=mix && fromcell = 7
  len1=0.75 && crane wall to Surtsey wall distance
  len2=0.75 && crane wall to Surtsey wall distance
  lengft=1.494 && cell height
  ku1=10.0  ku2=10.0 trapmul=1.0 trapmin=0.0 trapmax=1.0e20
  vnost=gft && adflow
eoi
eoi

cell=9 && basement, portions further from the cavity exit
&&
control nhtm=7 mxslab=11
  numtbc=1 maxtbc=5
eoi
geometry 1.8847 0.6249
atmos=3 pgas=1.99e+5 tgas=308.0
molefrac
n2=0.8762 o2=0.0979 h2=0.0259 && n2=0.3950 h2ov=.4600 h2=.0400
eoi
condense
&&
&& -----
&&
h-burn elev=2.572
  contburn
    shratio=20.0
    srtemp=893.0 && bulk spontaneous recombination
    mfsrb=0.95
    mforb=0.01
    debconc=1.e+6 && bsr on gas temp only
    srrate=4.05
eoi
&& for uchb case
  && flam=5.0  cfrmng=1.e-4 mormng=1.e-4 mfcig=1.e-4 mfoig=1.e-4
  && mfsig=0.999 && tactiv=0.4
eoi
&& overflow to cell 5
overflow=5
rad-heat
  gaswal 0.4485
  kmx=-0.8 && -0.791
  emsvt 0.8 0.8 0.8 0.8 0.8 0.8 0.8
  && cess
eoi

&& -----heat sink structures-----
struc
&& outgas && (de)activate outgassing model
&& concdata
&&   fh2oe=0.0386 fh2ob=0.200 fco2=0.0150
&&   eoi

```

```

&& RFC supports, cross beam
name=wall9s1 type=wall shape=slab chrlen=0.533 slarea=3.3747
  nslab=10 tunif=308.0
  compound= conc conc conc conc conc conc conc conc conc
  x=0.0 1.0e-4 3.0e-4 6.0e-4 1.2e-3 2.4e-3 5.0e-3 1.e-2 2.e-2 3.5e-2
  5.53e-2
  eoi

&& surtsey false floor
name=flor9s1 type=floor shape=slab chrlen=0.6 slarea=3.0161
  nslab=10 tunif=308.0
  compound= conc conc conc conc conc conc conc conc conc
  x=0.0 1.0e-4 3.0e-4 6.0e-4 1.2e-3 2.4e-3 5.0e-3 1.e-2 2.e-2 3.5e-2
  5.08e-2
  bouter tgas=308.0 eoi
  eoi

&& crane wall
name=wall9s2 type=wall shape=slab chrlen=0.625 slarea=4.0435
  nslab=10 tunif=308.0
  compound= conc conc conc conc conc conc conc conc conc
  x=0.0 1.0e-4 3.0e-4 6.0e-4 1.2e-3 2.4e-3 5.0e-3 1.e-2 2.e-2 3.5e-2
  5.71e-2
  eoi

&& biological shield, lower RFC wall
name=wall9s3 type=wall shape=slab chrlen=0.533 slarea=2.0547
  nslab=11 tunif=308.0
  compound= conc conc conc conc conc conc conc conc conc conc
  x=0.0 1.0e-4 3.0e-4 6.0e-4 1.2e-3 2.4e-3 5.0e-3 1.e-2 2.e-2 4.0e-2
  7.0e-2 0.1067
  eoi

&& underside of RFC
name=roof9s1 type=roof shape=slab chrlen=0.6 slarea=1.4090
  nslab=11 tunif=308.0
  compound= conc conc conc conc conc conc conc conc conc conc
  x=0.0 1.0e-4 3.0e-4 6.0e-4 1.2e-3 2.4e-3 5.0e-3 1.e-2 2.e-2 4.0e-2
  6.5e-2 9.4e-2
  eoi

&& underside of SG's, RCP's
name=roof9s2 type=roof shape=slab chrlen=0.368 slarea=0.5082
  nslab=6 tunif=308.0
  compound= fe fe fe fe fe fe
  x=0.0 1.0e-4 3.0e-4 6.0e-4 1.2e-3 2.2e-3 3.4e-3
  eoi

&& underside of grate at 592' level
name=roof9s3 type=roof shape=slab chrlen=0.6 slarea=0.7229
  nslab=3 tunif=308.0
  compound= fe fe fe
  x=0.0 1.0e-4 3.0e-4 5.57e-4
  eoi

```

CONTAIN DCH Models

Appendix

```

dch-cell
  sdeven=1.0
  && interact nonairborne debris
  && diatrap=0.01
    && thresh=1800.0 && stop reacting trapped debris when Fe freezes
  var-parm flag=2
    name=trapreac
    var-x=time x=5 0.0 3.0 4.0 5.0 15.0
    var-y=diatrap y=5 0.01 0.01 0.025 1.0 1.0
  eoi
  trapping
    tofku rhodg=mix && fromcell = 7
    len1=0.749 && 6V/S rule
    len2=0.749 && 6V/S rules
    lengft=0.625 && ave. cell height
    ku1=10.0 ku2=10.0 trapmul=1.0 trapmin=0.0 trapmax=1.0e20
    vnost=gft adflow=0.4533 && include eng. vent area also
  eoi
  eoi

  cell=10 && seal table room
  &&
  control nhtm=3 mxslab=10
    numtbc=1 maxtbc=5
  eoi
  geometry 0.1253 0.757
  atmos=3 pgas=1.99e+5 tgas=308.0
  molefrac
  n2=0.8762 o2=0.0979 h2=0.0259 && n2=0.3950 h2ov=.4600 h2=.0400
  eoi
  condense
  &&
  && -----
  &&
  h-burn elev=3.235
    contburn
      shratio=20.0
      srtemp=893.0 && bulk spontaneous recombination
      mfsrb=0.95
      mforb=0.01
      debconc=1.e+6 && bsr on gas temp only
      srrate=9.99
    eoi
  && for uchb case
    && flam=5.0 cfrmng=1.e-4 mormng=1.e-4 mfcig=1.e-4 mfoig=1.e-4
    && mfsig=0.999 && tactiv=0.4
  eoi
  && overflow to cell 5
  overflow=5
  rad-heat
    gaswal 0.259
    kmxx=-0.8 && -0.740
    emsvt 0.8 0.8 0.8
      && cess
  eoi

```

A27
CONTAIN DCH Models

Appendix

```
&& -----heat sink structures-----
struc
&& outgas && (de)activate outgassing model
&& concdata
&&   fh2oe=0.0386 fh2ob=0.200 fco2=0.0150
&&   eoi

&& roof of seal table room
name=roof10s1 type=roof shape=slab chrlen=0.407 slarea=0.1656
  nslab=10 tunif=308.0
  compound= conc conc conc conc conc conc conc conc conc
  x=0.0 1.0e-4 3.0e-4 6.0e-4 1.2e-3 2.4e-3 5.0e-3 1.e-2 2.e-2 3.2e-2
  4.57e-2
eoi

&& walls (all) of seal table room
name=wall10s1 type=wall shape=slab chrlen=0.757 slarea=1.433
  nslab=9 tunif=308.0
  compound= conc conc conc conc conc conc conc conc conc
  x=0.0 1.0e-4 3.0e-4 6.0e-4 1.2e-3 2.4e-3 5.0e-3 1.e-2 2.e-2 3.71e-2
eoi

&& floor of seal table room
name=flor10s1 type=floor shape=slab chrlen=0.382 slarea=0.1461
  nslab=9 tunif=308.0
  compound= conc conc conc conc conc conc conc conc conc
  x=0.0 1.0e-4 3.0e-4 6.0e-4 1.2e-3 2.4e-3 5.0e-3 1.e-2 2.e-2 3.05e-2
eoi

dch-cell
  sdeven=1.0
&& interact nonairborne debris
  && diatrap=0.01
    && thresh=1800.0 && stop reacting trapped debris when Fe freezes
  var-parm flag=2
    name=trapreac
    var-x=time x=5 0.0 3.0 4.0 5.0 15.0
    var-y=diatrap y=5 0.01 0.01 0.025 1.0 1.0
  eoi
  trapping
    tofku rhodg=mix && fromcell = 5
    len1=0.757 && cell height
    len2=0.431 && 6V/S rule
    lengft=0.757 && cell height
    ku1=10.0 ku2=10.0 trapmul=1.0 trapmin=0.0 trapmax=1.0e20
    vnost=gft && adflow
  eoi
eoi

cell=11 && pump deck level, near side
&&
control nhtm=7 mxslab=11
  numtbc=1 maxtbc=5
eoi
geometry 0.6603 0.62
atmos=3 pgas=1.99e+5 tgas=308.0
```

CONTAIN DCH Models

Appendix

```

molefrac
n2=0.8762 o2=0.0979 h2=0.0259 && n2=0.3950 h2ov=.4600 h2=.0400
eoil
condense
&&
&& -----
&&
h-burn elev=3.552
  contburn
    shratio=20.0
    srtemp=893.0  && bulk spontaneous recombination
    mfsrb=0.95
    mforb=0.01
    debconc=1.e+6 && bsr on gas temp only
    srrate=5.74
  eoil
  && for uchb case
    && flam=5.0  cfrmng=1.e-4 mormng=1.e-4 mfcig=1.e-4 mfoig=1.e-4
    && mfsig=0.999 && tactiv=0.4
  eoil
  && overflow to cell 5
  overflow=5
rad-heat
  gaswal 0.30875
  kmx=-0.8 && -0.7635
  emsvt 0.8 0.8 0.8 0.8 0.8 0.8 0.8
    && cess
eoil

&& -----heat sink structures-----
struc
  && outgas && (de)activate outgassing model
  && concdata
  && fh2oe=0.0386 fh2ob=0.200 fco2=0.0150
  && eoil
  && pump deck level ceiling (underside of operating floor)
  name=roof11s1 type=roof shape=slab chrlen=0.5 slarea=0.75
  nslab=10 tunif=308.0
  compound= conc conc conc conc conc conc conc conc conc
  x=0.0 1.0e-4 3.0e-4 6.0e-4 1.2e-3 2.4e-3 5.0e-3 1.e-2 2.e-2 4.0e-2
  7.62e-2
eoil

  && refueling canal wall surface + top of cross beam
  name=wall11s1 type=wall shape=slab chrlen=0.62 slarea=1.6157
  nslab=10 tunif=308.0
  compound= conc conc conc conc conc conc conc conc conc
  x=0.0 1.0e-4 3.0e-4 6.0e-4 1.2e-3 2.4e-3 5.0e-3 1.e-2 2.e-2 3.5e-2
  5.08e-2
eoil

  && inside surface of outer walls
  name=wall11s2 type=wall shape=slab chrlen=0.62 slarea=2.1438
  nslab=10 tunif=308.0
  compound= conc conc conc conc conc conc conc conc conc
  x=0.0 1.0e-4 3.0e-4 6.0e-4 1.2e-3 2.4e-3 5.0e-3 1.e-2 2.e-2 4.0e-2

```

CONTAIN DCH Models

Appendix

```

6.10e-2
eoI

&& steam gen & pump vertical surfaces
name=wall11s3 type=wall shape=slab chrlen=0.62 slarea=2.324
  nslab=6 tunif=308.0
  compound= fe fe fe fe fe fe
  x=0.0 1.0e-4 3.0e-4 6.0e-4 1.2e-3 2.2e-3 3.4e-3
eoI

&& underside grate above pumps
name=roof11s2 type=roof shape=slab chrlen=0.312 slarea=0.1951
  nslab=3 tunif=308.0
  compound= fe fe fe
  x=0.0 1.0e-4 3.0e-4 5.57e-4
eoI

&& top of pumps
name=flor11s1 type=floor shape=slab chrlen=0.229 slarea=0.0821
  nslab=6 tunif=308.0
  compound= fe fe fe fe fe fe
  x=0.0 1.0e-4 3.0e-4 6.0e-4 1.2e-3 2.2e-3 3.4e-3
eoI

&& upper surface of 592' level grating
name=flor11s2 type=floor shape=slab chrlen=0.5 slarea=0.588
  nslab=3 tunif=308.0
  compound= fe fe fe
  x=0.0 1.0e-4 3.0e-4 5.57e-4
eoI

dch-cell
  sdeven=1.0
&& interact nonairborne debris
  && diatrap=0.01
    && thresh=1800.0 && stop reacting trapped debris when Fe freezes
  var-parM flag=2
    name=trapreac
    var-x=time x=5 0.0 3.0 4.0 5.0 15.0
    var-y=diatrap y=5 0.01 0.01 0.025 1.0 1.0
  eoI
  trapping
    tofku rhodg=mix && fromcell = 5
    len1=0.62 && cell height
    len2=0.515 && 6V/S estimate
    lengft=0.62 && cell height
    ku1=10.0 ku2=10.0 trapmul=1.0 trapmin=0.0 trapmax=1.0e20
    vnost=gft && adflow
  eoI
eoI

cell=12 && pump deck level, far side
&&
control nhtm=7 mxslab=11
  numtbc=1 maxtbc=5
eoI

```

CONTAIN DCH Models

Appendix

```
geometry 0.814 0.62
  atmos=3 pgas=1.99e+5 tgas=308.0
  molefrac
  n2=0.8762 o2=0.0979 h2=0.0259 && n2=0.3950 h2ov=.4600 h2=.0400
  eoi
  condense
  &&
  && -----
  &&
  h-burn elev=3.552
  contburn
    shratio=20.0
    srtemp=893.0  && bulk spontaneous recombination
    mfsccb=0.95
    mfoccb=0.01
    debconc=1.e+6 && bsr on gas temp only
    srrate=5.36
  eoi
  && for uchb case
    && flam=5.0  cfrmng=1.e-4 mormng=1.e-4 mfcig=1.e-4 mfoig=1.e-4
    && mfsig=0.999 && tactiv=0.4
  eoi
  && overflow to cell 5
  overflow=5
  rad-heat
    gaswal 0.31925
    kmx=-0.8 && -0.7671
    emsvt 0.8 0.8 0.8 0.8 0.8 0.8 0.8
    && cess
  eoi

  && -----heat sink structures-----
  struc
  && outgas && (de)activate outgassing model
  && concdata
  && fh2oe=0.0386 fh2ob=0.200 fco2=0.0150
  && eoi
  && pump deck level ceiling (underside of operating floor)
  name=roof12s1 type=roof shape=slab chrlen=0.5 slarea=1.1224
  nslab=10 tunif=308.0
  compound= conc conc conc conc conc conc conc conc conc
  x=0.0 1.0e-4 3.0e-4 6.0e-4 1.2e-3 2.4e-3 5.0e-3 1.e-2 2.e-2 4.0e-2
  7.62e-2
  eoi

  && refueling canal wall surface + top of cross beam
  name=wall12s1 type=wall shape=slab chrlen=0.62 slarea=2.2047
  nslab=10 tunif=308.0
  compound= conc conc conc conc conc conc conc conc conc
  x=0.0 1.0e-4 3.0e-4 6.0e-4 1.2e-3 2.4e-3 5.0e-3 1.e-2 2.e-2 3.5e-2
  5.08e-2
  eoi

  && inside surface of outer walls
  name=wall12s2 type=wall shape=slab chrlen=0.62 slarea=2.6587
  nslab=10 tunif=308.0
```

CONTAIN DCH Models

Appendix

```

compound= conc conc conc conc conc conc conc conc conc
x=0.0 1.0e-4 3.0e-4 6.0e-4 1.2e-3 2.4e-3 5.0e-3 1.e-2 2.e-2 4.0e-2
5.71e-2
eoi

&& steam gen & pump vertical surfaces
name=wall12s3 type=wall shape=slab chrlen=0.62 slarea=2.324
nslab=6 tunif=308.0
compound= fe fe fe fe fe fe
x=0.0 1.0e-4 3.0e-4 6.0e-4 1.2e-3 2.2e-3 3.4e-3
eoi

&& underside grate above pumps
name=roof12s2 type=roof shape=slab chrlen=0.259 slarea=0.1341
nslab=3 tunif=308.0
compound= fe fe fe
x=0.0 1.0e-4 3.0e-4 5.57e-4
eoi

&& top of pumps
name=flor12s1 type=floor shape=slab chrlen=0.229 slarea=0.0821
nslab=6 tunif=308.0
compound= fe fe fe fe fe fe
x=0.0 1.0e-4 3.0e-4 6.0e-4 1.2e-3 2.2e-3 3.4e-3
eoi

&& upper surface of 592' level grating
name=flor12s2 type=floor shape=slab chrlen=0.5 slarea=0.6525
nslab=3 tunif=308.0
compound= fe fe fe
x=0.0 1.0e-4 3.0e-4 5.57e-4
eoi

dch-cell
sdeven=1.0
&& interact nonairborne debris
&& diatrap=0.01
&& thresh=1800.0 && stop reacting trapped debris when Fe freezes
var-parm flag=2
name=trapreac
var-x=time x=5 0.0 3.0 4.0 5.0 15.0
var-y=diatrap y=5 0.01 0.01 0.025 1.0 1.0
eoi
trapping
tofku rhodg=mix && fromcell = 9
len1=0.62 && cell height
len2=0.532 && 6V/S estimate
lengft=0.62 && cell height
ku1=10.0 ku2=10.0 trapmul=1.0 trapmin=0.0 trapmax=1.0e20
vnost=gft && adflow
eoi
eoi

cell=13 && upper Surtsey (near side)
&&
control nhtm=6 mxslab=10

```

CONTAIN DCH Models

Appendix

```

  eoi
  geometry 39.306 7.539
  atmos=3 pgas=1.99e+5 tgas=308.0
  molefrac
  n2=0.8762 o2=0.0979 h2=0.0259 && n2=0.3950 h2ov=.4600 h2=.0400
  eoi
  condense
  &&
  && -----
  &&
  h-burn elev=7.474
  contburn
  dftemp=400.0
  shratio=9.0
  srtemp=848.0 && bulk spontaneous recombination
  mfsrb=0.9
  mfocb=0.01
  debconc=1.e+6 && bsr on gas temp only
  srate=1.47
  eoi
  && for uchb case
  && flam=5.0 cfrmng=1.e-4 mormng=1.e-4 mfcig=1.e-4 mfoig=1.e-4
  && mfsig=0.999 && tactiv=0.4
  eoi
  && overflow to cell 5
  overflow=5
  rad-heat
  gaswal 2.489
  kmx=-0.8 && -0.80
  emsvt 0.8 0.8 0.8 0.8 0.8 0.8
  && cess
  eoi

  && -----heat sink structures-----
  struc
  && outgas && (de)activate outgasing model
  && condata
  && fh2oe=0.0386 fh2ob=0.200 fco2=0.0150
  && eoi

  && surtsey outer wall
  name=wall13s1 type=wall shape=slab chrlen=7.539 slarea=43.316
  nslab=8 tunif=308.0
  compound= fe fe fe fe fe fe fe
  x=0.0 1.0e-4 3.0e-4 6.0e-4 1.2e-3 2.4e-3 5.0e-3 9.e-3 1.588e-2
  bcoutter tgas=308.0 eoi
  eoi

  && surtsey ceiling
  name=roof13s1 type=roof shape=slab chrlen=3.66 slarea=5.2535
  nslab=8 tunif=308.0
  compound= fe fe fe fe fe fe fe
  x=0.0 1.0e-4 3.0e-4 6.0e-4 1.2e-3 2.4e-3 5.0e-3 9.e-3 1.588e-2
  bcoutter tgas=308.0 eoi
  eoi

```

CONTAIN DCH Models

Appendix

```

&& sides of steam generators and filler structures
name=wall13s2 type=wall shape=slab chrlen=1.0 slarea=5.961
  nslab=7 tunif=308.0
  compound= fe fe fe fe fe fe
  x=0.0 1.0e-4 3.0e-4 6.0e-4 1.2e-3 2.4e-3 4.0e-3 6.35e-3
  eoi

&& operating floor
name=flor13s1 type=floor shape=slab chrlen=1.33 slarea=1.771
  nslab=10 tunif=308.0
  compound= conc conc conc conc conc conc conc conc conc
  x=0.0 1.0e-4 3.0e-4 6.0e-4 1.2e-3 2.4e-3 5.0e-3 1.e-2 2.e-2 4.0e-2
  7.62e-2
  eoi

&& top of steam generators
name=flor13s2 type=floor shape=slab chrlen=0.47 slarea=0.347
  nslab=7 tunif=308.0
  compound= fe fe fe fe fe fe
  x=0.0 1.0e-4 3.0e-4 6.0e-4 1.2e-3 2.4e-3 4.0e-3 6.35e-3
  eoi

&& upper surface gratings above RCP's
name=flor13s3 type=floor shape=slab chrlen=0.312 slarea=0.1951
  nslab=3 tunif=308.0
  compound= fe fe fe
  x=0.0 1.0e-4 3.0e-4 5.57e-4
  eoi

dch-cell
  sdeven=1.0
  trapping
    tofku rhodg=mix && fromcell = 11
    len1=7.539 && cell height
    len2=4.15 && 6V/S rule
    lengft=7.539 && cell height
    ku1=10.0 ku2=10.0 trapmul=1.0 trapmin=0.0 trapmax=1.0e20
    vnost=gft && adflow
  eoi
  eoi

  cell=14 && upper Surtsey (far side)
  &&
  control nhtm=7 mxslab=10
  eoi
  geometry 41.046 7.539
  atmos=3 pgas=1.99e+5 tgas=308.0
  molefrac
  n2=0.8762 o2=0.0979 h2=0.0259 && n2=0.3950 h2ov=.4600 h2=.0400
  eoi
  condense
  &&
  && -----
  &&
  h-burn elev=7.474
  contburn

```

CONTAIN DCH Models

Appendix

```

dftemp=400.0
shratio=9.0
srtemp=848.0  && bulk spontaneous recombination
mfscb=0.9
mfocb=0.01
debcconc=1.e+6 && bsr on gas temp only
srrate=1.45
eo1
&& for uchb case
  && flam=5.0  cfrmng=1.e-4  mormng=1.e-4  mfcig=1.e-4  mfoig=1.e-4
  && mfsig=0.999 && tactiv=0.4
eo1
&& overflow to cell 5
overflow=5
rad-heat
  gaswal 2.489 && cell 13 value
  kmx=-0.8 && -0.80
  emsvt 0.8 0.8 0.8 0.8 0.8 0.8 0.8
    && cess
eo1

&& -----heat sink structures-----
struc
&& outgas && (de)activate outgasing model
&& concdata
&& fh2oe=0.0386 fh2ob=0.200 fco2=0.0150
&& eoi

&& surtsey outer wall
name=wall14s1 type=wall  shape=slab  chrlen=7.539  slarea=43.316
  nslab=8  tunif=308.0
  compound= fe fe fe fe fe fe fe
  x=0.0 1.0e-4 3.0e-4 6.0e-4 1.2e-3 2.4e-3 5.0e-3 9.e-3 1.588e-2
  bcoutter tgas=308.0 eoi
eo1

&& surtsey ceiling
name=roof14s1 type=roof  shape=slab  chrlen=3.66  slarea=5.2535
  nslab=8  tunif=308.0
  compound= fe fe fe fe fe fe fe
  x=0.0 1.0e-4 3.0e-4 6.0e-4 1.2e-3 2.4e-3 5.0e-3 9.e-3 1.588e-2
  bcoutter tgas=308.0 eoi
eo1

&& sides of steam generators and filler structures
name=wall14s2 type=wall  shape=slab  chrlen=1.0  slarea=5.961
  nslab=7  tunif=308.0
  compound= fe fe fe fe fe fe
  x=0.0 1.0e-4 3.0e-4 6.0e-4 1.2e-3 2.4e-3 4.0e-3 6.35e-3
eo1

&& RFC inside walls
name=wall14s3 type=wall shape=slab chrlen=0.772 slarea=5.060
  nslab=10 tunif=308.0
  compound= conc conc conc conc conc conc conc conc conc
  x=0.0 1.0e-4 3.0e-4 6.0e-4 1.2e-3 2.4e-3 5.0e-3 1.e-2 2.e-2 3.5e-2

```

CONTAIN DCH Models

Appendix

```

      5.08e-2
  eoi

  && operating floor
  name=flor14s1 type=floor shape=slab chrlen=1.33 slarea=4.24
  nslab=10 tunif=308.0
  compound= conc conc conc conc conc conc conc conc
  x=0.0 1.0e-4 3.0e-4 6.0e-4 1.2e-3 2.4e-3 5.0e-3 1.e-2 2.e-2 4.0e-2
  7.62e-2
  eoi

  && top of steam generators
  name=flor14s2 type=floor shape=slab chrlen=0.47 slarea=0.347
  nslab=7 tunif=308.0
  compound= fe fe fe fe fe fe
  x=0.0 1.0e-4 3.0e-4 6.0e-4 1.2e-3 2.4e-3 4.0e-3 6.35e-3
  eoi

  && upper surface gratings above RCP's
  name=flor14s3 type=floor shape=slab chrlen=0.259 slarea=0.1341
  nslab=3 tunif=308.0
  compound= fe fe fe
  x=0.0 1.0e-4 3.0e-4 5.57e-4
  eoi

  dch-cell
  sdeven=1.0
  trapping
    tofku rhodg=mix && fromcell = 12
    len1=7.539 && cell height
    len2=4.15 && cell 13 value
    lengft=7.539 && cell height
    ku1=10.0 ku2=10.0 trapmul=1.0 trapmin=0.0 trapmax=1.0e20
    vnost=gtf && adflow
  eoi
  eoi

  eof
  uo2d          debris
  molew      2.7007e+02
  temps      44
    3.0000e+02 4.0000e+02 5.0000e+02 6.0000e+02 7.0000e+02
    8.0000e+02 9.0000e+02 1.0000e+03 1.0500e+03 1.1000e+03
    1.1500e+03 1.2000e+03 1.2500e+03 1.3000e+03 1.3500e+03
    1.4000e+03 1.4500e+03 1.5000e+03 1.5500e+03 1.6000e+03
    1.6500e+03 1.7000e+03 1.7500e+03 1.8000e+03 1.8500e+03
    1.9000e+03 1.9500e+03 2.0000e+03 2.0500e+03 2.1000e+03
    2.1500e+03 2.2000e+03 2.2500e+03 2.3000e+03 2.3500e+03
    2.4000e+03 2.4500e+03 2.5000e+03 2.5500e+03 2.6000e+03
    2.6500e+03 2.7000e+03 2.7500e+03 2.8000e+03
  condt
    8.5417e+00 7.0075e+00 5.9438e+00 5.1651e+00 4.5726e+00
    4.1090e+00 3.7392e+00 3.4400e+00 3.3119e+00 3.1960e+00
    3.0912e+00 2.9964e+00 2.9107e+00 2.8335e+00 2.7639e+00
    2.7016e+00 2.6459e+00 2.5966e+00 2.5531e+00 2.5153e+00
    2.4829e+00 2.4555e+00 2.4331e+00 2.4154e+00 2.4023e+00

```

CONTAIN DCH Models

Appendix

2.3936e+00	2.3892e+00	2.3891e+00	2.3930e+00	2.4011e+00
2.4131e+00	2.4291e+00	2.4490e+00	2.4727e+00	2.5003e+00
2.5317e+00	2.5669e+00	2.6058e+00	2.6486e+00	2.6951e+00
2.7454e+00	2.7994e+00	2.8573e+00	2.9190e+00	
entht				
4.7186e+02	2.5643e+04	5.2885e+04	8.1370e+04	1.1071e+05
1.4069e+05	1.7121e+05	2.0218e+05	2.1783e+05	2.3358e+05
2.4942e+05	2.6535e+05	2.8137e+05	2.9749e+05	3.1369e+05
3.2998e+05	3.4636e+05	3.6283e+05	3.7940e+05	3.9608e+05
4.1286e+05	4.2977e+05	4.4681e+05	4.6401e+05	4.8139e+05
4.9897e+05	5.1681e+05	5.3492e+05	5.5337e+05	5.7221e+05
5.9149e+05	6.1130e+05	6.3172e+05	6.5283e+05	6.7473e+05
6.9752e+05	7.2134e+05	7.4631e+05	9.8223e+05	1.0131e+06
1.0439e+06	1.0748e+06	1.1056e+06	1.1365e+06	
rhot				
1.0964e+04	1.0940e+04	1.0915e+04	1.0887e+04	1.0858e+04
1.0827e+04	1.0795e+04	1.0761e+04	1.0743e+04	1.0725e+04
1.0707e+04	1.0688e+04	1.0669e+04	1.0649e+04	1.0629e+04
1.0609e+04	1.0588e+04	1.0567e+04	1.0546e+04	1.0524e+04
1.0502e+04	1.0479e+04	1.0457e+04	1.0433e+04	1.0410e+04
1.0386e+04	1.0362e+04	1.0338e+04	1.0313e+04	1.0288e+04
1.0263e+04	1.0237e+04	1.0211e+04	1.0185e+04	1.0158e+04
1.0132e+04	1.0105e+04	1.0077e+04	1.0050e+04	1.0022e+04
9.9942e+03	9.9660e+03	9.9375e+03	9.9088e+03	
spht				
2.3613e+02	2.6395e+02	2.7946e+02	2.8951e+02	2.9683e+02
3.0263e+02	3.0754e+02	3.1187e+02	3.1389e+02	3.1584e+02
3.1773e+02	3.1956e+02	3.2136e+02	3.2314e+02	3.2491e+02
3.2670e+02	3.2851e+02	3.3040e+02	3.3238e+02	3.3450e+02
3.3682e+02	3.3940e+02	3.4232e+02	3.4566e+02	3.4953e+02
3.5402e+02	3.5927e+02	3.6540e+02	3.7257e+02	3.8092e+02
3.9062e+02	4.0184e+02	4.1476e+02	4.2956e+02	4.4643e+02
4.6556e+02	4.8714e+02	5.1137e+02	6.1704e+02	6.1704e+02
6.1704e+02	6.1704e+02	6.1704e+02	6.1704e+02	
eoi				
zrd				
	debris			
molew	9.1220e+01			
temp	38			
3.0000e+02	4.0000e+02	5.0000e+02	6.0000e+02	7.0000e+02
8.0000e+02	9.0000e+02	1.0000e+03	1.0500e+03	1.1000e+03
1.1500e+03	1.2000e+03	1.2500e+03	1.3000e+03	1.3500e+03
1.4000e+03	1.4500e+03	1.5000e+03	1.5500e+03	1.6000e+03
1.6500e+03	1.7000e+03	1.7500e+03	1.8000e+03	1.8500e+03
1.9000e+03	1.9500e+03	2.0000e+03	2.0500e+03	2.1000e+03
2.1500e+03	2.2000e+03	2.2500e+03	2.3000e+03	2.3500e+03
2.4000e+03	2.4500e+03	2.5000e+03		
condt				
2.8000e+01	2.8000e+01	2.8000e+01	2.8000e+01	2.8000e+01
2.8000e+01	2.8000e+01	2.8000e+01	2.8000e+01	2.8000e+01
2.8000e+01	2.8000e+01	2.8000e+01	2.8000e+01	2.8000e+01
2.8000e+01	2.8000e+01	2.8000e+01	2.8000e+01	2.8000e+01
2.8000e+01	2.8000e+01	2.8000e+01	2.8000e+01	2.8000e+01
2.8000e+01	2.8000e+01	2.8000e+01	2.8000e+01	2.8000e+01
2.8000e+01	2.8000e+01	2.8000e+01	2.8000e+01	2.8000e+01
2.8000e+01	2.8000e+01	2.8000e+01	2.8000e+01	2.8000e+01
entht				

CONTAIN DCH Models

Appendix

5.2300e+02	3.0329e+04	6.1980e+04	9.4810e+04	1.2853e+05
1.6301e+05	1.9816e+05	2.3393e+05	2.5204e+05	2.7029e+05
3.3038e+05	3.4706e+05	3.6374e+05	3.8041e+05	3.9709e+05
4.1377e+05	4.3044e+05	4.4712e+05	4.6380e+05	4.8047e+05
4.9715e+05	5.1382e+05	5.3050e+05	5.4718e+05	5.6385e+05
5.8053e+05	5.9721e+05	6.1388e+05	6.3056e+05	6.4724e+05
8.8956e+05	9.0791e+05	9.2626e+05	9.4461e+05	9.6296e+05
9.8131e+05	9.9966e+05	1.0180e+06		
rhot				
6.5060e+03	6.5060e+03	6.5060e+03	6.5060e+03	6.5060e+03
6.5060e+03	6.5060e+03	6.5060e+03	6.5060e+03	6.5060e+03
6.5060e+03	6.5060e+03	6.5060e+03	6.5060e+03	6.5060e+03
6.5060e+03	6.5060e+03	6.5060e+03	6.5060e+03	6.5060e+03
6.5060e+03	6.5060e+03	6.5060e+03	6.5060e+03	6.5060e+03
6.5060e+03	6.5060e+03	6.5060e+03	6.5060e+03	6.5060e+03
6.5060e+03	6.5060e+03	6.5060e+03	6.5060e+03	6.5060e+03
6.5060e+03	6.5060e+03	6.5060e+03	6.5060e+03	6.5060e+03
sph				
2.8423e+02	3.0886e+02	3.2301e+02	3.3304e+02	3.4113e+02
3.4818e+02	3.5463e+02	3.6070e+02	3.6364e+02	3.6653e+02
3.3353e+02	3.3353e+02	3.3353e+02	3.3353e+02	3.3353e+02
3.3353e+02	3.3353e+02	3.3353e+02	3.3353e+02	3.3353e+02
3.3353e+02	3.3353e+02	3.3353e+02	3.3353e+02	3.3353e+02
3.3353e+02	3.3353e+02	3.3353e+02	3.3353e+02	3.3353e+02
3.3353e+02	3.3353e+02	3.3353e+02	3.3353e+02	3.3353e+02
3.6702e+02	3.6702e+02	3.6702e+02	3.6702e+02	3.6702e+02
3.6702e+02	3.6702e+02	3.6702e+02		
eo1				
zro2d				
debris				
mo1ew	1.2322e+02			
temp1	40			
3.0000e+02	4.0000e+02	5.0000e+02	6.0000e+02	7.0000e+02
8.0000e+02	9.0000e+02	1.0000e+03	1.0500e+03	1.1000e+03
1.1500e+03	1.2000e+03	1.2500e+03	1.3000e+03	1.3500e+03
1.4000e+03	1.4500e+03	1.5000e+03	1.5500e+03	1.6000e+03
1.6500e+03	1.7000e+03	1.7500e+03	1.8000e+03	1.8500e+03
1.9000e+03	1.9500e+03	2.0000e+03	2.0500e+03	2.1000e+03
2.1500e+03	2.2000e+03	2.2500e+03	2.3000e+03	2.3500e+03
2.4000e+03	2.4500e+03	2.5000e+03	2.550e+03	2.700e+03
condt				
2.0000e+00	2.0000e+00	2.0000e+00	2.0000e+00	2.0000e+00
2.0000e+00	2.0000e+00	2.0000e+00	2.0000e+00	2.0000e+00
2.0000e+00	2.0000e+00	2.0000e+00	2.0000e+00	2.0000e+00
2.0000e+00	2.0000e+00	2.0000e+00	2.0000e+00	2.0000e+00
2.0000e+00	2.0000e+00	2.0000e+00	2.0000e+00	2.0000e+00
2.0000e+00	2.0000e+00	2.0000e+00	2.0000e+00	2.0000e+00
2.0000e+00	2.0000e+00	2.0000e+00	2.0000e+00	2.0000e+00
2.0000e+00	2.0000e+00	2.0000e+00	2.0000e+00	2.0000e+00
2.0000e+00	2.0000e+00	2.0000e+00	2.0	2.0
enth1				
8.2319e+02	5.0045e+04	1.0369e+05	1.5985e+05	2.1771e+05
2.7687e+05	3.3709e+05	3.9824e+05	4.2913e+05	4.6023e+05
4.9152e+05	5.2301e+05	5.5468e+05	5.8653e+05	6.1856e+05
6.5077e+05	6.8315e+05	7.6298e+05	7.9326e+05	8.2353e+05
8.5381e+05	8.8408e+05	9.1436e+05	9.4463e+05	9.7491e+05
1.0052e+06	1.0355e+06	1.0657e+06	1.0960e+06	1.1263e+06
1.1566e+06	1.1868e+06	1.2171e+06	1.2474e+06	1.2777e+06
1.3079e+06	1.3382e+06	1.3685e+06	2.0622e+06	2.1793e+06

CONTAIN DCH Models

Appendix

SAND94-1073

CONTAIN DCH Models

Appendix

EXTERNAL DISTRIBUTION:

U.S. Nuclear Regulatory Commission (8)
Division of Reactor System Safety
Office of Nuclear Regulatory Research
ATTN: C. Ader, T-10K-8

A. Drozd
C. G. Gingrich, NLN-344
R. Lee, T-10K-8
J. Monninger, OWFN 8-D
A. Notafrancesco
A. Rubin, T-10K-8
T. Spies, T-10F-12

U.S. Nuclear Regulatory Commission (3)
Office of ACRS
ATTN: M. D. Houston, T-2E-26
T. Kress, T-2E-26
I. Catton
Washington, D.C. 20555-0001

U.S. Department of Energy (2)
Albuquerque Operations Office
Post Office Box 5400
ATTN: C. E. Garcia, Director
For: C. B. Quinn
R. L. Holton
Albuquerque, NM 87185

U.S. Department of Energy
Office of Nuclear Safety Coordination
ATTN: R. W. Barber
Washington, D.C. 20545

U.S. Department of Energy
Idaho Operations Office
850 Energy Drive
ATTN: S. W. Sorrell
Idaho Falls, ID 83401

U.S. Department of Energy
Scientific and Technical Information Center
Post Office Box 62
Oak Ridge, TN 37831

Argonne National Laboratory
9700 South Cass Avenue
ATTN: B. Spencer
Argonne, IL 60439

Battelle Columbus Laboratory (2)
505 King Avenue
ATTN: R. Denning
J. Gieseke
Columbus, OH 43201

Battelle Pacific Northwest Laboratory
Post Office Box 999
ATTN: M. Freshley
Richland, WA 99352

Brookhaven National Laboratory (3)
Building 130
32 Lewis
ATTN: R. Bari
T. Pratt
N. Tutu
Upton, NY 11973

Ebasco Services Incorporated
Applied Physics Department
Two World Trade Center
Attn: J. J. Shin
New York, NY 10048

EG&G Idaho
Post Office Box 1625/MS2508
ATTN: D. L. Knudson
Idaho Falls, ID 83415

Electric Power Research Institute (2)
3412 Hillview Avenue
ATTN: A. Michaels
M. Murillo
Palo Alto, CA 94303

Energy Research, Inc. (2)
Post Office Box 2034
ATTN: H. Esmali
M. Khatib-Rahbar
Rockville, MD 20852

Fauske & Associates, Inc. (2)
16W070 West 83rd Street
ATTN: R. Henry
M. G. Plys
Burr Ridge, IL 60952

General Electric Company
Advanced Boiling Water Reactor Program
175 Curtner Avenue
ATTN: W. Holtzclaw
San Jose, CA 95125

Knolls Atomic Power Laboratory
Post Office Box 1072
ATTN: J. McMullan
Schenectady, NY 12301

Levy & Associates
3880 South Bascom Avenue, Suite #112
ATTN: S. Levy
San Jose, CA 95124

Los Alamos National Laboratory
Post Office Box 1663
ATTN: B. Boyack, K-551
Los Alamos, NM 87545

Massachusetts Institute of Technology
ATTN: M. Golay
Cambridge, MA 02139

Oak Ridge National Laboratory (3)
Post Office Box 2009
ATTN: S. A. Hodge
C. Hyman
K. Smith, MS-8057
Oak Ridge, TN 37831-8057

Pennsylvania Power & Light Company
Two North Ninth Street
ATTN: T. S. Yih
Allentown, PA 18101

Purdue University
Heat Transfer Laboratory
School of Mechanical Engineering
ATTN: R. Viskanta
West Lafayette, IN 47907-1209

Purdue University
School of Nuclear Engineering
ATTN: M. Ishii
West Lafayette, IN 47907

Rensselaer Polytechnic Institute
Department of Nuclear Engineering &
Engineering Sciences
Tibbits Avenue, NES Building
ATTN: M. Podowski
Troy, NY 12180-3590

Science Applications International Corp.
2109 Air Park Road, S.E.
ATTN: D. R. Bradley
Albuquerque, NM 87106

Stone & Webster Engineering
Post Office Box 2325
ATTN: J. Metcalf, MS245-2
Boston, MA 02107

Texas A&M University
Department of Nuclear Engineering
ATTN: Y. A. Hassan
College Station, TX 77843

Jack Tills & Associates
Post Office Box 549
ATTN: J. Tills
Sandia Park NM 87047

University of California
Department of Chemical and
Nuclear Engineering
ATTN: T. Theofanous
Santa Barbara, CA 93106

University of Maryland
Department of Nuclear Engineering
ATTN: Professor K. Almenas
College Park, MD 20742

University of Missouri
Nuclear Engineering Department
ATTN: S. K. Loyalka
Columbia, MO 65211

University of New Mexico
Department of Chemistry and
Nuclear Engineering
ATTN: F. E. Haskin
Albuquerque, NM 87131

University of Wisconsin
Department of Nuclear Engineering
153 Engineering Research Building
1500 Johnson Drive
ATTN: M. L. Corradini
Madison, WI 53706

Westinghouse Bettis Atomic Laboratory
Post Office Box 79
ATTN: J. W. Wolfe, ZAP 34N
West Mifflin, PA 15122

Westinghouse Savannah River (3)
Woodside Executive Park
1359 Silver Bluff Road
ATTN: K. O'Kula
Aiken, SC 29808-0001

AECL Research
Whitshell Laboratories
ATTN: S. R. Mulpuru
Pinawa, Manitoba R0E 1L0
CANADA

Ontario Hydro
700 University Avenue
ATTN: O. Akalin
Toronto, Ontario M5G 1X6
CANADA

FOREIGN DISTRIBUTION:

IAEA
Division of Nuclear Reactor Safety
Wagranerstrasse 5
Post Office Box 100
A/1400 Vienna
ATTN: M. Jankowski
AUSTRIA

Belgonucleaire SA
Rue du Champ de Mars 25
ATTN: H. Bairiot
B-1050 Brussels
BELGIUM

Director, Research, Science Education CEC
Rue de la Loi 2000
1049 Brussels
ATTN: W. Balz
BELGIUM

Commission on the Use of Atomic Energy for
Peaceful Purposes - 69 Shipchenski
Prokhotod Boulevard, 1574, Sofia
ATTN: Y. Yanev
BULGARIA

AECL CANDU
Sheridan Park Research Community
2251 Speakman Avenue
ATTN: V. J. Nath
Mississauga, Ontario L5K 1B2
CANADA

AECL Research
Chalk River Research Laboratories
ATTN: B. H. McDonald
Chalk River, Ontario K0J 1JO
CANADA

Nuclear Research Institute
250 68 Rez
ATTN: J. Kujal
CZECH REPUBLIC

State Office for Nuclear Safety
Slezska 9
ATTN: J. Stuller
120 00 Prague 2
CZECH REPUBLIC

RISO National Laboratory
Department of Energy Technology
Post Office Box 49
DK-4000 Roskilde
ATTN: P. B. Fynbo
DENMARK

Finnish Center Radiation & Nuclear Safety
Department of Nuclear Safety
Post Office Box 268
SF-00101 Helsinki
ATTN: J. V. Sandberg
FINLAND

Tech Research Centre of Finland (VTT)
Nuclear Engineering Laboratory (YDI)
PL 169
00181 Helsinki
ATTN: L. Mattila
FINLAND

Cadarache Center for Nuclear Studies (3)
F-13108 Sait Paul-Lez-Durance Cedex
ATTN: M. Schwartz
F. Serre
A. Meyer-Heine
FRANCE

Inst. de Protection et de Surete Nucleaire
CEN/FAR-B.P. No. 6
F-92265, Fontenay-aux-Roses
ATTN: J. Bardelay
Cedex, FRANCE

Battelle Institute e. V.
Am Romerhof 35
D-6000 Frankfurt am Main 90
ATTN: D. T. Kanzleiter
GERMANY

Gesellschaft fur Reaktorsicherheit (3)
Forschungsgelände
8046 Garching
ATTN: K. Trambauer
G. Weber
M. Sonnenkalb
GERMANY

Gesellschaft fur Reaktorsicherheit mbH
Postfach 101650
Glockengasse 2
D-5000 Köln 1
ATTN: J. Langhans
GERMANY

Ruhr-University of Bochum
Department of Nuclear & New Energy System
ATTN: U. Brockmeier
GERMANY

University of Stuttgart
IKE
Pfaffenwaldring 31
ATTN: U. Bieder
D-7000 Stuttgart 80
GERMANY

Technische Universität München
Forschungsgelände
8046 Garching
ATTN: Professor Dr. I. H. Karwat
GERMANY

Kernforschungszentrum Karlsruhe (4)
Post Office Box 3640
ATTN: V. Scholtysek
75 Karlsruhe
GERMANY

Research Centre Rossendorf, Inc.
Forschungszentrum Rossendorf
Postfach 19
ATTN: Dr. H. Funke
DO-8051 Dresden
GERMANY

Institute for Electric Power Research
Division of Nuclear & Power Engineering
Post Office Box 233
ATTN: Z. Techy
H-1368 Budapest
HUNGARY

Hungarian Atomic Energy Commission
H-1374 Budapest, Post Office Box 565
ATTN: S. Elo
Budapest
HUNGARY

CEC Joint Research Center (3)
I-21020 Ispra (Varese)
ATTN: P. Fasoli-Stella
A. Markovina
R. Ricchena
ITALY

Nucleare e della Protezione Sanitaria
(DISP) (ENEA)
Ente Nazionale Energie Alternative
Viale Regina Margherita, 125
Cassella Postale M. 2358
ATTN: G. Petrangeli
1-00144 Roma A.D.
ITALY

ENEL-CRTN
Via Monfalcone 15
ATTN: E. Borioli
20132 Milan
ITALY

Toshiba Corporation
Nuclear Safety Engineering Section
8, Shinsugita-Cho, Isogo-Ku
Yokohama 235
ATTN: M. Naito
JAPAN

Power Reactor Nuclear Fuel Development
Corporation (PNC)
9-13, 1-Chome
ATTN: H. Hiroi
Minato-Ku, Tokyo
JAPAN

Nuclear Power Engineering Center
Fujitakano Building
17-1, 3-Chome, Toranomon, Minato-Ku
ATTN: Kenji Takumi
Tokyo, 105
JAPAN

Japan Atomic Energy Research Institute (2)
Tokai-mura
Naku-gun
ATTN: K. Soda
J. Sugimoto
Ibaraki-ken, 319-11
JAPAN

POSTECH
Department of Mechanical Engineering
Post Office Box 125
Kyungbuk 790-600
ATTN: M. H. Kim
KOREA

Korea Atomic Energy Research Institute
150 Dukjin-dong, Yoosung-gu
ATTN: Hee-Dong Kim
Taejon 305-353
KOREA

Korea Institute of Nuclear Safety
Safety Review and Assessment Division
Post Office Box 16, Daeduk-Danji
ATTN: J. J. Lee
Taejon, 305-353
KOREA

VATESI
Gediminis Prospect 36
ATTN: P. Vaisnys
Vilnius
LITHUANIA

Com. Nacional de Seguridad Nucl. Salvag
Colonia Narvarte Delegation B. Juarez
ATTN: Dr. Abrtshsm #779
C.P. 03020
MEXICO

Atomic Energy Council
67, Lane 144 Keelung Road
Section 4, Taipei, Taiwan
ATTN: S. J. Shieh
REPUBLIC OF CHINA

Institute of Nuclear Energy Research
Post Office Box 3
Lungtan, Taiwan 325
ATTN: S. I. Chang
REPUBLIC OF CHINA

Nuclear Safety Institute
Russian Research Center KI
1 Kurchatov Square
ATTN: V. Asmolov
123182 Moscow
RUSSIA

Russian Academy of Sciences
Nuclear Safety Institute
52, B. Tulskaia
ATTN: V. F. Strizhov
113191 Moscow
RUSSIA

Nuclear Regulatory Authority, Slovak Republic
Post Office Box 24
820 07 Bratislava 27
ATTN: J. Misak
SLOVAK REPUBLIC

Jozef Stefan Institute
Jamova 39
ATTN: B. Mavko
61111 Ljubljana
SLOVENIA

Catedra de Tecnologia Nuclear
E.T.S. Ingenieros Industriales
Universidad Politecnica
Jose Gutierrez Abascal, 2
28006-Madrid
ATTN: L. Herranz
SPAIN

Consejo de Seguridad Nuckan
SOR Angela de la Cruz No. 3
ATTN: J. Bagues
28056 Madrid
SPAIN

Consejo de Seguridad Nuclear
Justo Dorado 11
ATTN: J. E. deCarlos
28040 Madrid
SPAIN

E.T.S. Ingenieros Industriales
Jost Gutierrez Abascal, 2
ATTN: A. Alonso
28006 Madrid
SPAIN

Royal Institute of Technology
Nuclear Power Safety
S-100 44 Stockholm
ATTN: B. R. Sehgal
SWEDEN

Swedish Nuclear Power Inspectorate
Post Office Box 27106
S-102 52 Stockholm
ATTN: W. Frid
SWEDEN

Studsvik Nuclear
S-611 82, Nykoping
ATTN: K. O. Johansson
SWEDEN

Swiss Federal Nuclear Safety Inspectorate
CH-5303 Wurenlingen
ATTN: S. Chakraborty
SWITZERLAND

Paul Scherrer Institute
ATTN: P. Hosemann
CH-5232 Villigen, PSI
SWITZERLAND

Institute of Nuclear Energy Research
Post Office Box 3
ATTN: Sen-I Chang
Lung-Tan
TAIWAN 325

Netherlands Energy Research
Foundation (ECN) (2)
Postbus 1
1755 ZG Petten
ATTN: K. J. Brinkman
P. M. Stoop
THE NETHERLANDS

N. V. Kema
Post Office Box 9035
ATTN: P. Kloeg
6800 ET Arnhem
THE NETHERLANDS

AEA Culham Laboratory (2)
Abingdon
Oxfordshire, OX14-3DB
ATTN: B. D. Turland
D. F. Fletcher
UNITED KINGDOM

AEA Winfrith (3)
Dorchester
Dorset DT2 8DH
ATTN: S. Kinnersley
P. N. Smith
B. Bowsher
UNITED KINGDOM

Nuclear Electric
Berkeley Nuclear Laboratory, Berkeley
ATTN: C. Chapman
Gloucestershire GL 13 9PB
UNITED KINGDOM

CEGB, Booths Hall
Chelford Road, Knutsford
Cheshire WA16 8QG
ATTN: N. E. Butterly
UNITED KINGDOM

AERE Harwell
Didcot
ATTN: A. L. Nichols
Oxfordshire OX11 ORA
UNITED KINGDOM

UKAEA, Risely Nuclear Laboratories (2)
Risley, Warrington
ATTN: A. T. D. Butland
I. H. Dunbar
Cheshire WA3-4NE
UNITED KINGDOM

INTERNAL DISTRIBUTION:

MS0619 Print Media (12615)
MS0736 N. R. Ortiz (6400)
MS0739 K. D. Bergeron (6421) (5)
MS0739 R. K. Cole, Jr. (6421)
MS0739 R. G. Gido (6421)
MS0739 R. O. Griffith (6421)

MS0739 K. K. Murata (6421)
MS0739 R. C. Smith (6421)
MS0739 D. W. Stamps (6421)
MS0739 E. L. Tadios (6421)
MS0739 D. C. Williams (6421)
MS0742 J. E. Kelly (6414)
MS0744 D. A. Powers (6404)
MS0747 A. L. Camp (6412)
MS0747 S. E. Dingman (6412)
MS0748 F. E. Harper (6413)
MS0899 Tech Library (13414) (5 cys)
MS1137 M. D. Allen (6422)
MS1137 T. K. Blanchat (6422)
MS1137 M. M. Pilch (6422)
MS1139 K. O. Reil (6423)
MS1139 R. O. Gauntt (6423)
MS0100 Document Processing (7613-2) for
DOE/OSTI (2 cys)
MS9018 Central Technical Files (8523-2)